THE UNIVERSITY *of* EDINBURGH

A STUDY OF THE CHARACTERISTIC RADIATION EMITTED FROM X-RAY TUBES

by Peter Tothill B.Sc.

Thesis presented for the Degree of Doctor of Philosophy of the University of Edinburgh in the Faculty of Medicine, July 1964.

CONTENTS

CHAPTER 1

Introduction

1.1 Nature of X-ray emission

X-rays are produced when fast-moving electrons strike a target. While most of the ensuing interactions with the atoms of the target result in collisional losses of energy, appearing as heat, a small proportion give rise to the emission of radiation. These last interactions are of two types: in the first, an electron may be ejected from a shell close to the nucleus. When an electron from an outer shell fills the vacant position, a quantum of characteristic radiation is emitted - K characteristic if a K electron was ejected, L radiation from the loss of an L electron, etc. The spectrum of the radiation arising in this way consists of discrete lines, the energy of each corresponding to the difference in energy between the binding energies of the appropriate shells. In addition to the direct ejection of an inner electron by a bombarding electron, a fluorescence interaction may occur, in which the energy for the electron removal arises from the absorption of higher energy radiation produced elsewhere in the target.

The other type of radiative interaction occurs when a bombarding electron passes very close to a nucleus and suffers a drastic change of direction accompanied by a loss of energy. This energy appears as a photon of "bremsstrahlung". Depending on the orbit described by the electron, the photon may have any energy up to that of the electron. Interactions of this type give rise to the continuous spectrum of X-rays. The total spectrum then consists of a continuum ending at the maximum energy of the electrons, with superimposed lines of characteristic radiation. The

relationship/

relationship between the two types of radiation forms the subject of this study.

1.2 Scope of the investigation

The main purpose of the investigation was to provide further information about X-ray beams used in medical diagnosis and radiotherapy. In order to study the effects of such beams, a knowledge of their "quality" as well as their quantity is usually required. This quality is completely specified only by giving the spectral energy distribution. The determination of this distribution is difficult, and simpler methods of specification are usually adopted. These are nearly always based on attenuation measurements. The presence of characteristic radiation in the beam under consideration influences the significance of some of the parameters considered. It is therefore necessary to have some knowledge of the relationship between the amount of characteristic radiation and the continuous radiation in X-ray beams under various operating conditions.

Since medical and many other X-ray sets operating under conditions which involve the emission of characteristic radiation almost invariably have tubes with targets of tungsten, attention was confined to this material. Moreover, as only a small proportion of such sets (such as apparatus used for superficial X-ray therapy) have windows capable of transmitting the low energy L characteristic radiation of tungsten, the investigation has included only a study of the K radiation.

A considerable attention has been paid to the accurate determination of the wavelengths of the characteristic radiation emitted by practically/

practically all the elements, since these are of importance in X-ray diffraction studies. A number of investigators have concerned themselves with the quantity of characteristic radiation emitted from elements used as targets in tubes employed for such diffraction studies. These are usually materials of lower atomic number, and the X-ray energies are invariably much lower than those we shall consider.

Apart from a few deductions from attenuation data, which may not have much validity, the only previous determinations of the quantity of tungsten K radiation have arisen from scintillation spectrometry investigations.

For the correction or interpretation of the attenuation data already referred to, the relationship required is the ratio of the quantity of characteristic radiation to that of the continuous radiation (or the total beam). Since the detector used in attenuation measurements is nearly always an air ionization chamber, it is most appropriate that the ratio is expressed in terms of the unit used for such detectors, namely the röntgen. However, measurements made by some methods may involve expression of the ratio in other units, such as photon flux or intensity. Under some circumstances, an interchange may be made between such systems of units.

1.3 Possible methods of determining the ratio of characteristic to total radiation

Several possible methods are available for investigating the relationship between characteristic and total radiation. These will be considered in turn:

(a) Crystal diffraction methods.

All the earlier determinations of X-ray spectra were made with crystal/

crystal spectrometers. Such instruments have an extremely good resolution and are capable of measuring X-ray wavelengths with very great accuracy. They also provide the only means available of studying in detail all the lines which comprise the characteristic radiation. There are, however, limitations imposed on the delineation of the complete spectrum by the existence of multiple orders of diffraction. The Bragg formula governing the angular relationships states that reinforcement will occur when $2d \sin \Theta = n\lambda$, where d is the separation of successive planes, Θ is the angle of incidence, λ the wavelength and n an integer. Thus it can be seen that for any given angular setting of the detector and crystal, there are many values of λ which will satisfy the equation, leading to the superposition of spectral curves. This is particularly serious when λ is small as in our case, and it is very difficult to determine in this way the continuous spectra of high energy radiation.

It may be that relative changes in the intensity of the characteristic lines with operating voltage and filtration could be studied with such a spectrometer, and a calibrating procedure such as that to be described in connection with proportional counter measurements used to derive the relationship to the total beam. However, no crystal diffraction apparatus was available for this investigation.

(b) Proportional counters.

These devices do not rely on dispersion of the beam to obtain a spectral distribution, but upon the relationship (ideally linear) between the energy of the ionizing radiation and the size of the electrical pulse emerging from the apparatus. If the distribution of pulse sizes is investigated/

investigated it may be possible to derive the corresponding energy distribution in the spectrum of the incident beam. Such devices have a much poorer resolution than the crystal diffraction spectrometer, but since a much greater fraction of the beam enters the detector, their sensitivity is much higher. While solid state detectors are growing in importance, they have not yet been developed far enough for the study of X-ray spectra in the energy range considered in this investigation, and the main types of proportional counter to be considered are the scintillation counter and the gas proportional counter.

(i) Scintillation counters. When a scintillation counter is used to detect X or γ photons, the radiation is allowed to fall on a phosphor, usually a crystal of sodium iodide, activated by a small inclusion of thallium. The absorption of the photon in the phosphor leads to the emission of many photons of light, which are in turn detected by a sensitive photomultiplier tube, resulting in an electrical pulse which can be further amplified and counted. The size of the output pulse is very nearly proportional to the energy of the photon of ionizing radiation. Sodium iodide is particularly suitable as a phosphor as it can be grown in large, clear crystals transparent to the fluorescent light, it contains material of relatively high atomic number, which leads to good absorption of the primary photons and the spectral distribution of the emitted light matches the response of commonly available photomultiplier tubes.

An X or γ ray spectrum can be investigated by scintillation methods by incorporating a pulse-height analyser in the electronic circuitry, so that a pulse height distribution may be obtained. Many factors lead to corrections/

corrections being necessary to convert such a distribution to the energy spectrum of the incident radiation. These include the non-linear response of the spectrometer to photons, the crystal efficiency, the escape of iodine K X-rays, the Compton effect and the spectrometer resolution. These corrections are complex, and computer techniques are often used.

The main limitation of scintillation spectrometry is the relatively poor resolution obtainable, due principally to the random nature of the emission of electrons in the photomultiplier tube. The resolution is worse at low energies and the Kα and Kβ characteristic lines of tungsten are not resolved, for example. Despite this, however, scintillation spectrometry offers the best means of studying the complete X-ray spectrum. This application was first made by Johansson in 1951 and the method has been developed by many others. In particular, Cormack (1955) and his colleagues in Canada and a group of workers at Lund University in Sweden have made notable contributions. From the latter laboratory Hettinger and Starfelt in 1958 published what were probably the first reliable values of the contribution of the K characteristic radiation of tungsten to the emission from X-ray tubes.

As much attention had already been paid to the investigation of X-ray spectra by this method, and it seemed unlikely that a significant fresh contribution could be made, it was decided to explore other methods. As will be seen later, some use has been made of the results of Hettinger and Starfelt, and comparisons made with their findings.

(ii) Gas proportional counters. The gas proportional counter (more commonly known simply as the proportional counter) consists of an ionization/

ionization chamber in which the electrode configuration and applied voltage are such as to permit a limited amount of ionization by collision of the gas molecules. By this means, the passage of a single electron can give rise to a measurable pulse. Moreover, the size of the output pulse is proportional to the energy expended in the gas by the initiating electron. It is this property which gives rise to the possibility of using the counter for X or γ ray spectrometry. This depends on the emission of photoelectrons within the counter following photoelectric absorption by the gas of the counter. Because the absorption of all but the lowest energy X-rays is very low, the sensitivity of the counter to medium and high energy X and γ rays is also low. In addition, the absorption coefficient of the filling gases used varies rapidly with changing X-ray energy, so there are not many circumstances in which a proportional counter can be used to derive a complete spectrum. The outstanding advantage of the gas proportional counter over the scintillation counter is its better resolution. For example, the resolution of a 60 keV line, expressed as full width at half height, might be 6% for a proportional counter and 16% for a sodium iodide scintillation counter.

Inert gases are normally used as a filling for proportional counters, usually with the addition of a small proportion of organic gas. The efficiency of detection of X or γ rays may be improved by using the higher atomic number gases krypton or xenon, but they have some disadvantages, as will be seen later, and they are too expensive to permit gas flow operation. Consequently, argon is the most commonly used filling gas. The relative insensitivity to higher energy radiation may be on occasion an advantage in reducing/

reducing a background or other unwanted radiation response.

Proportional counters have been used to study X-ray spectra at low energies. For example, Dyson and Cosslett (Dyson 1959, Cosslett and Dyson 1957) have investigated both continuous and characteristic X-ray production in various target materials at energies up to about 15 kV. Dolby (1960) has worked at even lower energies and describes the use of a proportional counter to measure the intensities of the carbon and aluminium K - lines excited at tube potentials between 1 and 10 kV. At these energies, the absorption in argon is quite high, and the efficiency of detection ranges from 20 - 100% To the best of the author's belief, no reports have appeared of the use of the proportional counter to study the K characteristic radiation from tungsten. It was originally intended in the present investigation to use such a counter to measure only relative intensities of K-radiation under various operating conditions, but, as will be described in Chapter 2, a method was devised of calibrating the counter to yield a direct comparison between the characteristic and the total radiation.

(c) The use of filters.

All materials placed in a beam of X-rays give rise to attenuation, and the attenuation coefficients of the materials vary markedly with the energy of the beam, as well as with the atomic number of the material. The dependence upon energy means that different parts of an X-ray spectrum will be attenuated by varying amounts, and filters can be used to change the energy distribution within a spectrum and therefore the quality of the radiation.

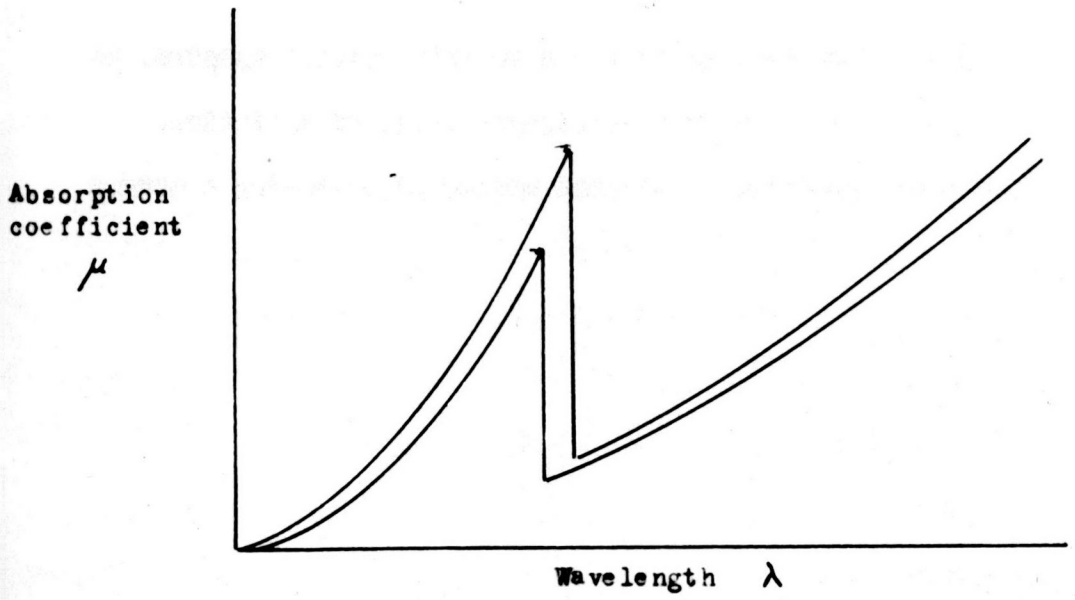

Figure 1

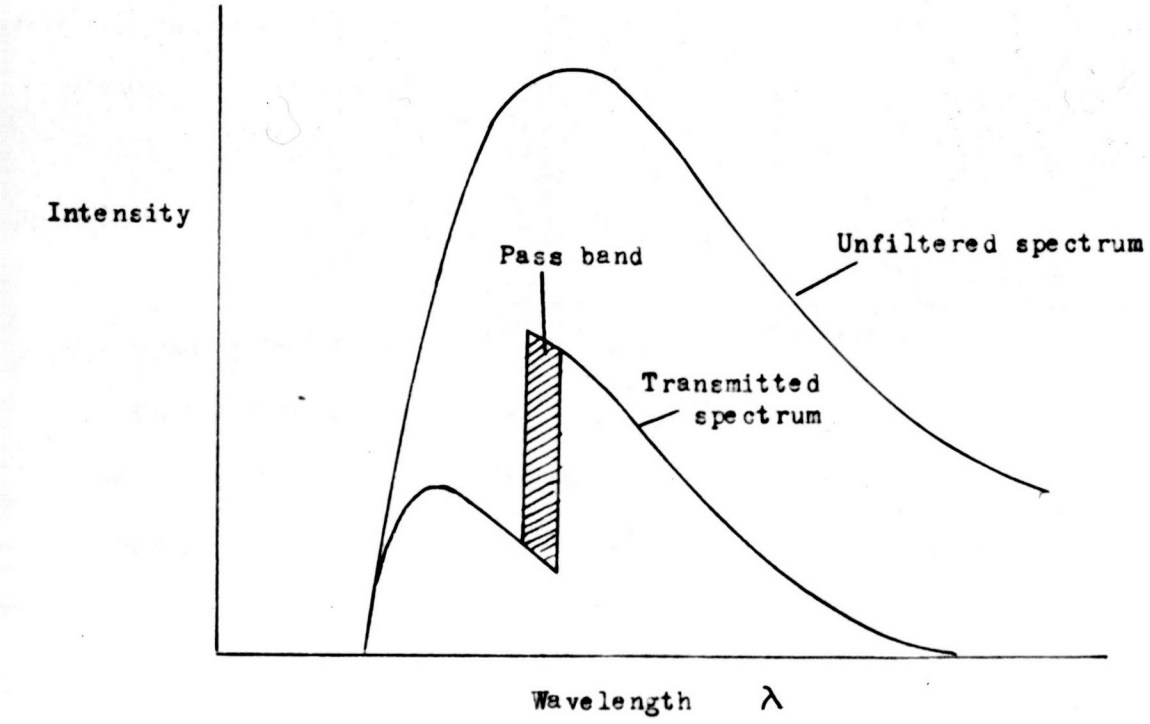

Figure 2

It is not possible, as is the case with optical spectra, to select with a single filter a narrow wavelength range of radiation. However, in 1928 Ross described an elegant method of selecting a narrow wavelength band of X-rays with balanced filters. This relies on the similarity of the attenuation coefficient-wavelength relationship of elements of adjacent atomic number over the whole wavelength range except in the immediate vicinity of an attenuation discontinuity.

The principle is illustrated in Figure 1, where attenuation coefficient is plotted against wavelength for a pair of filters, differences being exaggerated for clarity. If the thicknesses are chosen correctly, transmitted spectra should be identical for all wavelengths except those lying within the narrow band between the absorption limits, as is shown in Figure 2. If measurements made with one filter in the beam are subtracted from those obtained with the other, any differences must be due to wavelengths between the absorption limits. The degree of monochromatism thus obtained is sufficient for many studies, and the "resolution" obtainable is better than that offered by the gas proportional counter or scintillation spectrometer, while the intensity or sensitivity obtainable is much greater than is found with crystal diffraction methods.

The method has been developed and reviewed by Kirkpatrick (1939 and 1944) and applied by many workers in a variety of investigations. As an example of an application requiring the selection of narrow band of wavelengths from a general beam, Spiers (1946) used filters of silver and tin to simulate a monochromatic beam for measuring the X-ray transmission of a number of materials.

Balanced/

Balanced filters have been used to investigate characteristic X-ray production. For example, Kirkpatrick and Baez (1947) used filters of molybdenum and rhodium to isolate the Kα line of silver, Smick and Kirkpatrick (1945) used an iron-cobalt pair to study the nickel K lines, and Bendit (1958) investigated the Kα characteristic radiation from copper with nickel and iron filters. The method does not seem to have been used to study tungsten K characteristic emission, possibly because the filter elements involved are in the rare earth series, and until fairly recently were not obtainable in sufficient quantity and purity at a reasonable price. The use of balanced filters in the present study is described in Chapter 3.

(d) Theoretical calculation.

The final method to be considered in order to relate characteristic to continuous X-ray production is the theoretical one. Many attempts have been made to explain and predict the production of X-rays under various operating conditions. It is probable that neither the theories nor the fundamental data are sufficiently accurate to permit precise appraisal of the parameters in which we are interested. Nevertheless, it seemed worth while to develop a theoretical approach in order to examine the importance of various factors. The results are presented in Chapter 4.

CHAPTER 2

Proportional Counter Measurements

2.1 Assessment of possible performance

As mentioned in the introduction, a proportional counter was first considered as a means of examining the K-characteristic radiation from tungsten and its dependence on tube voltage and filtration only in a relative manner. Subsequently a method was devised of calibrating the counter with a radioisotope source, which made it possible to relate the characteristic radiation to the total exposure rate in the beam.

Before embarking on the construction of a counter, some consideration was given to the performance that could be expected. First consider the resolution that might be obtainable. The spread in pulse height distribution is governed in theory by fluctuations inherent in the mechanism of detection and multiplication, namely the statistical fluctuations in the initial number of ion pairs formed by radiation of a given energy, and the size of the avalanche in the multiplication process. Gatrousis, Heinrich and Crouthamel (1961) have shown that the relative standard deviation of the output pulse size

$$\frac{\sigma_p}{\bar{P}} = \frac{0.16}{E^{\frac{1}{2}}}$$

where E is the energy of the radiation expressed in keV. For 60 keV

$$\frac{\sigma_p}{\bar{P}} = 2.1\%$$

and the resolution expressed as full width at half maximum

$$= 2.36 \frac{\sigma_p}{\bar{P}} = 4.9\%$$

In/

In addition to the theoretical limitation of resolution, there may be other practical factors in the design and construction of the counter and in the associated electronic equipment which increase the spread in pulse height distribution. The best experimental values for resolution at about 60 keV are around 6% (Bisi and Zappa (1955), West and Bradley (1957), Gatrousis and Crouthamel (1961)). Such a resolution should be adequate to separate the Kα from the Kβ lines of tungsten, though not, of course, the $K\alpha_1$ from the $K\alpha_2$.

The next matter to be considered is the efficiency of detection to be expected. This is determined by the photoelectric absorption coefficient of the filling gas. The absorption in 5 cm of three inert gases at atmospheric pressure at various photon energies is given in Table 1.

TABLE 1

	% absorption in 5 cm of		
keV	Argon	Krypton	Xenon
10	35	53	99
20	5.5	60	50
40	1.0	15	52
60	0.32	5.5	22
80	0.14	2.5	12
100	0.08	1.5	7

It will be seen that the absorption decreases rapidly with increasing photon energy, and that, as the absorption coefficient is nearly proportional to Z^4, there is a big difference between the gases. Argon is a relatively inefficient detector of the 60 keV characteristic radiation from tungsten, but then we have a high intensity available in the X-ray beam,

and/

and are likely to be embarrased by too high, rather than too low a count-rate.

Another factor enters into the choice of counting gas, namely the presence of "escape peaks". If an incident X-ray photon ejects an electron from the K shell of the counter gas, the photoelectron produced will have an energy $E_p = E_i - B_k$, where E_i is the energy of the incident photon and B_k the binding energy of the K shell electrons. The photoelectron is immediately absorbed in the counter gas. The K shell vacancy is filled by the transition of an electron from an outer shell. The excited atom then reorganises either by the emission of an X-ray or an Auger electron. In the latter case the total ionization produced by the photoelectron and the Auger electron is detected and a pulse corresponding to the full energy of the incident X-ray quantum appears.

On the other hand, if reorganisation is by the emission of a K X-ray quantum, characteristic of the counter gas, only the photoelectron energy E_p will be detected unless the K quantum is itself absorbed by the photoelectric process in the L or M shells of the gas. Since materials are relatively transparent to their own K radiation, these last interactions are somewhat unlikely. The probability that an ionized atom reorganises by the emission of an X-ray is determined by the fluorescence yield. This varies markedly with atomic number, being 0.11 for argon, and 0.85 for xenon. Thus with an argon filling, escape peaks are barely noticeable, whereas with xenon they predominate. The difference between the energies of the full and escape peaks is equal to the energy of the K X-ray of the gas, 2.9 keV for argon, 34 keV for xenon. The argon escape peak is barely resolved, while for krypton and xenon it is quite separate. With xenon, especially, the escape peak is much larger than the full energy peak. This complication

may/

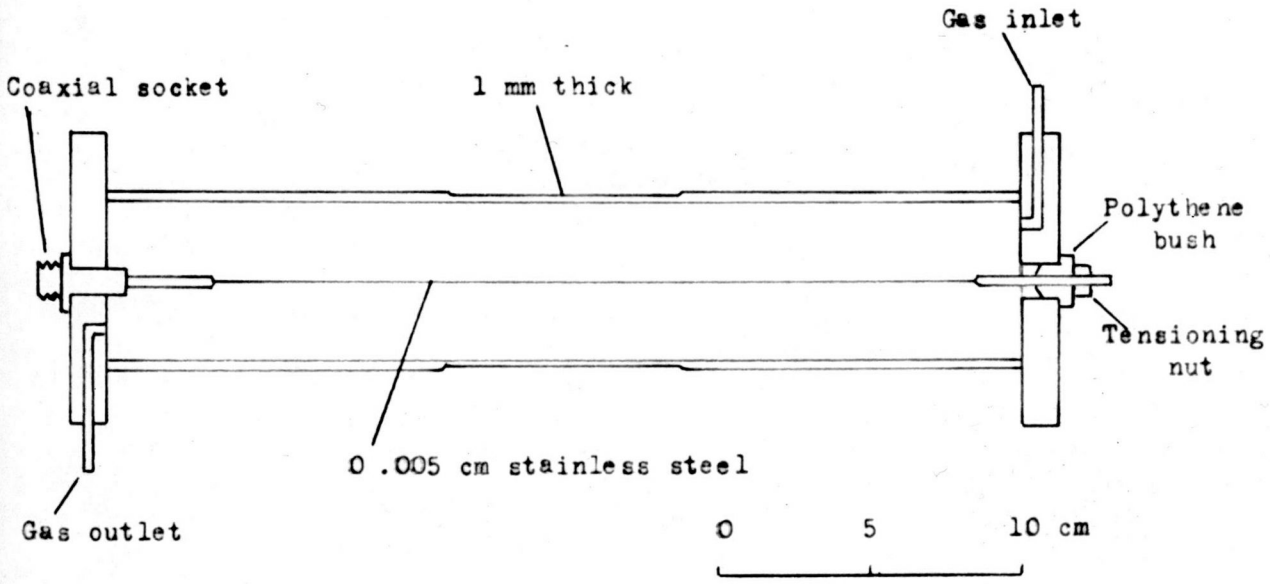
Gas inlet
Coaxial socket
1 mm thick
Polythene bush
Tensioning nut
0 .005 cm stainless steel
Gas outlet
0
5
10 cm

Figure 3

may make the interpretation of spectra difficult.

A final consideration in the choice of counter gas is cost. Argon is relatively inexpensive and can be used in a flow system. Krypton and xenon are much too expensive for this and can only be used in sealed counters. This in turn places greater demands on constructional methods and limits the materials that can be used.

As pure inert gases exhibit some metastability, an impurity whose ionization potential is less than that of the inert gas is usually added to stabilize the multiplication process. In the counter to be described, the filling used was a mixture of 90% argon and 10% methane.

2.2 Description of counter constructed

Most proportional counters have been constructed of metal. However, Gatrousis, Heinrich and Crouthamel (1961), have pointed out the advantages of low atomic number materials, notably the absence of fluorescent X-ray production. The counter constructed for this investigation is similar to one described by them, but differing in detail to incorporate materials readily available. The main features are illustrated in Figure 3.

The body consists of a Perspex tube, 30 cm long and 5.4 cm internal diameter. The central position is reduced in thickness to approximately 1 mm to reduce attenuation of the incident X-rays (calculations show that attenuation of 60 keV X-rays is 1.7%, of 10 keV X-rays 20%). The tube is cemented with Araldite at each end into grooves turned in Perspex end plates, into which are drilled holes for the entry and exit of the counting gas. The central electrode consists of a stainless steel wire 0.005 cm in diameter, stretched between a standard coaxial socket at one end

and/

and a screwed rod at the other. The latter serves to apply tension, and is housed in a polythene bush. The ends of the central electrode are effectively thickened by 3 mm brass rods; this lowers the electric field strength and reduces end effects. The length of the counter also ensures a uniform field distribution over the central portion used for X-ray detection. The inside of the tube is rendered conducting by a coating of colloidal graphite.

The pulses produced in a proportional counter are quite small (in our case approximately 1 mV) and a fair degree of amplification is needed. This was provided by a Dynatron linear amplifier, type 1430. In the early stages of the investigation a variety of auxilliary apparatus was used to determine the pulse height distribution. The final arrangement used for the X-ray spectra was to feed the pulses from the amplifier to an Isotope Developments Ltd. type 1750 ratemeter. This has a built-in pulse height analyser and provision for a recorder output. The recorder used was a Record recording milliammeter. The ratemeter was modified slightly to permit external control of the bias voltage, and this was provided by attaching a pair of precision potentiometers to the driving mechanism of the recorder. In this way the bias voltage could be swept in synchronisation with the recorder chart. The synchronisation was not changed when the recorder speed was altered; the latter could be achieved by changing gear ratios.

The counting gas, 90% argon + 10% methane, was passed through a bubbler after leaving the counter, and the internal pressure thus maintained slightly above atmospheric. On first operating the counter a fairly long flushing period was required, but subsequently this could be reduced/

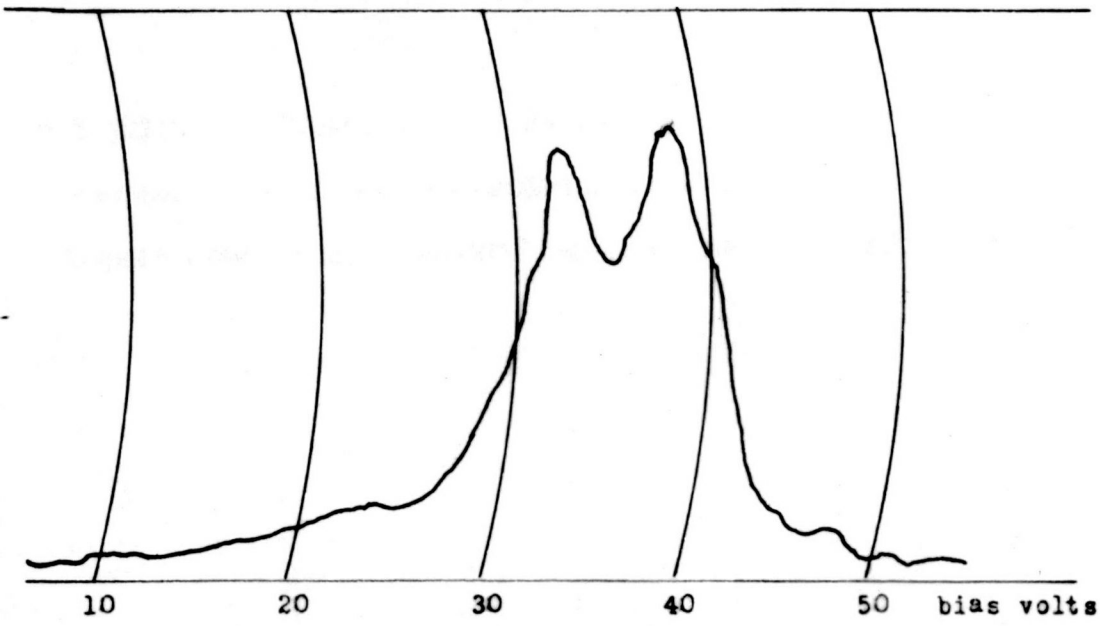

Figure 4. L characteristic radiation from lead excited by 80 kVp X-rays

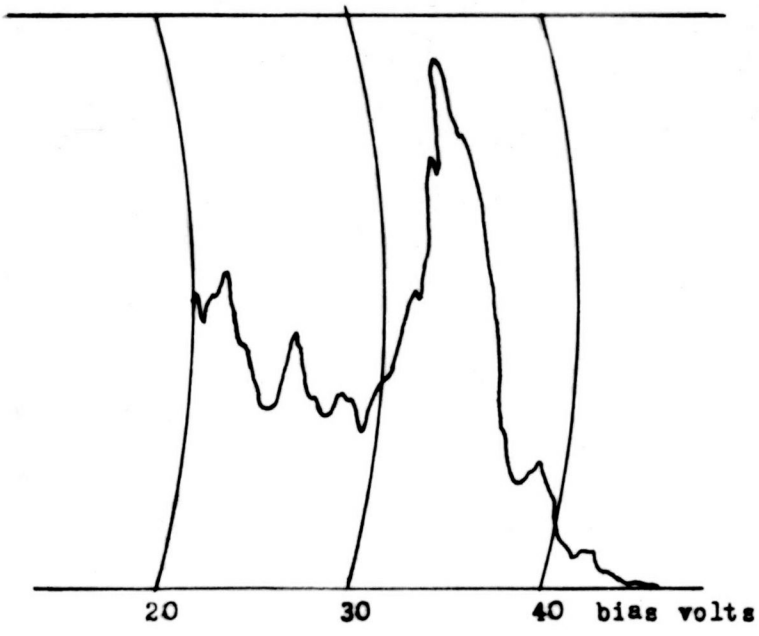

Figure 5. K characteristic radiation from tungsten excited by 140 kVp X-rays

reduced to a few minutes. For the best stability, however, flushing for at least half an hour was desirable and resolution continued to improve even after that. Flow rates of about two bubbles a second were adequate after the flushing period at a higher rate.

2.3 Tests of counter

Early tests of the counter were made with radioisotope sources. The 14 keV γ ray from cobalt-57 was well displayed, while the 122 keV peak, although 15 times as abundant, did not appear, illustrating the marked reduction of counting efficiency with increasing energy. A thallium-204 beta source was used to excite characteristic radiation from tungsten and lead. The L lines appeared and the α and β groups were well resolved. The source was not sufficiently active for the K lines to give good peaks.

Most valuable as a source was the isotope americium-241. It has a long half-life and its principal γ-ray has an energy of 59.6 keV, very close to the Kα emission of tungsten. A resolution of 8% could regularly be obtained for this peak.

The X-ray apparatus first used in conjunction with the proportional counter was a General Electric KX-10 medium voltage therapy set operating up to 140 kVp and 5 mA. It was quite simple to use the X-rays to excite fluorescent radiation from tungsten and other materials, and now the K characteristic was displayed, as well as the L lines. These are illustrated in Figures 4 and 5. Examination of the direct beam posed more problems. The chief difficulty was that of the relatively enormous intensity of the beam. Proportional counters have much shorter resolving times than Geiger-Müller counters (approximately 1 μs) but there is a limit to the count-rate that can be recorded. In our case the limit was set more by the associated electronic/

electronic apparatus than the counter itself. The most dramatic illustration of the saturation that arises was the way the recorded count-rate apparently decreased with an increase of X-ray intensity.

There was a limit to the extent to which distance could be used to reduce intensity, as the counter could not be placed further than 3½ metres from the X-ray tube. Recourse was therefore made to collimation. At the counter the beam was limited by a lead diaphragm, and at the tube by a pinhole. At first a hole made by a number 80 drill (0.34 mm diameter) was used, but later a smaller hole was obtained (approximately 0.2 mm) by inserting a length of wire in the hole, hammering the lead around it and then withdrawing it.

An attempt was made to assess the saturation count-rate of the counter together with its associated apparatus, using the β radiation from two thallium-204 sources. The larger was placed at a number of distances to get different count-rates and the effect of the addition of β rays from the other source on the count-rate noted. The reduction of the effect of the addition was then an indication of saturation. The result was not necessarily directly applicable to the X-ray case as there were pulses below the threshold of the bias control that could still contribute to saturation, and there might well be a different proportion of these in the two cases. However, it seemed that saturation could be avoided by keeping the total counting rate above the threshold below 10,000 c/s.

The counter was shielded with lead to limit detection to the centre portion, where it was controlled by various apertures in lead sheet. It was found that there was still an appreciable response when the direct beam was blocked at the tube pinhole, indicating that leakage of radiation through/

through the tube housing could not be ignored in comparison with the very low exposure rate in the direct beam necessary to avoid saturation. This was overcome by encasing the tube housing in a further 3 mm thickness of sheet lead.

A number of factors influenced the choice of scanning speed of the bias voltage, channel width of the pulse height analyser and time constant of the ratemeter. The narrower the channel width, the better the resolution that could be expected. On the other hand, since the total count-rate was limited by saturation considerations, a narrow channel width gave rise to a low counting rate, with more statistical fluctuations. These could be minimised by operating with a longer time constant, but this in turn called for a slow scanning speed in order to avoid distortion of the trace. A limit was set to the latter by the stability of the tube output. A variety of operating conditions was tried, particularly in the earlier stages, before the bias control was coupled to the recorder. Scanning was then manual, and although synchronisation was not so accurate, it was possible to experiment with different ratios of scanning speed to recorder speed. Typical conditions were: ratemeter range 30 or 100 c/s., time constant 5 s, scanning speed 1 V/10 s , chart speed 1 in/min, giving a relationship of 6 V/min and a scan time from 5 - 50 V of 7.5 min.

2.4 Calibration of counter with americium-241 source

Attempts were next made to quantitate the measurement of the Kα characteristic peaks in relation to the total radiation, using the americium-241 source of nominal activity 1 mc. The principal γ-ray lines of ^{241}Am are given by Strominger, Hollander and Seaborg (1958) as: 26.4 keV, 3.3%,

33.2 keV/

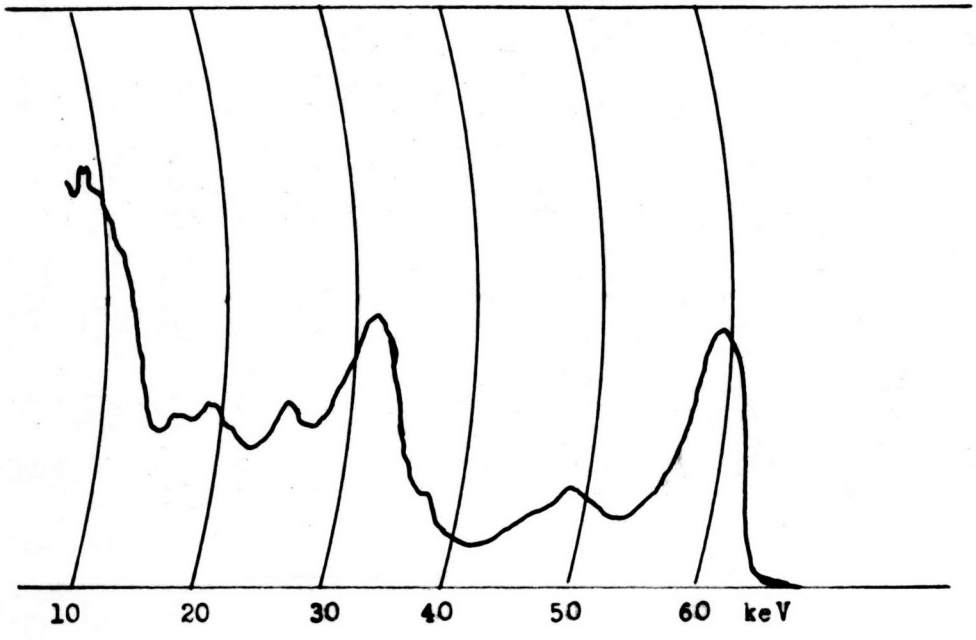

Figure 6. Spectrum of 1 mc source of americium-241

33.2 keV, 0.2%, 43.5 keV, 0.24% and 59.6 keV, 40%. There are also the L X-rays of neptunium, and West (1953) shows the principal energies to be approximately 13, 17 and 21 keV. It will be seen that the predominant feature of the spectrum is the line at 59.6 keV. This is very close in energy to the Kα characteristic lines of tungsten, $K\alpha_1$ 59.4 keV and $K\alpha_2$ 58.2 keV. Thus if the exposure rate from the 59.6 keV americium radiation could be determined at the counter and related to the area under the observed peak on the chart, this relationship could be used to calibrate the area under the tungsten Kα peak in terms of exposure rate and thence compare it with the total radiation in the beam measured by some other means.

The spectrum of americium-241 as observed with the proportional counter did not agree exactly with the figures quoted above, and it was felt that the anomalies should be cleared up before attempting to determine the exposure rate corresponding to the 59.6 keV peak. A sample of the spectrum is shown in Figure 6, and it will be seen that there are two unexplained peaks, a prominent one at 31.5 keV, and a smaller one at about 50 keV.

The source consisted of a solution of 1.5 ml volume, and was still in the glass bottle in which it had been delivered from the Radiochemical Centre. It seemed possible that the strange peaks might be due to the excitation of fluorescent radiation in the material of the bottle. Consideration of the elements that would give rise to characteristic radiation of these energies showed that the 31.5 keV peak might be due to barium or caesium, though both were unexpected. The higher energy peak would have to arise from one of the rare earths and this seemed improbable.

The americium solution formed too large and ill-defined a source

for/

for accurate calibration of the counter, so it was decided to concentrate it and transfer it to a smaller vessel offering less attenuation of the γ-radiation. A portion of the solution was pipetted into a small polythene vial and evaporated slowly by leaving it in a dessicator under reduced pressure. Then more solution was added, until all had been transferred, together with several rinsings from the bottle. Checks were made at each stage on the amount of activity in each vessel. The final volume was approximately 0.1 ml.

The americium-241 spectrum now appeared very different. As expected, the lower energy peaks were now very much enhanced relative to the 59.6 keV peak. More important was the disappearance of the 31.5 keV peak. This supported the idea of fluorescent emission from the bottle, and it was possible to demonstrate the peak again by using the bottle as either a "transmission" or "reflection" source, with excitation by the americium-241. To check on the element concerned, a polythene bottle was filled with barium hydroxide and used in place of the bottle as a "reflector". A fluorescent peak was produced, agreeing with that from the bottle to within the resolution of the counter.

There remained the peak at 50 keV. It was found that this could be produced also by "reflection" from the empty bottle. In addition, a variety of other materials, which could not give fluorescent radiation of this energy, led to its appearance. It was eventually realised that it must be due to Compton scattered radiation. There is a maximum intensity of Compton photons when the scattering angle is 180°, and then the energy of the scattered photon is

$$E_o \Big/ 1 + \frac{E_o}{510} \quad (1 - \cos \phi)$$

where/

where E_o is the energy of the incident photon in keV. For E_o = 60 and ϕ = 180°, scattered energy = 49 keV.

Although the lower energy lines appear prominently on the measured spectra, owing to the greatly increased absorption in argon, the 59.6 keV line will dominate as far as exposure rate is concerned. However, the specific gamma-ray constant (Γ) is a minimum at 60 keV and rises quite considerably at lower energies, so the lower energy emissions will contribute more to air ionization than their relative abundances would indicate. Thus, although the 26.4 keV line has an abundance of 8% of that of the 59.6 keV line, the variation of specific gamma-ray constant with energy leads to it being 26% as effective in giving rise to ionization current. In order to produce a more nearly monochromatic radiation, therefore, it was necessary to attenuate the lower energy lines by filtration. Calculation showed that 0.5 mm copper or 1 cm aluminium would attenuate the 26.4 keV line to 1% or less of its original intensity, while halving the intensity of the 59.6 keV peak. 0.25 mm copper reduces the 26.4 keV line to 2.6%, and the 59.6 keV line to 68%, although the increase in Γ means that the lower energy line may be no longer negligible. These calculations were confirmed by measuring spectra with absorbers placed between the americium source and the counter. 0.25 mm copper suppressed the 26.4 keV peak almost entirely, while 0.5 mm copper did so completely.

2.5 Calibration of 1 mc americium-241 source

Having established that a virtually monochromatic beam of 59.6 keV energy could be obtained, the next step was to deduce the exposure rate at a given distance from the source. The activity was not known with sufficient accuracy/

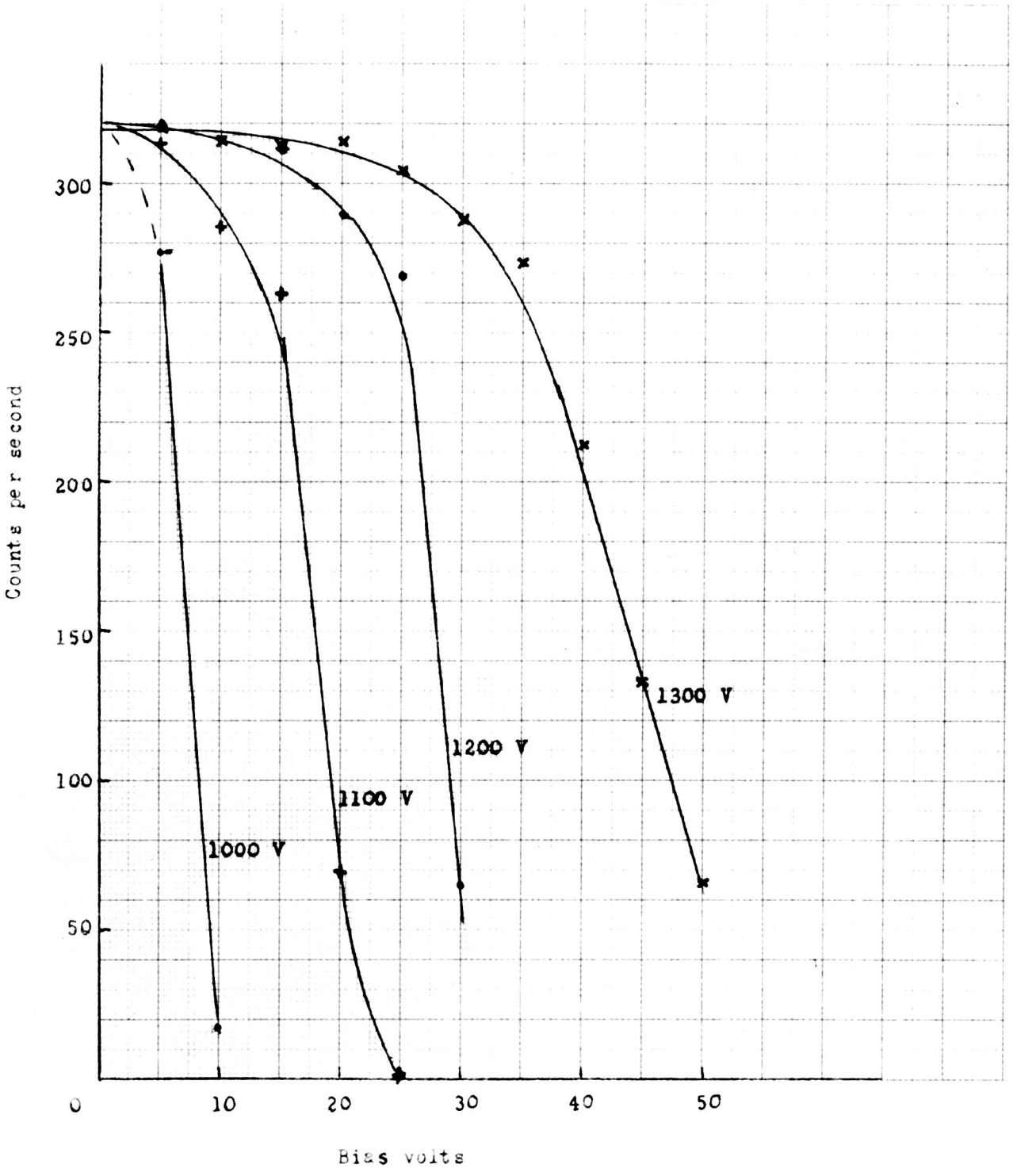

Figure 7. Count rate from americium-241 source with defined solid angle geometry.

accuracy to permit direct calculation. Nor was the activity sufficient to permit measurement by ionization chamber. The method chosen was calibration of the effective disintegration rate by defined solid angle γ counting, relating this to the exposure rate with a calculated value of the specific gamma ray constant.

The detector chosen for the calibration was a sodium iodide crystal 2.5 cm thick, coupled to a photomultiplier tube. This thickness was sufficient to give complete absorption of the gamma ray. The solid angle through which radiation was detected was defined by a hole 1.07 cm in diameter placed over the crystal, and 30 cm from the source. A filter of 0.57 mm copper was interposed to eliminate the lower energy radiation. The photomultiplier was connected to an amplifier and scaler and count-rates determined for a variety of settings of bias and E.H.T. voltage. The results are plotted in Figure 7. The curves were extrapolated to zero bias voltage.

The count-rate obtained has to be corrected for attenuation of the γ-ray in the crystal mount. This is stated by the manufacturers to be of 0.022 in thick duralumin. This aluminium alloy contains approximately 4% copper and 0.5% manganese, which increase the attenuation coefficient. Making allowances for these inclusions, the attenuation of 60 keV radiation is to 0.925. Thus the measured count-rate of 320 c/s becomes corrected to 346 c/s. The solid angle subtended by the hole

$$= \frac{1.07^2 \times \pi}{4 \times 30^2}$$

and the effective disintegration rate

$$= \frac{4\pi \times 4 \times 30^2}{1.07^2 \times \pi} \times 346$$

$$= 4.35 \times 10^6 \text{ d.p.s.}$$

This corresponds to

$$\frac{4.35 \times 10^6}{3.7 \times 10^7} = 0.118 \text{ mc}$$

(allowing for the 40% abundance of the 59.6 keV line and absorption in the copper filter, this represents an activity of 0.69 mc). Γ for 60 keV is given by Johns (1961) as 0.34 R/hr/mc at 1 cm. We have, therefore, 0.34 x 0.118 R/hr at 1 cm, or 0.67 mR/min.

2.6 Preliminary measurements with KX-10 set

As mentioned previously, preliminary X-ray measurements were made with the KX-10 set. As the beam defined by a pinhole near the tube was non-uniform at the detector position 3.5 m away, it was decided to define the beam further by an aperture in a lead sheet, placing alternately the proportional counter and an ionization chamber behind it. With the smallest pinhole already described, it was possible to use an aperture of 0.5 in without causing saturation of the counter.

To measure the total exposure rate of the beam passing through the aperture, one of the ionization chambers designed for the balanced filter measurements, to be described in Chapter 3, was used. The ionization current was measured with an Isotope Developments Ltd. vibrating reed electrometer, type 1880. This instrument has a maximum sensitivity of 10 mV full scale, and it was necessary to pass the ionization current through a resistor of $10^{12}\Omega$ in order to obtain a reasonable reading. The combination of 0.5 in aperture and ionization chamber were calibrated against a Baldwin-Farmer dosemeter at a relatively high exposure rate by removing the pinhole and

operating/

operating at 50 cm from the tube focus.

2.7 Operation with Siemens 250 kVp set

While some results were obtained with the KX-10 set, the maximum voltage of 140 kVp limited the range, and stability of operation of the set was not as good as might be desired. All subsequent measurements were carried out with the Siemens set. The Siemens Stabilipan has a nominally constant potential generator giving a maximum tube voltage of 250 kVp and current of 15 mA.

Initially a similar arrangement to that adopted with the KX-10 set was used, namely a fixed aperture and alternate measurements with the counter and ionization chamber. Some difficulty was experienced in obtaining a sufficiently low intensity to avoid saturation of the counter. Pinhole pictures showed that the focal spot was square, with bands of relatively high emission near two parallel edges and less emission in the centre. This central portion was therefore used, a 1 mm pinhole being placed at 13 cm from the tube focus, the beam limited further by a 5 mm aperture at 50 cm and the detectors used at 4 m, the greatest distance that could be achieved. A hole of diameter 0.25 in served as the aperture over the detectors.

2.8 Optimum conditions for counter

Before further X-ray measurements with the proportional counter, the operating conditions were varied in order to determine the optimum. The parameters to be varied were the high voltage on the counter, the attenuation used in the amplifier and its differential and integral time constants, and the channel width of the pulse height analyser. Some of these are interrelated,

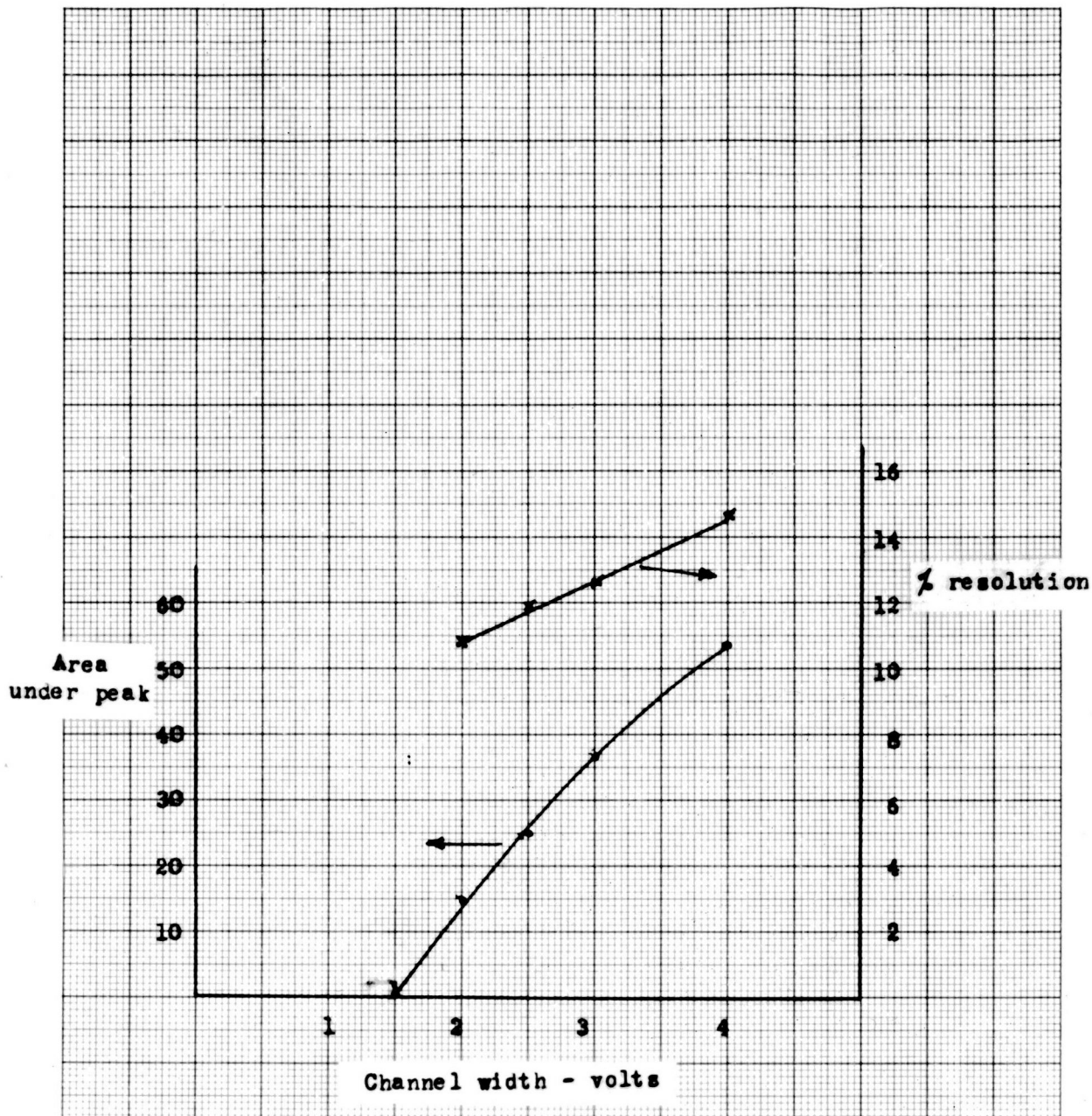
Area under peak
60
50
40
30
20
10
16
14
12
10
8
6
4
2
% resolution
1
2
3
4
Channel width - volts

Figure 8

as the amplification factor has to be lowered when the high voltage is increased in order to maintain the required relationship between photon energy and bias voltage. The effects to be studied were the resolution and sensitivity of the counter. It is obvious that good resolution is desirable. There is a limit to the degree to which sensitivity can be sacrificed in favour of resolution, as the total count-rate is limited by the possibility of saturation, and statistical considerations determine the lowest acceptable count-rate within the analyser channel.

The americium-241 was set up over the counter and the various parameters already mentioned varied in turn. The chart recorder with the coupled bias sweep was used to display the spectrum of the 59.6 keV peak. The area under the curve was measured to establish sensitivity and its width at half maximum height to assess resolution. As a result it was found that best results were obtained with the amplifier attenuation set at 20 dB (the full gain of the amplifier with its associated head amplifier was about 120 dB) and both differential and integral time constants at 1.6 μs. Under these conditions a high voltage of 1600 V was required to place the 59.6 keV peak at approximately 30 V on the bias scale. There was no clear-cut optimum setting of channel width, as resolution only improved as sensitivity was lowered. The results are illustrated in Figure 8. It will be seen that the setting of the channel width on the analyser was obviously in error. It was finally decided to operate at a nominal channel width of 3 V, corresponding probably to a real width of 1.5 V.

Since it was necessary when using the americium source for calibrating the counter to have it fairly close (less than 5 cm) to the aperture in order to get a reasonable sized peak on the chart, it was

essential/

essential that the effective distance should be known accurately. To this end, spectral scans were performed with different distances between the bottom of the source holder and the top of the lead sheet. Peak areas on the chart were measured and an inverse square law plot gave a straight line and indicated that the effective distance was 1.5 cm more than that measured.

The gearing used to couple the chart recorder to the bias potentiometers did not lead to an integral relationship between bias voltage and distance on the chart. In any case there was a possibility that the relationship might not be quite linear. Accordingly the recorder was run with the bias sweep operating and the time taken for the bias to change by 5 V measured with a stop watch. This was repeated over the whole of the bias range; the times could then be converted to distance on the chart. There was a slight departure from linearity. A graph was constructed which could be used to convert distance on the recorder chart into bias voltage.

For X-ray scanning it was found that a chart speed of 1 in/min gave reasonable results when a ratemeter time constant of 1 sec was used. If a time constant of 5 sec was necessary (for example when a lower count-rate range was used) the chart speed was lowered to 0.5 in/min in order to avoid distortion of the trace. At the higher speed a scan over the full bias range of 5 - 50 V took just over 5 min.

During a long run with the counter there was some drifting of peak position. This would alter the effect of the channel width in terms of photon energy and might be expected to alter the area under the peak. In order to correct for this, a series of scans was carried out with the

americium source, the peak position being deliberately varied by changing the E.H.T. A plot of peak area against peak bias voltage then served to correct the observed X-ray peak areas.

2.9 Ionization chamber for measuring total exposure rate

To measure the total exposure rate the same ionization chamber as before was used behind the 0.25 in aperture. Once again it was necessary to use a $10^{12}\Omega$ resistor with the I.D.L. electrometer. This made the time constant very long and a single measurement of exposure rate took about half an hour.

In order to calibrate the ionization chamber it was placed behind the same 0.25 in aperture alongside the chamber of a Baldwin-Farmer dosemeter at approximately 60 cm from the focus of the Siemens tube. The pinhole was removed. The ionization current was now very much higher, of course, and a resistor of $10^{9}\Omega$ was used with the electrometer. The value of this resistor, and of the $10^{12}\Omega$, was measured with an A33B resistance measuring unit attached to an E.I.L. Vibron 33B electrometer. The Baldwin-Farmer dosemeter had itself been calibrated against a standard instrument at different values of beam half-value-layer and so a calibration chart for the experimental chamber could be drawn up.

The sequence of measurements of the characteristic radiation was to carry out a series of scans with the proportional counter behind the aperture, followed by an americium calibration, then the ionization chamber measurements at a series of X-ray energies. Finally another americium calibration was followed by a repeat of the X-ray spectral scans.

2.10 Improved technique of operating with Siemens set

Some/

Some results were obtained with the technique described. However, it was realised that there were drawbacks to the method. The very long time constant of the electrometer made measurements tedious and it was difficult to be sure that the final voltage reading had been reached. Accuracy of measurement of the ionization current was also not high when lower X-ray tube potentials were being used, as the potential across the high resistance was then less than 10 mV. It was also a disadvantage not to be able to measure the characteristic radiation with the proportional counter simultaneously with the measurement of the total radiation in the beam by the ionization chamber. Reliance had to be placed on the constancy of output of the X-ray set, and although this was well stabilised, it was realised that it would be preferable for the measurements to be simultaneous.

The consideration which had prompted the use of a fixed aperture with alternate placings of the two detectors behind it was the possible non-uniformity of the beam, consisting as it did of a portion of the pinhole image of the focal spot. This was investigated further by exposing a film at the detector position 4 m from the target with the pinhole at 13 cm in place, but the diaphragm at 50 cm removed. The whole focal spot image was then about 28 cm square and it appeared that the centre of this area offered a large enough beam of sufficient uniformity to accommodate both detectors at the same time. This was further investigated by making measurements with the ionization chamber (with no limiting aperture) at different positions within the area of interest. The exposure rate did not vary by more than a few percent.

Accordingly, a fresh aperture was placed at 50 cm from the target, $^{3}/_{4}$" x $^{1}/_{2}$" in size, over the central part of the focus image. This included

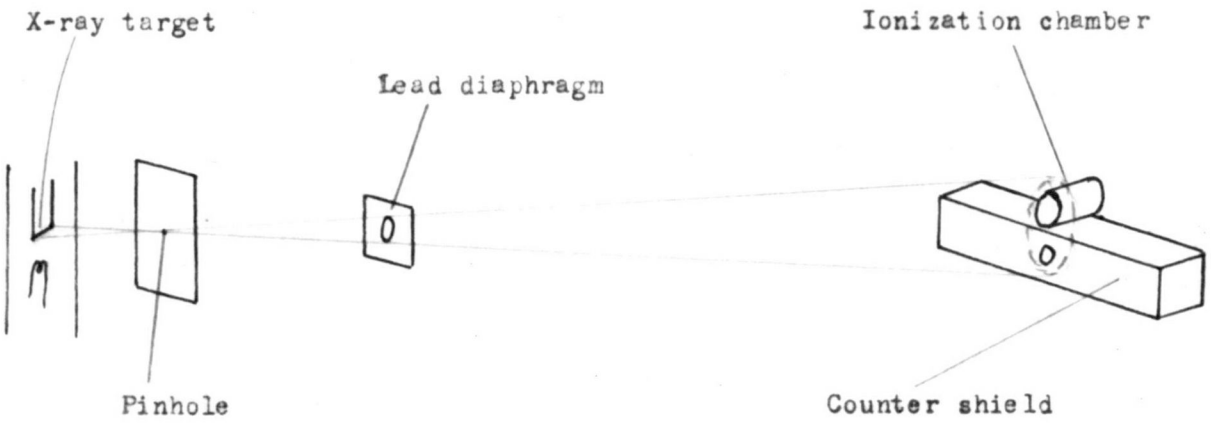

Figure 9

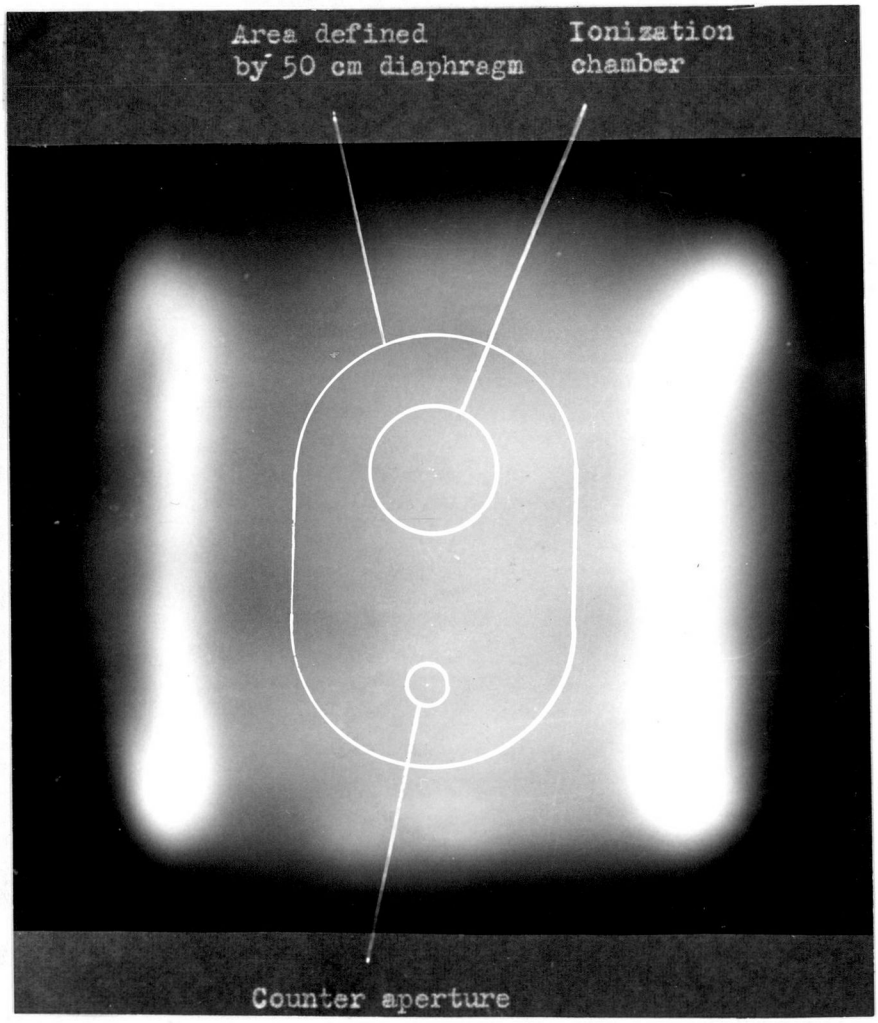

Figure 10. Image of the focal spot at 150 cm from the target

the uniform relatively low intensity part of the image, excluded the higher intensity "bars" at the edges, and produced a beam, 17.5 x 12 cm at 4 m capable of including both detectors. The ionization chamber, without any limiting aperture, was arranged alongside the proportional counter. The arrangement of the apparatus is illustrated in Figure 9, while Figure 10 shows an image of the focal spot at 150 cm from the target, with the beam defined by the 50 cm diaphragm indicated, together with the positions of the detectors. The positioning of the detectors was set by fluoroscopy or the use of a G.M. counter and checked by exposing films before and after a series of measurements.

As the full volume of the ionization chamber was now being used, the ionization currents were higher, and it was possible to reduce the resistance to $10^{11}\Omega$. An aperture of 1.6 cm diameter over the counter was found to be suitable, the ratemeter range was 300 c/s, its time constant 1 s, and the chart speed 1 in/min. The time constant of the electrometer was such that for a given setting of tube voltage and current, two proportional counter spectral scans could be carried out while an ionization current determination was made. Calibration of the ionization chamber against the Baldwin-Farmer dosemeter was carried out as before, this time the electrometer resistance being reduced to $1.25 \times 10^{8}\Omega$.

2.11 Calibration of 100 mc americium-241 source

At this time a more active source of americium-241 became available. This was a standard Radiochemical Centre sealed source of nominal activity 100 mc. This was ideal for calibration purposes, the source, of active diameter 0.72 cm, being contained in a housing with a front face of stainless steel/

steel 0.3 mm thick. This attenuated the lower energy radiation markedly, although examination with the proportional counter showed that there was still some present. Virtually monochromatic radiation was obtained by the addition of a copper filter 0.57 mm thick. The higher activity meant that the source could be further from the counter aperture during calibration (distances of 15 to 25 cm were used), increasing the accuracy. As before, scans were performed with the range of nominal distances, an inverse square law plot leading to the effective separation of source and aperture. More important, the higher activity enabled a different means of assessing the exposure rate due to the 59.6 keV γ-ray to be used.

This method involved direct measurement with an ionization chamber. The source, with a filter of 0.57 mm copper, was arranged at a given distance from the side of the 35 cc ionization chamber which was normally used with an E.I.L. type 37A dosemeter. Since the latter was not sufficiently sensitive to measure the ionization current, the chamber was connected to the I.D.L. 1880 electrometer, fitted with a resistance of $10^{11}\Omega$. A range of distances from 4 to 10 cm between the copper filter and the side of the chamber was used and an inverse square law graph plotted to determine the effective separation. In fact, this was close to the distance between the centre of the chamber and the estimated centre of the source.

The ionization chamber was then calibrated. First, the half-value-layer of the filtered americium γ-ray beam was determined and found to be 0.50 mm copper. Then the operating conditions of the KX-10 X-ray set were altered until a beam of the same half-value-layer was obtained. This occurred at 120 kVp with a filter of 0.57 mm copper. Then this quality was used to calibrate the E.I.L. chamber against the Baldwin-Farmer dosemeter,

a/

a resistance of $10^9\Omega$ being fitted in the electrometer.

The exposure rate for the filtered americium source deduced from these experiments was 40.6 mr/min or 2.43 r/hr at 1 cm, from which exposure rates at other distances could be calculated. Using the figures for specific gamma ray constant and abundance already mentioned in section 2.5, and allowing for attenuation in 0.3 mm stainless steel and 0.57 mm copper, an activity of 61 mc was deduced, as compared with the nominal activity of 100 mc. However, it is to be expected that there would be appreciable self absorption in the source itself, which would account for this discrepancy. The drawing supplied by the Radiochemical Centre suggests a source thickness of 1 mm , while calculations of the specific activity show that, owing to the long half-life, there must be at least 27 mg of element present, having a very high absorption coefficient at this energy.

As a check on these measurements, a defined solid angle calibration was carried out for the new source in the same way as for the smaller one. A 1 in sodium iodide crystal was again used as detector, the distance between source and aperture this time being 200 cm. The deduced exposure rate at 1 cm was 2.43 r/hr and the calculated activity 61 mc, in excellent agreement with the ionization chamber measurements.

This last calibration enabled the effective activities of the two americium sources to be compared, a ratio of 65:1 being obtained. A more direct comparison was also made with a scintillation counter detector and a ratio of 61:1 established.

2.12/

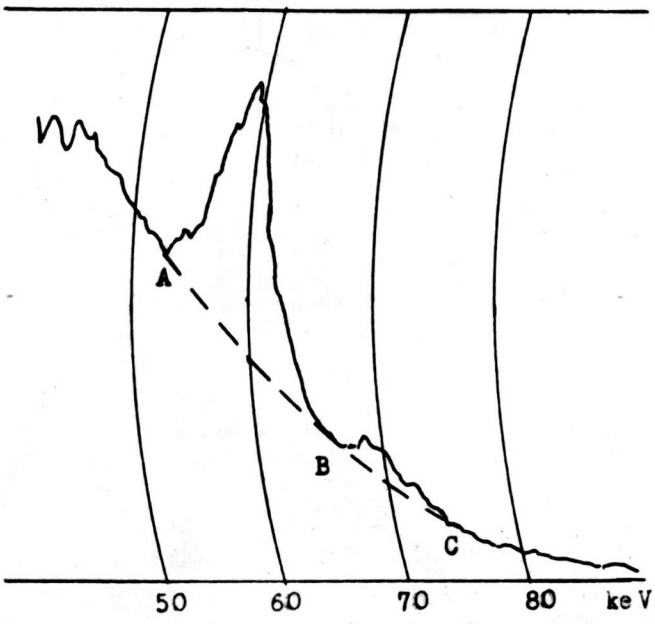

Figure 11

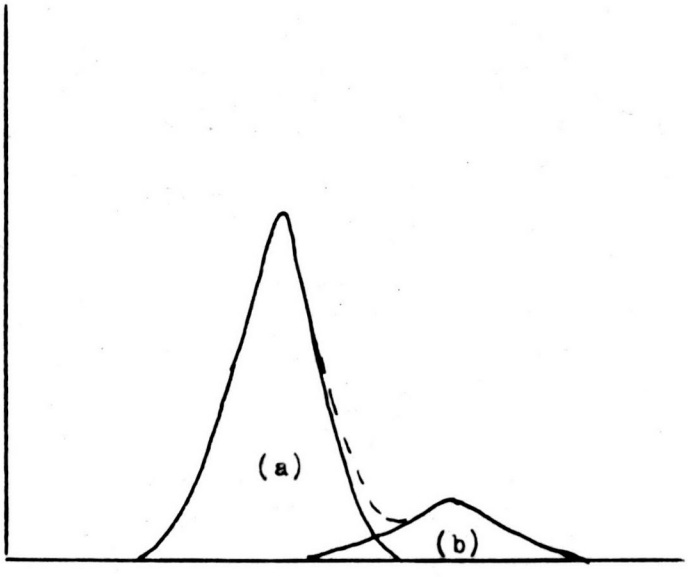

Figure 12

2.12 Interpretation of X-ray pulse-height distribution

We must now consider the interpretation of the X-ray pulse-height distribution and the derivation of the area of the Kα peak from it. A typical chart is shown in Figure 11. In order to determine the base line it is tempting to draw in the line A B C , but some calculations show that this is not justifiable. The situation is perhaps best illustrated by synthesising a spectral distribution. As a starting point we may represent the Kα peak by an experimentally determined americium-241 spectrum, as shown at (a) in Figure 12. In this case the resolution was 8%. The X-ray peak will be slightly wider, owing to the 1.2 keV separation of the $K\alpha_1$ and $K\alpha_2$ peaks, which are, of course, not resolved. The position of the Kβ peak is easily determined from the relationship between photon energy and bias voltage. The height of this peak requires further consideration. Beckmann's (1955) figures for the relative intensity of the various lines of the tungsten characteristic radiation give a ratio of Kβ/Kα of 0.31. In addition, the counter is less sensitive to the higher energy radiation. Using values of the photoelectric absorption coefficient of argon, we get a sensitivity ratio of 0.66 for the energies of the Kβ and Kα lines. These two factors lead to a ratio of 0.20 for the areas of the Kβ and Kα peaks. The width of the Kβ peak will be greater than that of the Kα in terms of bias voltage, since the percentage resolution is the same, and therefore its height will be correspondingly less. Incorporating this effect, we find that the height of the Kβ peak is 0.18 that of the Kα, and again using the americium spectrum we can draw in the Kβ peak. This is shown at (b) in Figure 12 as is also the combination of the two peaks. If this is now superimposed on an assumed curve for the continuous radiation (Figure 13)

a/

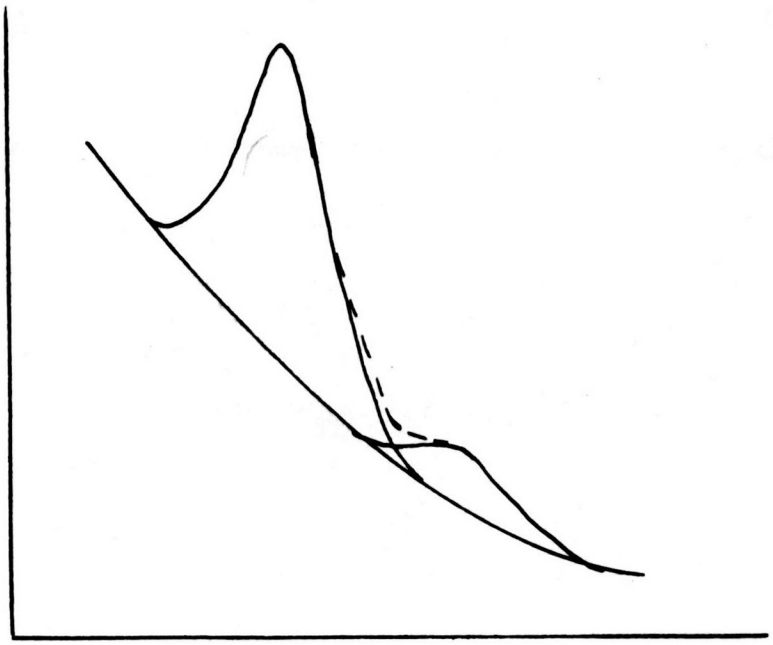

Figure 13

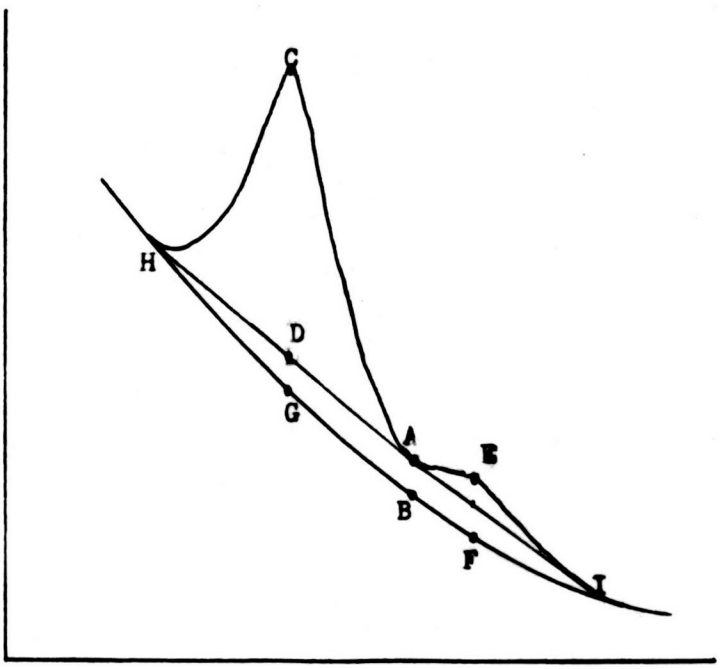

Figure 14

a scan very like that observed experimentally with X-rays is obtained. It is clear that as the two peaks are not completely separated, the baseline cannot be simply drawn.

It is of interest to calculate the resolution needed to achieve complete separation of the peaks. Taking 1% of the peak height as the limit, and assuming a Gaussian distribution, separation just occurs if the resolution is 5.5%. This is close to the theoretical limit of resolution of a proportional counter at this energy, and unlikely to be achieved in a practical instrument. Similar calculations show that the degree of overlap will be such that there will be interference with the peak height itself if the resolution is worse than 12%. This should not happen with our counter.

Several possible methods of deducing the position of the baseline were considered. The first involved the use of the synthetic model deduced above. A line is drawn to join the minima in the curve, as H A I in Figure 14. The height from this line to the Kα peak is measured, C D. Other distances on the model, such as D G , A B and E F , are measured, and the relationships between them and C D established. Then on the experimental X-ray curve C D can be measured and the other distances deduced, giving sufficient points to draw in the baseline curve H G B F I.

One disadvantage of this method is that the relationships depend on the resolution of the counter, which is somewhat variable, and to a lesser extent on the shape of the baseline curve which varies a good deal with tube voltage and filtration. In addition, owing to statistical fluctuations, it is difficult to establish the position of point A accurately. This method was therefore not pursued further.

It/

It was thought better to determine the baseline position by considering points on the experimental spectral scan outside the influence of the characteristic peaks and deducing the expected variation between these points. In order to be sure of clearing the peaks, energies of 50 and 80 keV were chosen as the reference points. The predominant factor governing the shape of the curve between these two points is the variation of photoelectric absorption of argon with energy. The other factor is, of course, the shape of the continuous spectrum itself. Over this range, the argon absorption coefficient varies with energy according to a power law, and a straight line plot is obtained on log log graph paper. If, for example, it is assumed that the true continuous spectrum is a straight line between 50 and 80 keV, the effect of the variation in absorption coefficient is to alter the picture to a curve, concave upwards, which seems very plausible as a baseline, particularly for high kVp, lightly filtered radiation. However, reflection shows that this cannot be a universal model, as filtration of the incident beam will change the shape of the continuous radiation curve. We shall return to this point after considering another matter.

2.13 Anomaly in pulse height distribution - scatter background

It was noticed that filtration of the incident beam with successive thicknesses of copper did not have the expected effect on the heights of the spectral scan, particularly at lower energies. For example, the addition of 0.9 mm copper to the unfiltered beam produced an attenuation of the 50 keV height of only about half that expected from absorption calculations. At lower energies the difference was much greater. The first possible cause of this anomaly to be investigated was the filter thickness. The filters

were/

were those used clinically with the X-ray set and were made up of copper, 1 mm aluminium and a thin plastic cover. Since they could not easily be dismantled, transmission measurements were made with radiation of different energies. The larger americium source with 0.57 mm copper filter provided a monochromatic beam of 59.6 keV. The source was then used to excite characteristic radiation from barium (32 keV) and erbium (49 keV). In all cases there was good agreement between the observed and the calculated transmission. This confirmed the correctness of the stated filter thicknesses, and also the contention that filtration should have a predictable effect on the heights of an observed spectral scan.

The reason for the observed anomaly was suggested when higher energy radiation, from iodine-131, was used to simulate the continuous spectrum. It was found that filtration had no appreciable effect on the height of the curve from 40 keV upwards. Even the addition of 2 mm lead had very little effect. Such an absorber should eliminate the lower energies completely, and it is clear that in this case the low energy part of the spectrum at least, must arise from scatter within the counter or from its housing generated by higher energy radiation capable of penetrating the absorbers with little attenuation. In the X-ray case the low energy part of the observed spectrum will be a combination of the true continuous spectrum, which will be subject to the calculated transmission of filters, and a "scatter background", much less attenuated.

The magnitude of this scatter background was estimated from the effect of filtration on the observed spectral heights. It was assumed that the scatter background was due to radiation of effective energy some 60% of the peak voltage on the tube. For example, for 250 kVp, an effective

energy/

energy of 150 kVp was taken. This is little attenuated by the filters used, to 0.92 for 0.4 mm copper and to 0.81 for 0.9 mm copper. This small degree of attenuation means that the value assumed for the effective energy of the radiation producing the scatter background is not critical. It is then necessary to calculate the attenuation of the true continuous radiation component of the beam at the energy considered, and adjust the proportions of the true continuous and background components until the sum fits the experimentally observed heights. An example is shown in Table 2 where the height of the curve at 50 keV is considered for an accelerating potential of 250 kVp.

TABLE 2

Filter	% transmission		Attenuation of background	Deduced %			
	Observed	Calculated		Scatter		True	
2 mm Al	100	100	1	12	+	88	= 100
0.5 mm Cu	46	39	.92	11	+	35	= 46
1 mm Cu	20.5	12	.81	10	+	10.5	= 20.5

It is seen that, although the scatter background is relatively unimportant for a beam with no additional filtration, when the total filtration is 1 mm copper, the scatter background contributes half the totalheight of 50 keV. There were some other conditions of aperture size and pinhole in which the scatter background was even higher. Similar manipulations were carried out to assess the scatter background at 80 keV, and it was found to be much less important.

2.14/

2.14 Derivation of baseline curve in spectrum

Having established the heights on the curves at 50 and 80 keV, corresponding to the true continuous spectrum and the scatter background, it remains to derive the baseline curve at intermediate energies, which again will be made up of two components. In this derivation a number of requirements must be met:

(1) the curve must look right, i.e. it must blend smoothly with the experimental curve below 50 keV and above 80 keV,

(2) the areas of the Kα and Kβ peaks must be in the right relationship,

(3) the areas of the Kα peak measured with different filtrations of the beam must agree with calculated transmissions,

(4) the effect of filtration on the true continuous spectrum must also follow calculation.

It is necessary to make some assumption about the shape of the scatter background curve and the effect of filtration upon it. It is also necessary to assume a shape for the true continuous spectrum; the validity of this assumption can then be tested by considering the requirements above. Any failure to meet these requirements will lead to modifications of the proposed curve until all points are satisfied.

The only clue to the shape of the scatter background curve came from the spectra derived with the proportional counter from heavily filtered high energy radiation such as that from iodine-131. These suggested that the curve was concave upwards, but not as much as would arise from an exponential/

exponential distribution between the end points. Accordingly a shape between a linear and an exponential curve was chosen and seemed to fit in reasonably well with the other requirements.

As a starting point for the derivation of the proportional counter curve corresponding to the true continuous spectrum it was assumed that the spectrum for unfiltered radiation was a straight line. The variation of argon absorption coefficient with energy modified this to the curve that would be found on the proportional counter record in the absence of scatter background. The effect of filtration on this curve was then calculated, scatter background added and the requirements (1) - (4) investigated. Under some operating conditions it was clear that the curve obtained was too concave upwards, i.e. that the true continuous curve should be concave downwards in this energy range, which might be expected from known spectral shapes. In this case a useful assumption was a power law variation of the total continuous plus scatter radiation. The scatter could then be subtracted and the effect of filtration calculated.

Once the baseline was established, the Kα and Kβ peaks were drawn in where they overlapped, bearing in mind the information obtained from the synthesis of the curves already discussed. The areas between these peaks and the baseline were then measured with a planimeter. As calculated previously, the Kβ area was only one fifth of that of the Kα peak, and it could not be determined very accurately, especially as the curve was subject to statistical fluctuations. However, its measurement did provide a useful check of the baseline position, as in criterion (2) already discussed. The area of the Kα peak was the item of chief interest. Before considering the final assessment of its variation with operating voltage and filtration in comparison/

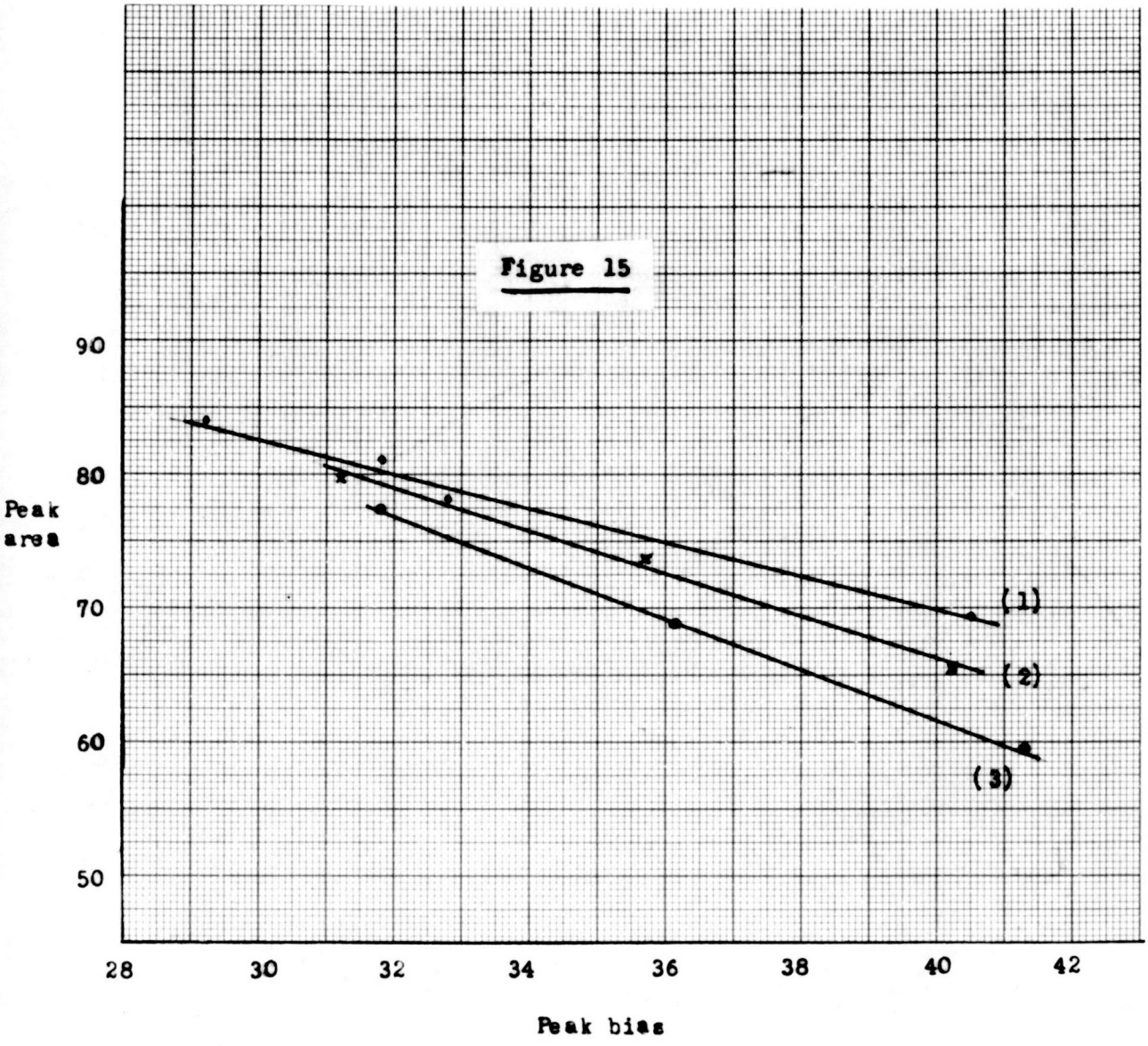
Figure 15
90
80
70
60
50
Peak area
28
30
32
34
36
38
40
42
Peak bias
(1)
(2)
(3)

comparison with the total exposure rate, we must deal with some further anomalies that came to light during the course of a series of measurements.

2.15 Variation of sensitivity of counter

It was found that results for the ratio of peak area/total radiation from experiments performed on two different occasions agreed well at lower energies, but diverged as the energy increased. The ionization chamber results agreed well, and the most likely explanation seemed to be that there was a progressive change of sensitivity of the proportional counter throughout one, at least, of the measurements, which were quite prolonged. It has already been described how peak area was found to vary as peak bias voltage drifted and how corrections were made for this. These corrections were derived from scans of the americium-241 peak at different counter voltages performed at some stage during the X-ray measurements. However, these scans had been performed only once or twice on a given day, and it now appeared that there might be a sensitivity variation over and above that arising from peak bias voltage changes.

This possibility was investigated by scanning the americium-241 spectrum at a number of settings of counter voltage at intervals after the counter was first operative. The results are illustrated in Figure 15, where the area under the peak is plotted against peak bias voltage. It is seen that there is, indeed, a drift of counter sensitivity over and above that due to any change of bias voltage. This might be due to changes in the associated electronic equipment, but more likely to the counter itself, where variations in gas flow and progressive removal of gaseous or vapour impurities might play their part. To combat this drift, calibrating scans

of/

of the americium peak were performed at frequent intervals during subsequent X-ray investigations. Even greater variations of sensitivity were found on occasion.

2.16 Discrepancy in ionization chamber measurements - improvement in pinhole

The next discrepancy came to light when results obtained with the proportional counter were being compared with those from the filtration method to be described in the next chapter. While the values for the ratio of peak to total radiation were in general similar as derived by the two methods, there was a noticeable difference in the shape of the curve relating this ratio to tube operating voltage. To determine which parameter was responsible for the difference, the graphs of variation of total exposure rate and peak exposure rate with tube voltage as measured by the two techniques were separately compared, normalisation being effected at one particular point. The curves for peak exposure rate against voltage at several different filtrations agreed well. On the other hand, if the total exposure rate curves were matched for low tube voltages, they diverged progressively for higher voltages, the values of exposure rate determined during the proportional counter experiments rising more steeply above about 170 kVp.

This finding was rather surprising, as the same ionization chamber was used to measure total exposure rate in both series of experiments. The differences between the two series were that the filtration measurements were performed with the chamber in the full beam at about 65 cm from the target, while those in the other series called for beam restriction by the pinhole, and an operating distance of 400 cm. To test whether the increased operating distance was the cause of the discrepancy, due to attenuation of the lower energy components of the radiation by the intervening air, a series of

measurements/

measurements was made with the ionization chamber at different distances from the tube, but without any severe collimation of the beam. When the results were normalised at 250 kVp and 2 mm aluminium total filtration, there was a slight difference between the exposure rates at 65 and 400 cm at voltages below 200 kVp and for the unfiltered beam. There was no difference for beams filtered with 0.5 or 1 mm copper. Air filtration was not, therefore, the cause of the anomaly.

It seemed, therefore, that the use of the pinhole was introducing the observed effect. The thickness of the lead used for this pinhole was 0.6 cm, and calculation showed that a transmission of approximately 0.02% could be expected for 250 kVp radiation. Since the pinhole limited the proportion of radiation proceeding in a direction perpendicular to the tube axis to about 0.15%, it seemed that the penetration might be something like 10% of the "useful" beam. This was checked experimentally by using the ionization chamber in its normal position at 400 cm. Measurements were made with the pinhole in its usual position and then with a sheet of lead 0.6 cm thick in the same place. The exposure rate in the latter case at 250 kVp was 11% of that with the pinhole operating. While this confirmed the calculated figure, it was not sufficient to explain the discrepancy altogether, especially as the measured transmission of the 0.6 cm lead was very much less at 220 kVp.

It was then noticed that the pinhole was damaged. The tube side of the hole had been burred over, reducing the opening considerably, but leaving a thin edge. This would be relatively opaque to low energy radiation, but increasingly transparent as the voltage increased. This explained the anomaly satisfactorily. A new pinhole was made, still with a 1 mm diameter hole, with the ends countersunk to avoid further damage. The thickness was

increased/

increased to 1.2 cm to avoid any penetration.

When this pinhole was put into use with the ionization chamber and proportional counter set-up as before, it was found that the count-rate and exposure-rate were much higher, as might be expected. It was necessary to reduce the aperture over the counter to 0.9 cm diameter. When suitably normalised the ionization chamber measurements now agreed well with those obtained during filtration measurements.

2.17 Another anomaly in spectrum - random coincidences

On calculating the results of the proportional counter measurements it was found that the scatter background at 50 keV was now less than previously observed, probably as there was less high energy radiation relative to that in the 50 - 80 keV band. However, yet another oddity now appeared. It was found that the 80 keV heights of the spectral curves were apparently more subject to attenuation by copper filtration than calculations suggested. It is possible that this phenomenon may have been present previously, but masked by greater scatter background, which leads to an apparently lower attenuation.

In contradistinction to the cause of the scatter background, it seems that part, at least, of the spectral height at around 80 keV must arise from lower energy radiation. This could only happen if there were summation of effectively coincident pulses arising from the finite resolving time of the counter and its associated amplifier. The counting-rate in the lower energy ranges of the spectrum was certainly very much higher than in the region of interest, owing to the greater efficiency of the counter at lower photon energies. The appearance of random coincidences varies as the square of the count-rate.

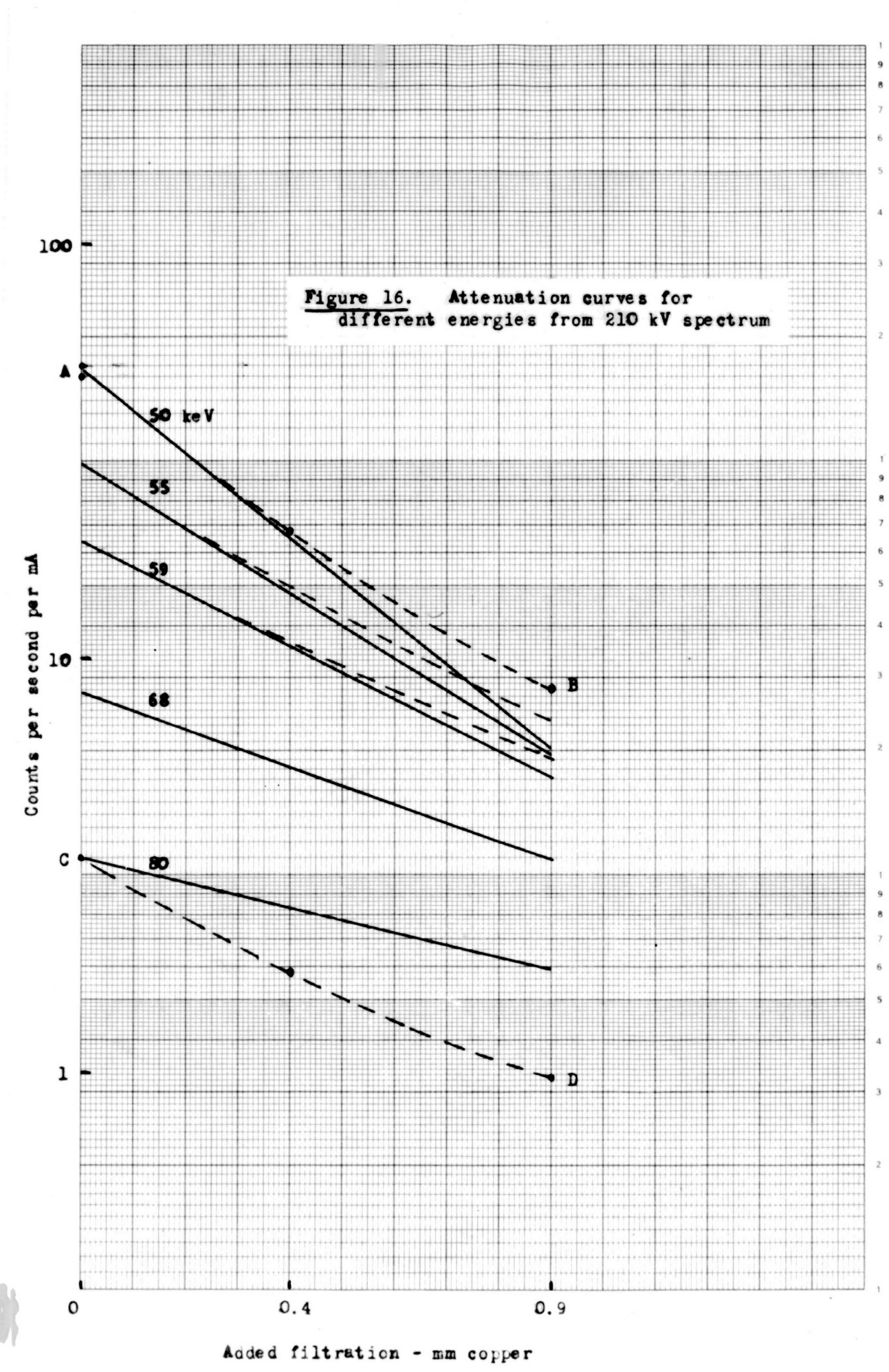

Figure 16. Attenuation curves for different energies from 210 kV spectrum

This explanation was investigated with the larger americium-241 source. This was placed at different distances from the counter to vary the count-rate, and it was found that when the count-rate in the peak was greater than about 1000 c/s, there was indeed a high energy "tail" to the spectrum, ending, as one would expect, at twice the peak bias. The effect of copper filtration on one such spectrum was investigated. The peak was set at a bias of 19 V and the peak count-rate at approximately 5000 c/s. At a bias voltage of 35 V, corresponding to 108 keV, the count-rate was 42 c/s. The addition of 0.57 mm copper reduced the count-rate at 35 V bias to 10.5 c/s. This attenuation to 25% is characteristic of 50 keV radiation for this thickness of filter. Thus the presence of easily attenuated radiation at the 80 keV point on the X-ray spectrum is explained.

2.18 New method of derivation of baseline curve

The existence of this phenomenon, manifesting itself as an apparent change in scatter background from positive to negative as higher energies were considered, made it difficult to apply the method previously described for the derivation of the baseline position. A different empirical approach was therefore made, though retaining the same criteria of acceptability. A power law variation of height of the baseline with photon energy was assumed for the unfiltered radiation. Then attenuation curves were plotted for a number of different energies, as illustrated in Figure 16. The calculated attenuation was drawn in at each energy, and the observed values at 50 keV (A B) and 80 keV (C D). The deviation from the calculated figures was then shared out between the intermediate energies. The results were cross plotted on log-log paper to smooth them and the peak areas measured.

Finally/

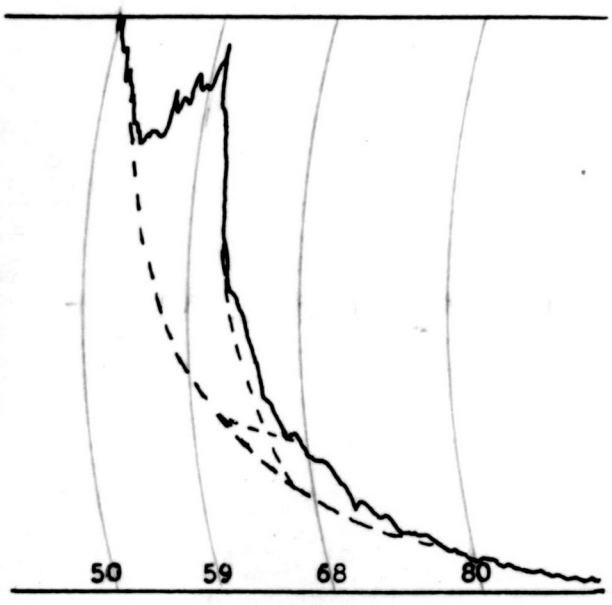

210 kVp, 5.8 mA, 2 mm Al
total filtration

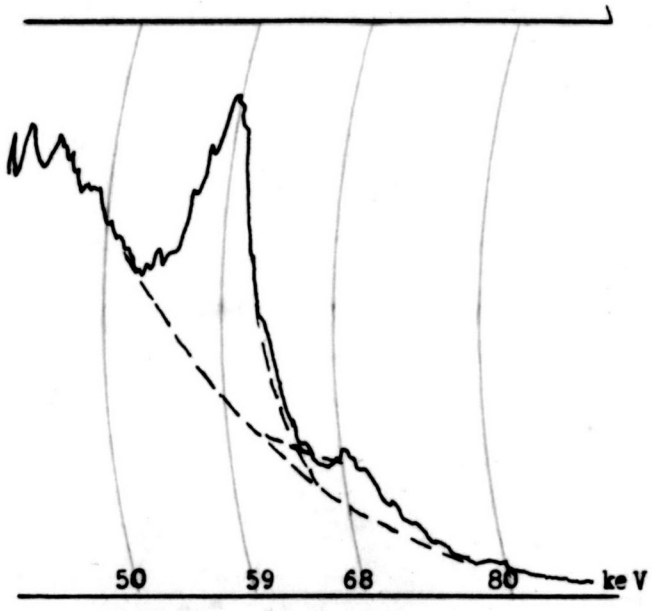

210 kVp, 9.5 mA, 0.5 mm Cu
total filtration

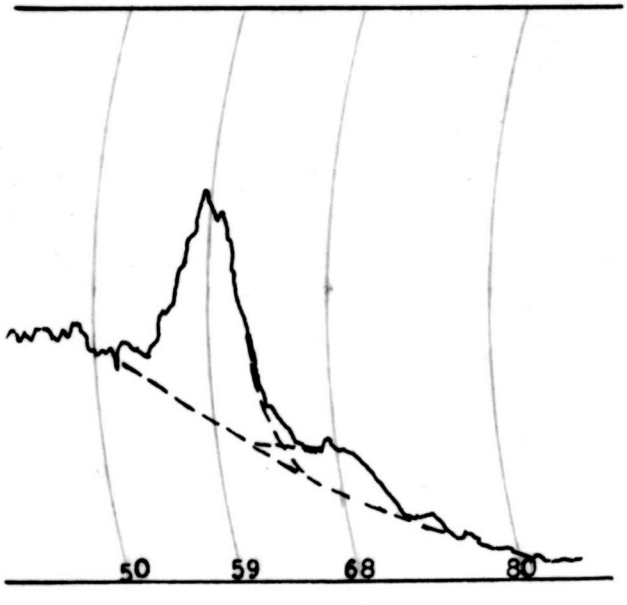

210 kVp, 14.5 mA, 1.0 mm
total filtration

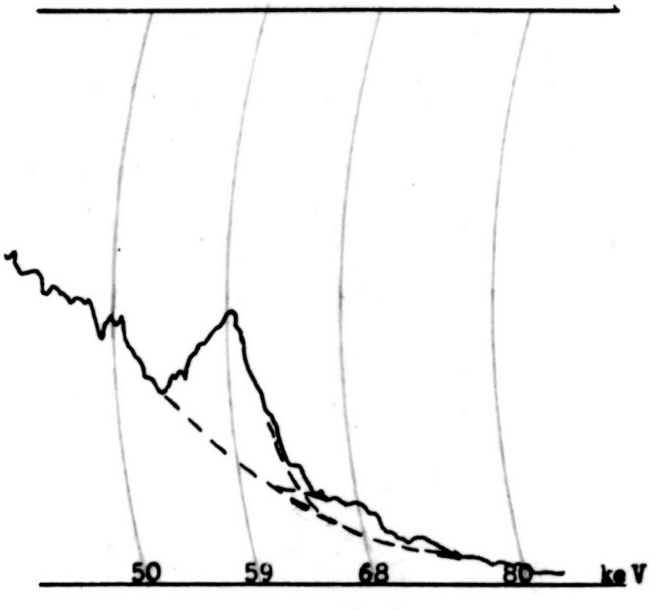

130 kVp, 14.5 mA, 0.5 mm Cu
total filtration

Figure 17

Figure 18

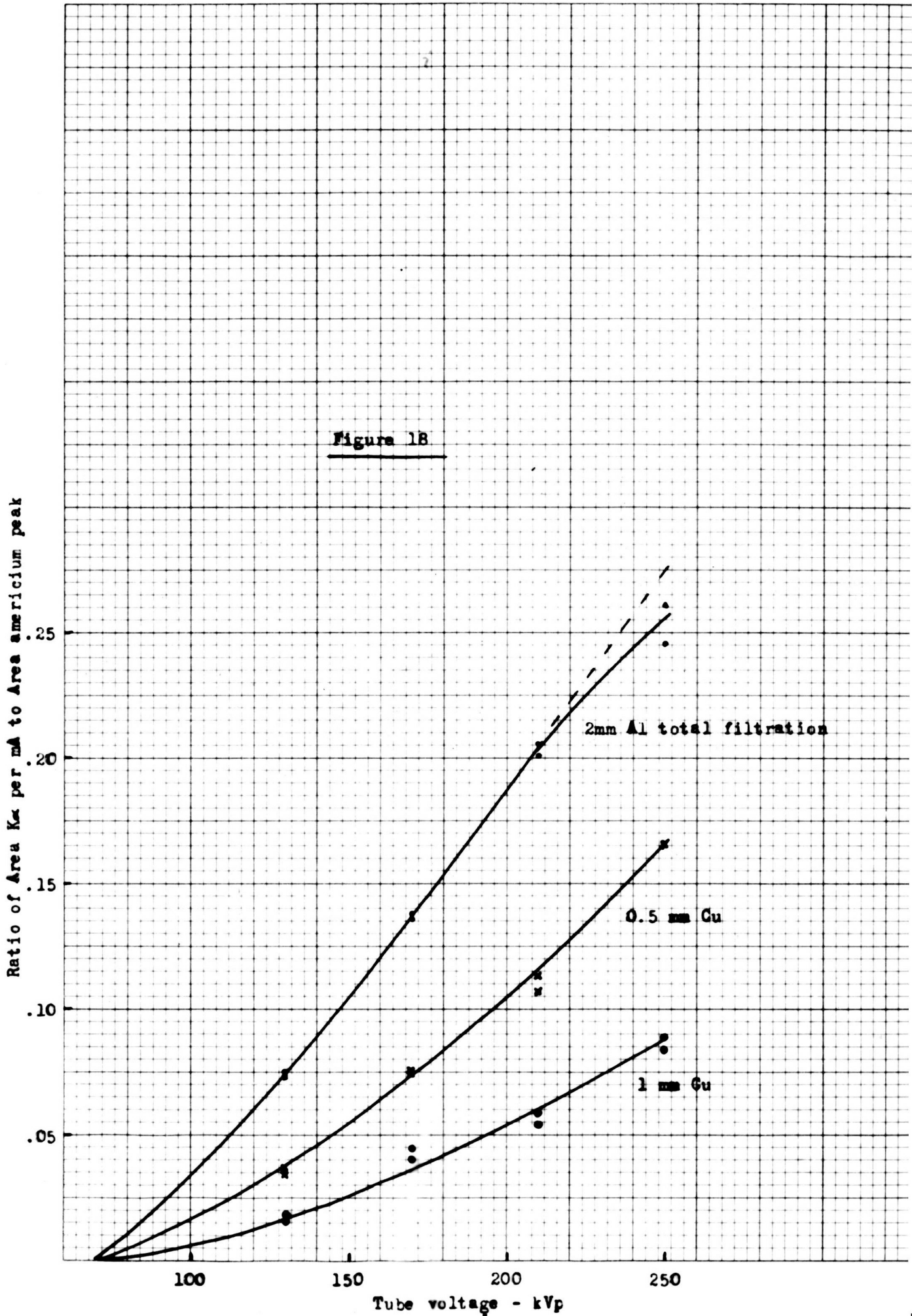
Ratio of Area Kα per mA to Area americium peak
.25
.20
.15
.10
.05
2mm Al total filtration
0.5 mm Cu
1 mm Cu
100
150
200
250
Tube voltage - kVp

Finally, adjustments were made to give the right ratio of peak areas and the right attenuation of the Kα peak.

2.19 Results of proportional counter experiments

We may now turn to the results of the proportional counter experiments, after the various corrections had been made. A number of pulse height distributions obtained under various conditions are shown in Figure 17. In order to ensure that the 50 keV point was on the chart, while maintaining the peak area as large as possible, it was necessary to vary the tube current over the range 4 -15 mA. The results were therefore expressed as exposure rates per mA. Early measurements had shown that within the experimental error, both peak area and total exposure-rate varied linearly with tube current.

When peak areas had been measured, they were divided by the area of the appropriate americium scan for the corresponding peak bias voltage. Americium scans were performed at three different values of peak bias four times during the course of the last series of measurements and peak area plotted against peak bias for each. On this occasion there was little change of sensitivity with time; however, in each case the X-ray scan was related to the americium scan nearest in time. The variation with tube voltage of the area under the Kα peak per mA divided by the area of the americium-241 peak is illustrated in Figure 18. The americium source with its filter of 0.57 mm copper was placed at 10 cm from the aperture over the counter, and the previously determined value of the exposure rate at this distance was used to convert the area ratios into equivalent exposure rates.

The readings of the electrometer connected to the ionization chamber

were/

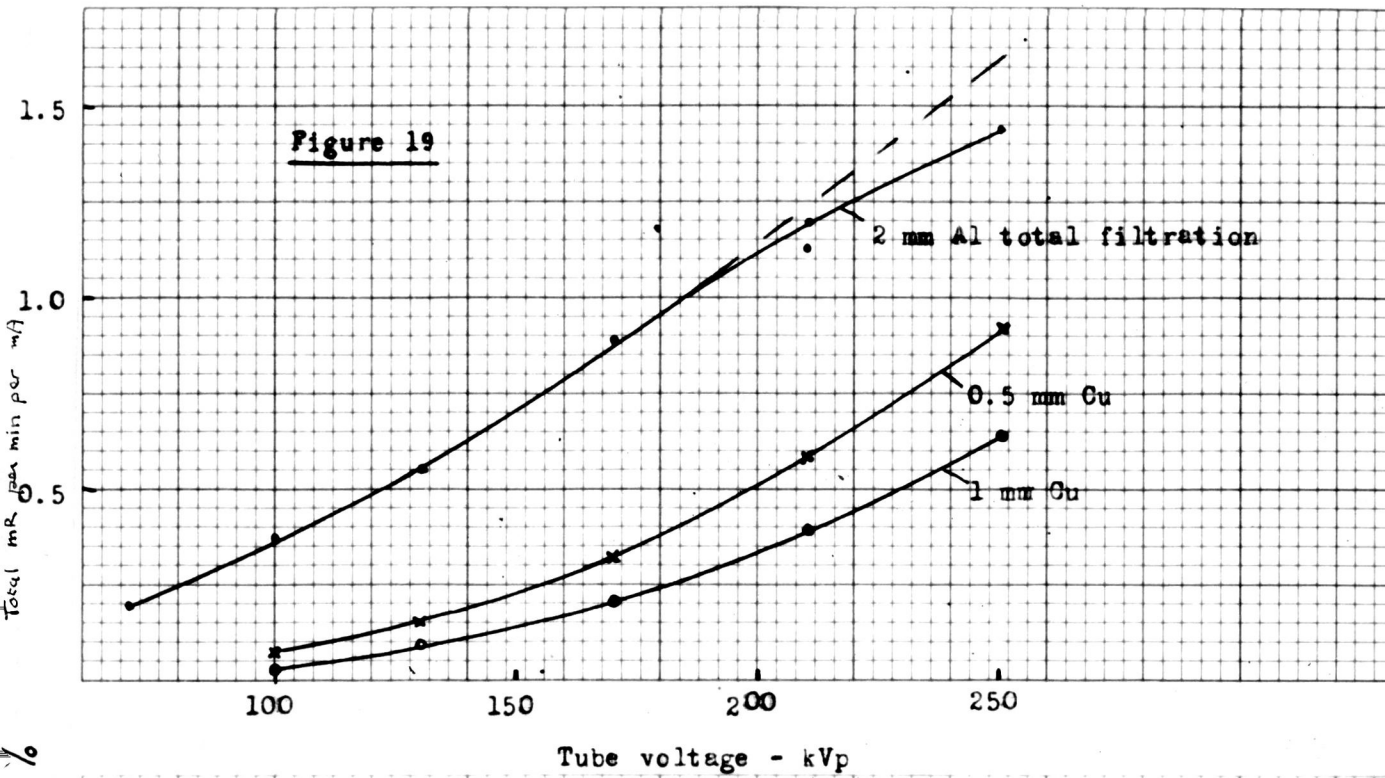
Figure 19
2 mm Al total filtration
0.5 mm Cu
1 mm Cu
1.5
1.0
0.5
100
150
200
250
Tube voltage - kVp

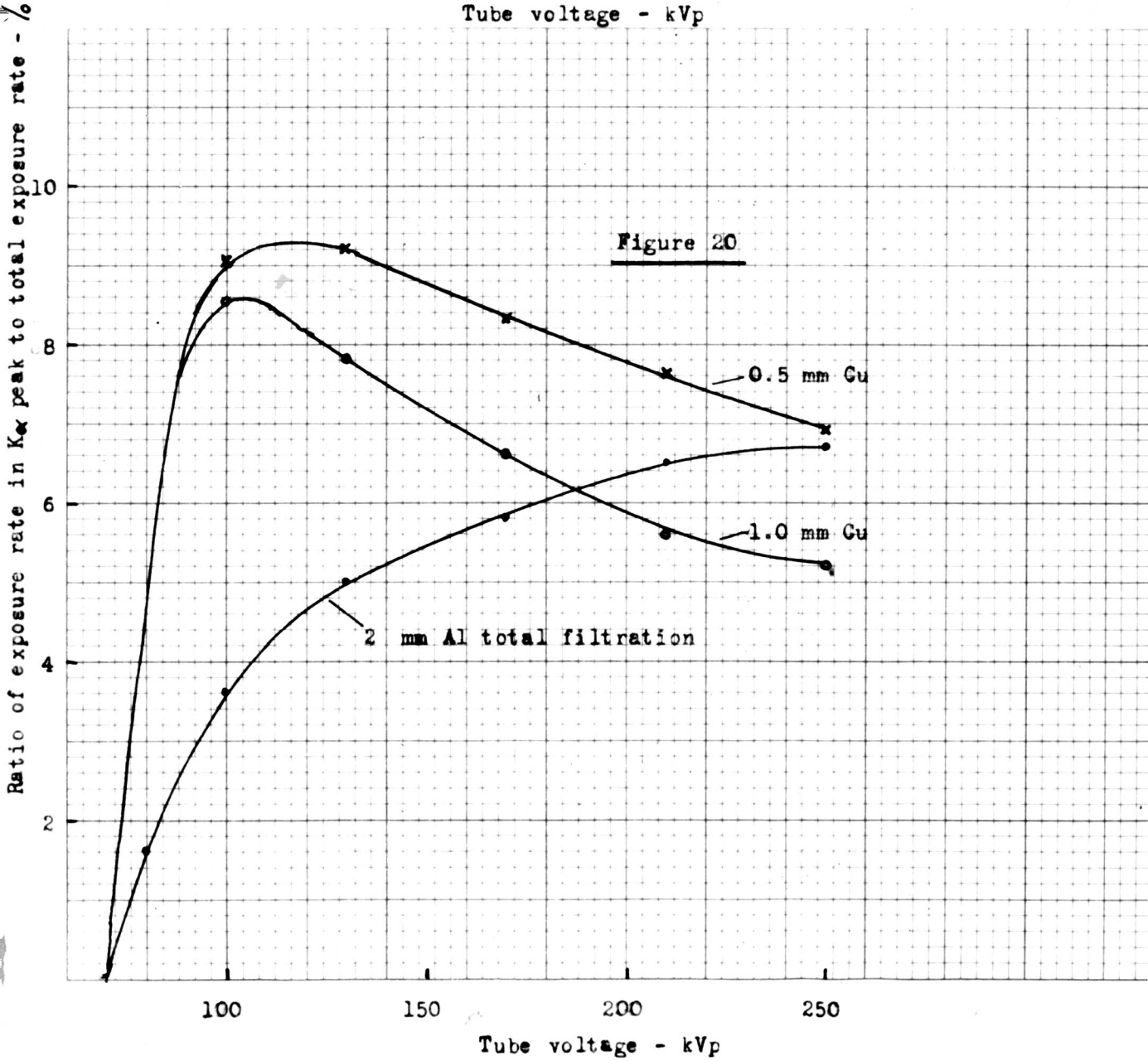
Figure 20
0.5 mm Cu
1.0 mm Cu
2 mm Al total filtration
10
8
6
4
2
100
150
200
250
Tube voltage - kVp

were also converted into exposure rates using the calibration against the Baldwin-Farmer dosemeter. These results are plotted against tube voltage in Figure 19. Finally the ratio of the peak to total exposure rates was derived from the smoothed curves and is plotted against tube voltage in Figure 20. It was unnecessary to correct for any non-uniformity across the beam, as replacing the counter by the ionization chamber at the end of the measurements had shown that the exposure rate in this position was identical with that in the original chamber position.

2.20 Discussion of results of proportional counter experiments

It may be noticed that the 250 kVp, 2 mm aluminium filtration points on both the peak and total exposure rate graphs do not quite fall on the continuously rising curves that might be expected. Indeed, this was contrary to the results of earlier experiments, from which a portion of curve such as that shown dotted might be expected. It was likely that this departure was due to inaccurate registration or reading of the tube current. This was only 3.7 mA for this measurement and the meter could not be read to better than 0.2 mA. Substituting 3.5 mA would, in fact, remove the discrepancy. In any case, it was of no consequence in determining the peak to total ratio.

It is somewhat difficult to assess the accuracy of the determinations of peak/total ratio, since the limited accuracy of an individual determination of peak area, for example, can be improved by plotting the results against tube voltage and working from the smoothed curve. In particular, the peak area at lower voltages was quite small, and due to statistical fluctuations could not be determined accurately - perhaps no better than 20% for 130 kVp, 1 mm copper filtration, for example. However, the area/kVP curve can be extrapolated

to/

to zero at 69 kVp, the K absorption limit for tungsten, and this makes it easier to draw the lower energy part of the curve. During some earlier proportional counter experiments, spectral scans had been carried out at tube voltages down to 90 kVp, using a larger aperture over the counter in order to improve the accuracy. These served to confirm the shape of this part of the curve. The random errors introduced in individual measurements of peak area, modified by smoothing the curves, perhaps results in an accuracy of 5%. The ionization current readings should be more accurate than this, and should not contribute appreciably to the overall inaccuracy of the determinations.

There remain the possibilities of systematic errors, arising from the calibration of the ionization chamber, measurement of high resistances and assessment of the exposure rate from the americium-241 source. The last involved the measurement of distances, resistances and electrometer potentials. Each individual measurement could be made with an accuracy of perhaps 1 - 2%, but many steps were involved, and the overall error might again be 5%. Since the same Baldwin-Farmer dosemeter was used to calibrate the ionization chambers used for both the total X-ray and the americium-241 exposure rates, its absolute calibration accuracy was not important, merely its energy dependence. The combination of all the assessments of accuracy leads to a figure of 7%.

Further discussion of the results of the proportional counter experiments and comparison with other results will be deferred to Chapter 5, but it may be useful here to summarise some of the points dealt with in this chapter. The proportional counter described had sufficiently good resolution to separate the Kα and Kβ peaks of the characteristic radiation from tungsten, though/

though with some overlap. The marked variation of counter sensitivity with X-ray energy makes the interpretation of the pulse height distribution curves difficult, but methods have been described for deriving the effective baseline of the peak spectra. A study of the effect of filtration upon the pulse height distribution revealed two apparent anomalies, attributed to "scatter background" and "pulse pile-up", which were allowed for. Changes of counter sensitivity were corrected by frequent calibrating scans with the americium-241 source, and simultaneous measurements with both detectors improved the accuracy of determination of the relationship between the characteristic and total radiation. Assessment of the exposure rate from the americium-241 source enabled it to be used as a means of quantitating this relationship.

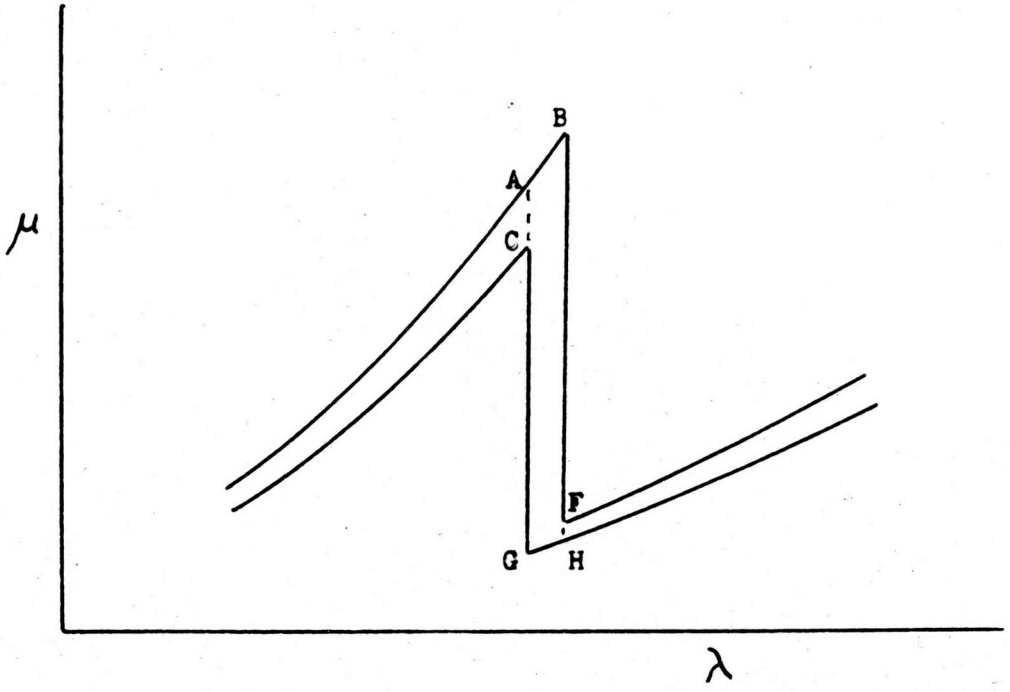

Figure 21

Pass band shaded horizontally, error area vertically

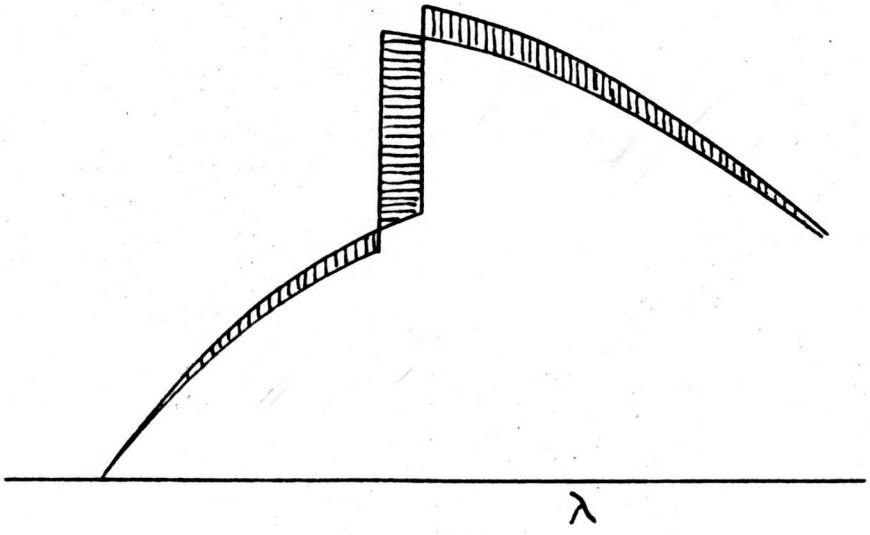

Figure 22

CHAPTER 3

Balanced Filter Experiments

3.1 Examination of Kirkpatrick's conclusions on balanced filters

The general principles of the use of balanced filters, as first suggested by Ross, were outlined in the introduction. It was also mentioned that Kirkpatrick had developed the theory and practice of such use. Before proceeding to describe the application of this method to our particular problem, it may be worth examining some of Kirkpatrick's conclusions.

In his first paper (Kirkpatrick 1939) he investigates the possibility of balance. It is convenient for our discussion to reproduce his Figure 2 (our Figure 21). In this, the linear attenuation coefficient, μ, is plotted against wavelength, λ, for two materials of adjacent atomic number, the dissimilarity of the K jumps, CG and BF, being exaggerated for clarity. For perfect balance it is necessary for the ratio μ_1/μ_2 to be constant for all wavelengths outside the pass band. This result is possible only if μ_1 and μ_2 can be represented by the same function of λ apart from a constant of proportionality. The function may change over different parts of the spectrum provided that the two filter elements change together. In practice the identity of function is not found. The causes of imperfect balance may be considered in two parts - differences in K jumps for the two elements, and changes in the ratio μ_1/μ_2 at wavelengths away from the absorption edge.

Kirkpatrick introduces the concept of an "error area", the difference, apart from that in the pass band, between the areas under the curves representing the spectra transmitted by the separate filters. This

is/

is illustrated in Figure 22 (Kirkpatrick's Figure 1). Clearly, balance may be obtained at any given wavelength by suitable choice of filter t thicknesses, when $\mu_1 t_1 = \mu_2 t_2$. This balance point could be, for example, at the short wavelength side of the pass band (in Figure 21, if μt were substituted for μ as the ordinate, A would coincide with C). In general, absorption jumps vary from element to element, and there will then not be perfect balance at the long wavelength side (for example, point F would come below H in the case shown in Figure 21). Kirkpatrick shows, however, that balance can be achieved on both sides of the pass band by the addition of a thin filter of low atomic number to one member of the balanced pair.

This removes the biggest cause of the error area, but there remains the variation of μ_1/μ_2 at other wavelengths due partly to the scatter component of the attenuation coefficient, since this is not proportional to a power of λ . In his second paper Kirkpatrick (1944) argues that balance may be obtained at any number of different wavelengths by varying the thickness of different parts of the filters. In practice this would call for a knowledge of attenuation coefficients to a high degree of accuracy and a crystal diffraction spectrometer for checking balance at different wavelengths. It did not appear feasible in our case.

Kirkpatrick showed that the intensity of the transmitted band has a maximum value when the filter thickness = $\log r/\mu_2 (r - 1)$, where r is the ratio of the attenuation coefficients on the short (μ_S) and long (μ_L) wave sides of the jump. However, in his second paper he suggests that such a maximum may sometimes be less desirable than a large ratio of pass band power to "error power". He concludes that an increase in this ratio may be achieved/

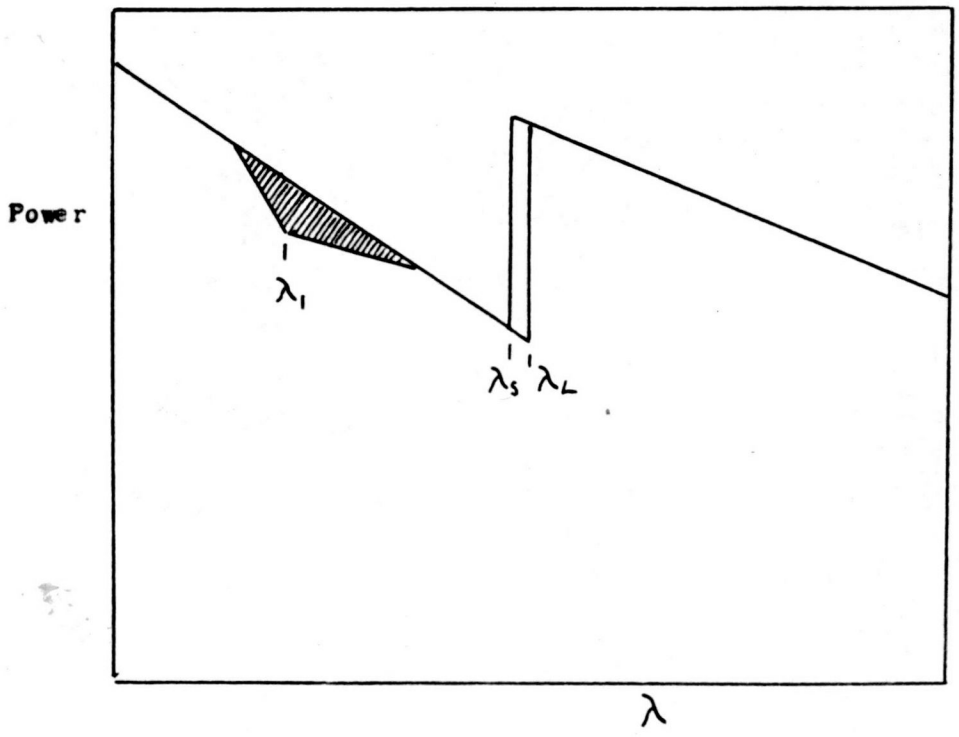

Figure 23

achieved by increasing the filter thickness above the optimum. This conclusion is based on the assumption of a rectangular spectral distribution of breadth twice the mean wavelength of the pass band, and an imperfect balance everywhere outside the pass band represented by $\Delta \mu t$. Since it is possible to achieve balance either side of the pass band, this latter assumption is not a realistic one, and it is of value to examine the effect of a different assumption on the conclusion about filter thickness.

The more likely departure from balance would arise from a difference between the attenuation coefficients over part of the spectrum, and this may be represented in its effect in simplified form as the shaded triangular area in Figure 23, which illustrates the transmission of a rectangular spectrum. For simplicity of presentation, we assume that μ is identical for the two filters for all wavelengths outside the pass band and the error area, and therefore the thickness, t, is the same for each filter. The effect of increasing the thickness of the filters on the ratio of this error area to the pass band area will depend on the wavelength chosen, λ_1 , but we may insert plausible values. The error area is proportional to $(e^{-\mu_1 t} - e^{-(\mu_1 + \Delta\mu_1)t})$ where μ_1 is the attenuation coefficient of one filter at wavelength λ_1 and $\Delta \mu_1$ is the difference between the two coefficients. The pass band area is proportional to $(e^{-\mu_L t} - e^{-\mu_s t})$ so that the ratio pass band area/error area is proportional to $(e^{-\mu_L t} - e^{-\mu_s t}) \Big/ (e^{-\mu_1 t} - e^{-(\mu_1 + \Delta \mu_1)t})$. Assume that $\mu_s = 100$, $\mu_L = 20$, values near those found in the practical case. The maximum pass band/

band transmission is at t = log 5 / 20(5-1), = 0.02cm. We can now calculate the effect of increasing t two- or three-fold on the pass band area, on the error area and on the ratio of one to the other. Consider two values of λ_1 the first chosen so that $\mu_1 = 20$ and $\Delta \mu_1 = 2$. This represents a wavelength about half that of the pass band and in our particular case a part of the spectrum contributing substantially to the total radiation. Secondly, let $\mu_1 = 40$ and $\Delta \mu_1 = 5$. This corresponds to a wavelength intermediate between the first λ_1 and the pass band. The results are presented in Table 3.

TABLE 3

t	0.02	0.04	0.06
Pass band area $\alpha(e^{-20t} - e^{-100t})$	0.538	0.431	0.300
Error area (1) $\alpha(e^{-20t} - e^{-22t})$	0.023	0.036	0.035
Ratio (1) Pass band area/ Error area	20.6	12.7	8.9
Error area (2) $\alpha(e^{-40t} - e^{-45t})$	0.045	0.035	0.023
Ratio (2) Pass band area/ Error area	12.1	11.7	12.5

It will be seen that for the error area at the lower wavelength, increasing the filter thickness above the calculated optimum actually reduces the ratio of/

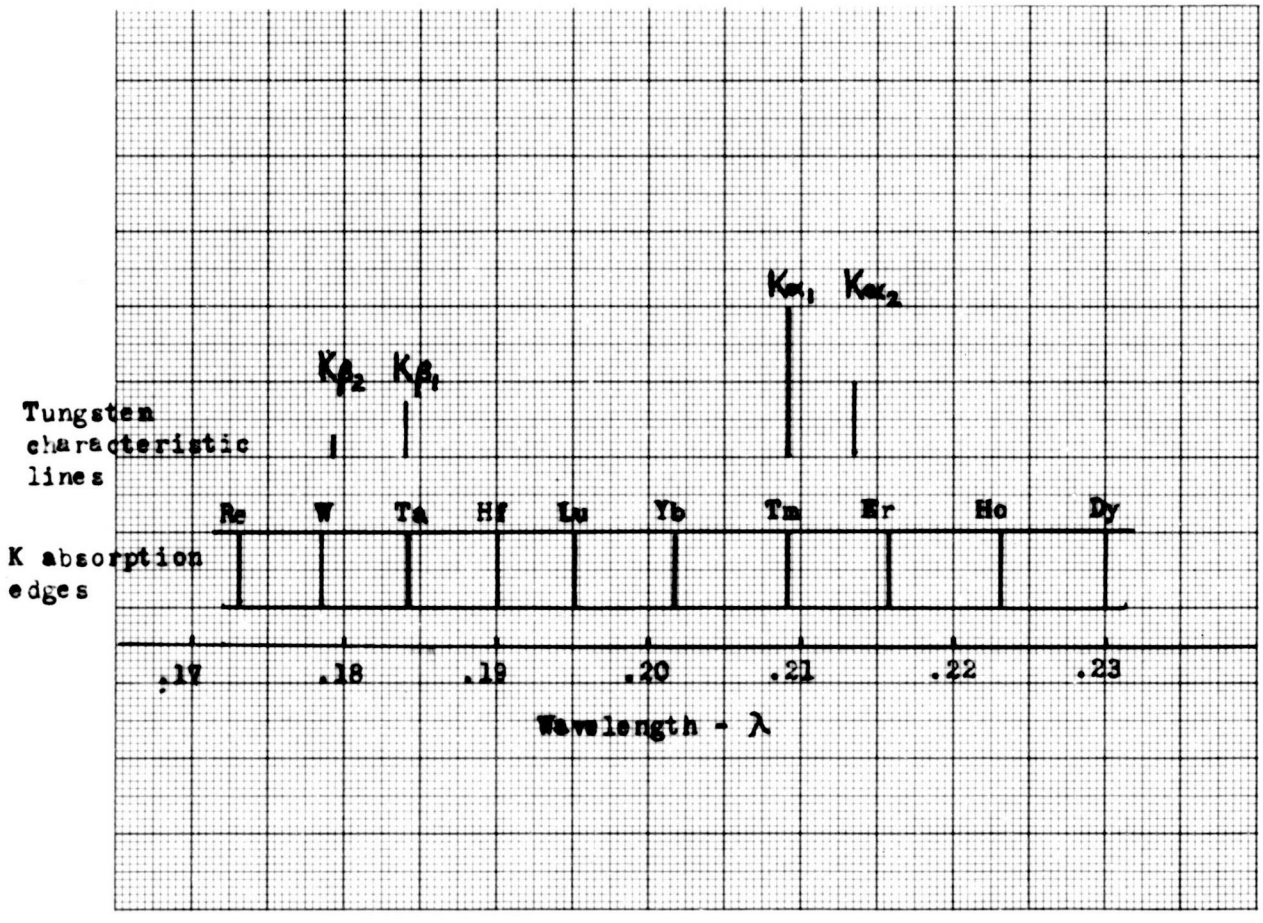
Tungstem characteristic lines
K absorption edges
Re
W
Ta
Hf
Lu
Yb
Tm
Er
Ho
Dy
.17
.18
.19
.20
.21
.22
.23
Wavelength - λ

Figure 24

of the pass band area to error area, while at the longer wavelength considered there is little change. Since the form of the error area postualted is much nearer to that likely to be found in practice than that assumed by Kirkpatrick, it is concluded that it is not desirable to increase the thickness of the filters above the optimum for maximum transmitted intensity.

3.2 Filter elements necessary to examine tungsten K characteristic radiation

We may now turn to the consideration of the filters necessary to isolate the characteristic radiation from tungsten. The wavelengths of the K characteristic lines of tungsten and the absorption edges of the appropriate elements are illustrated in Figure 24. It is clear that the $K\alpha_2$ line lies within the pass band of a thulium-erbium pair, but the $K\alpha_1$ line is so close to the thulium absorption edge that more detailed consideration is required to decide on the appropriate pair. Similarly $K\beta_2$ is between the absorption edges of tungsten and tantalum, but the $K\beta_1$ line is very close to the tantalum edge and it is not clear whether it is on the long or short wavelength side.

Some values of the wavelengths in question as reported by various workers are shown in Table 4, and displayed graphically in Figure 25. The wavelengths are in Angstrom units. It seems likely that common sources were used by some of the authors.


Ta edge
4
5
6
7
W Kβ1
2
1
4
3
.1835
.1840
λ
.1845

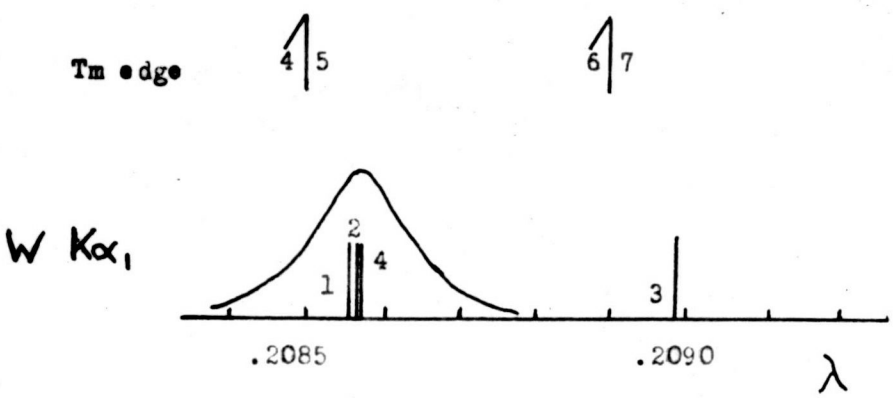
Tm edge
4
5
6
7
W Kα1
2
1
4
3
.2085
.2090
λ

Figure 25

TABLE 4

Reference	W $K\alpha_1$	W $K\beta_1$	Tm K edge	Ta K edge
1	.20856	.18397		
2	.20857	.18399		
3	.208992	.184363		
4	.208575	.183997	.2085	.18360
5			.2085	.1836
6			.2089	.18393
7			.2089	.18393

Reference

1 Williams (1932) quoted by Compton and Allison

2 Compiled by J. M. Cork in Handbook of Physics and Chemistry

3 Compiled by Cochran and Scott in Kaye and Laby

4 Blokhin (1957) compiled from many sources

5 Cabrera (1923) quoted by Compton and Allison

6 Barrett (1952) reproduced in Handbook of Physics and Chemistry

7 Compiled by Cochran and Scott in Kaye and Laby

It will be seen that all the results for the tantalum absorption edge place it on the short wavelength side of the $K\beta_1$ line, although the spread between the results is as big as the mean difference between the wavelengths of the line and the edge. It is probably reasonable to conclude that the tungsten

$K\beta_1$/

$K\beta_1$ line lies between the absorption edges of tantalum and hafnium, and not with the $K\beta_2$ line between the edges of tungsten and tantalum.

The position of the $K\alpha_1$ line is not so certain, as some combinations of figures place the thulium edge on the long wavelength side, though the majority favour the short wavelength side. Blokhin's figures are the most recent and perhaps the most reliable, and they support the idea that the W $K\alpha_1$ line is along with the $K\alpha_2$ line, between the erbium and thulium absorption edges.

3.3 Effect of width of line

The wavelengths are so close that the effect of the possible finite width of the line has to be borne in mind. Both the classical and quantum theories of X-ray line production predict a dispersion of the lines, and this is found in practice. The value of the full width at half maximum height for the $K\alpha_1$ line of tungsten was found by Barnes and Palmer (1933) to be 0.15 X.U. The effect of such a width on our filter problem is shown in Figure 25, where the dispersed shape is superimposed over Blokhin's figure for the wavelength of the tungsten $K\alpha_1$ line. It is clear that this finite width may well mean that, although the bulk of the $K\alpha_1$ line is in the thulium-erbium pass band, part of it may be excluded. The finite width of the absorption edge may also influence partial exclusion.

The question of the relative wavelengths of the tungsten $K\alpha_1$ line and the thulium edge could probably be solved satisfactorily only by the use of the same crystal diffraction spectrometer to measure both quantities, and also the transmission of the line through the filter. Some evidence on the question was obtained in the present study, and this will be described later.

We/

We can make certain of including both the $K\alpha_1$ and $K\alpha_2$ lines in a pass band by using filters of ytterbium and erbium, though this might be expected to increase the difficulties of obtaining balance outside the pass band. The relative intensities of the K characteristic lines are $K\alpha_1$ 100, $K\alpha_2$ 50, $K\beta_1$ 35 and $K\beta_2$ 15, so obviously the best results will be obtained by measuring $K\alpha_1$ and $K\alpha_2$.

3.4 Likely magnitude of error area

Let us next make use of absorption data to investigate the possibilities of balance and the likely magnitude of the error area. Accurate experimental absorption coefficients for the rather exotic elements thulium and erbium were not available, so it was decided to make use of Victoreen's (1949) empirical method to calculate them. Since we are concerned with the differences in behaviour of two adjacent elements, the absolute values of absorption coefficient are less important than relative values. Victoreen considers that his results have an accuracy of about 1%, and this is not sufficient for our purpose. However, it is likely that relative values are much better than this for materials of adjacent atomic number. Victoreen's formula is

$$\frac{\mu}{\rho} = (C \lambda^3 - D \lambda^4) + \sigma_e W_o \frac{Z}{A}$$

where $\frac{\mu}{\rho}$ is the mass attenuation coefficient, λ the wavelength and C and D constants for a particular element which change at an absorption edge. The second term represents the scattering coefficient which can be calculated from the Klein-Nishina formula. Victoreen gives values for C and D for all elements for wavelengths less than the K absorption edge, but his 1949 paper does not include values for the wavelength range between the K and L edges.

C_L/

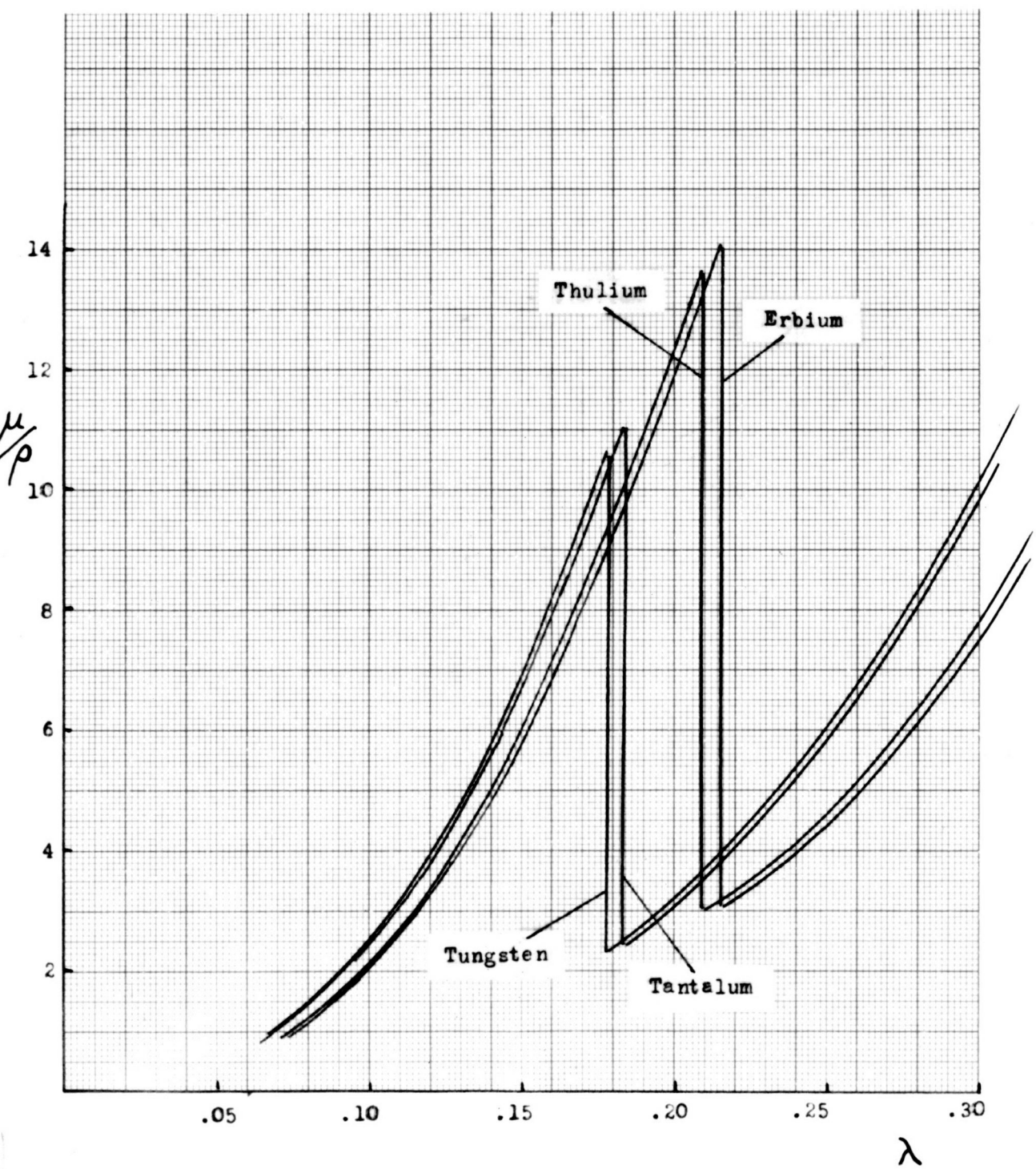
14
12
10
8
6
4
2
μ/ρ
Thulium
Erbium
Tungsten
Tantalum
.05
.10
.15
.20
.25
.30
λ

Figure 26

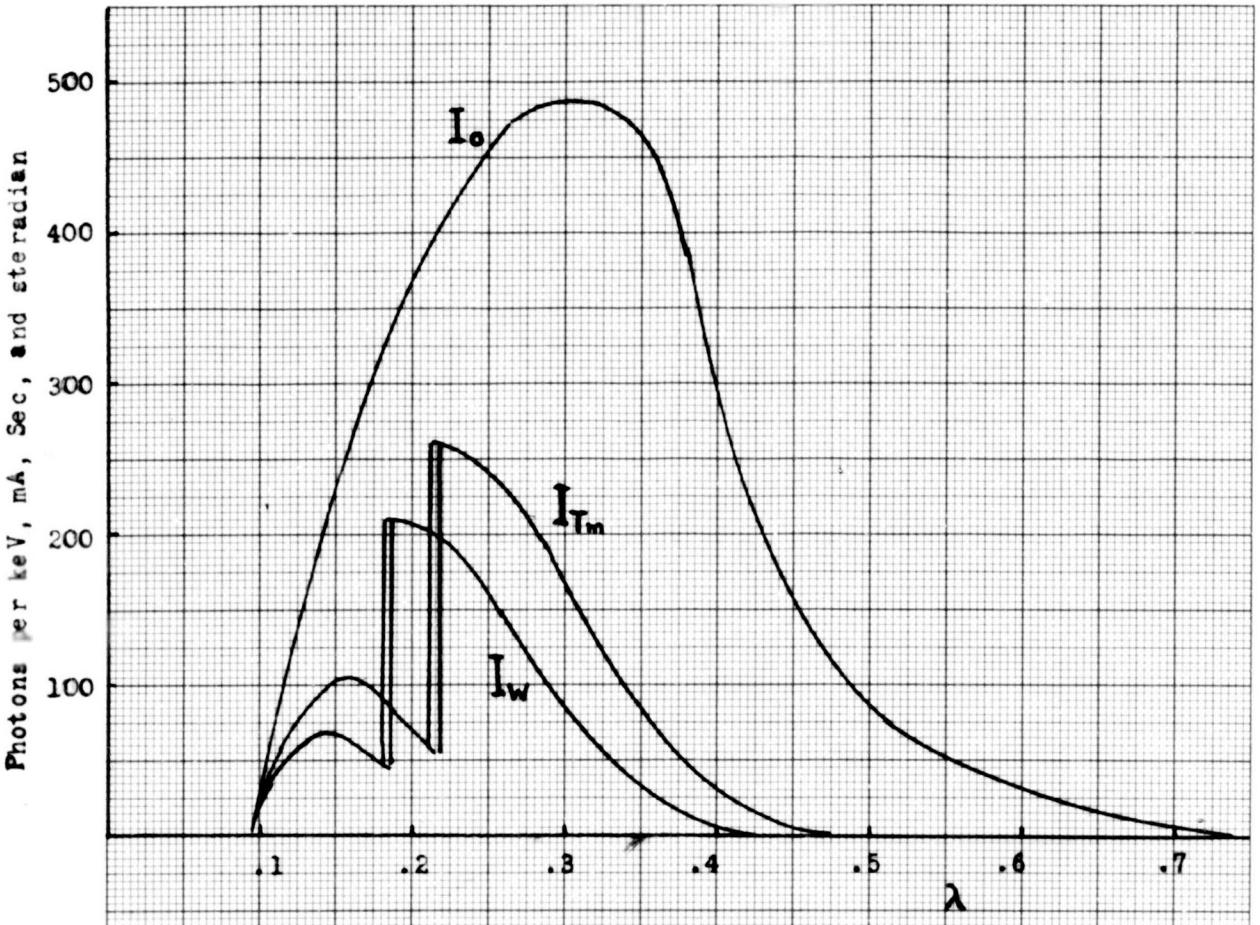

Figure 27

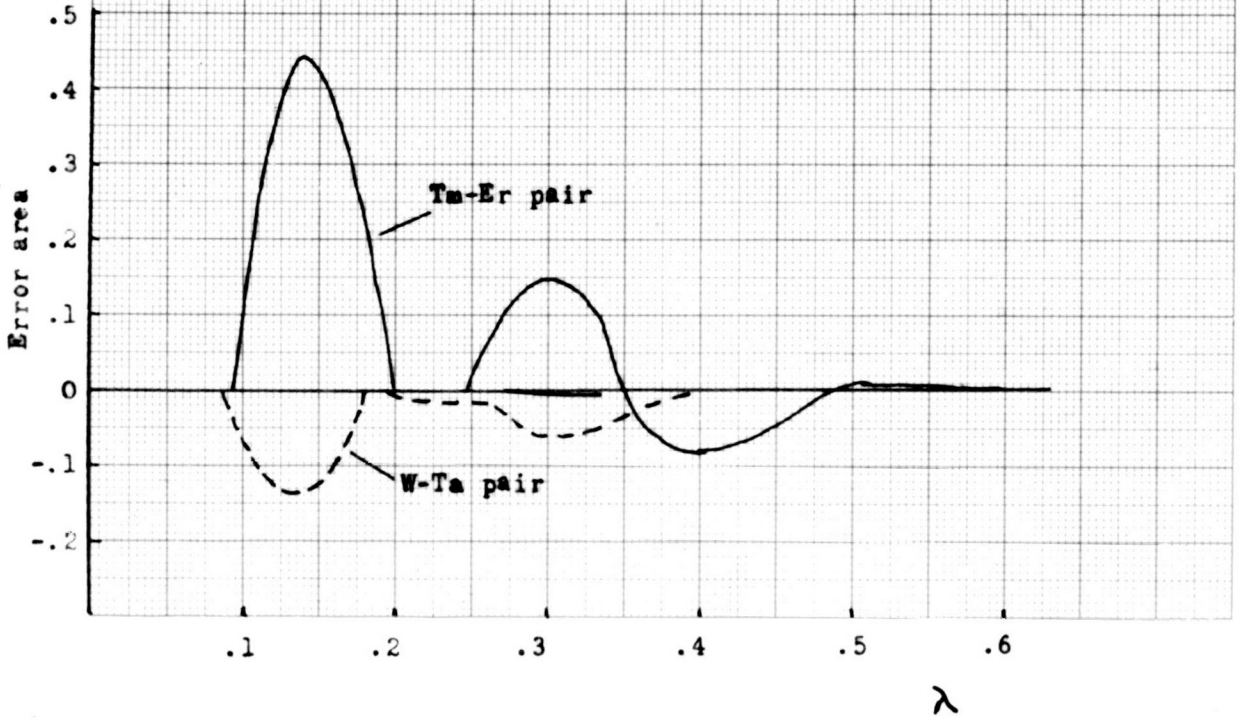

Figure 28

C_L and D_L are given for a few elements in an earlier paper (Victoreen 1948) and these were plotted against atomic number and values for thulium, erbium, tungsten and tantalum interpolated. It is perhaps because of the uncertainty of C_L and D_L that the calculated values of $\frac{\mu}{\rho}$ for tungsten for wavelengths greater than the K absorption edge are some 25% higher than those quoted in a more recent survey (Grodstein 1957). However, our contention that relative attenuation will still be accurate, is probably not affected. There is excellent agreement between the two sources of tungsten attenuation coefficient for wavelengths below the K absorption edge.

Using Victoreen's formula and constants, values of $\frac{\mu}{\rho}$ were calculated for thulium, erbium, tungsten and tantalum. It was necessary to make the calculation to five significant figures in order to show up differences in attenuation of the "balanced" filters. The results are plotted in Figure 26. The effects of filters of optimum thickness on an assumed rectangular spectrum were calculated, but the concept of pass band area does not have any significance in our case, so the effects on an experimental spectrum were investigated. The spectrum chosen was one at 140 kVp, published by Hettinger and Starfelt (1958). This was re-plotted on a wavelength scale, omitting the characteristic peak. The ordinate units were unchanged. The spectrum (I_o) is plotted in Figure 27 together with the attenuated spectra (I_{Tm} and I_w) after passage through filters of thickness to give optimum pass band transmission. It has been assumed that balance was achieved on either side of the pass band.

The error area is much too small to be seen on such a plot, but is itself plotted on a larger scale in Figure 28. Measuring areas under the curves/

curves, we find that, for the thulium-erbium pair, the error area totals 0.044 units, compared with a total area of the incident spectrum of 154 units. Hettinger and Starfelt give the ratio of K photons to total photons at this tube voltage as 0.14, i.e. K photons/continuous spectrum = 0.16. The $K\alpha_1$ and $K\alpha_2$ lines constitute 75% of the K radiation, and assuming that both are in the pass band, the number of characteristic photons in the band is 0.12 of the incident continuous radiation, corresponding to 0.12 x 154 = 18.5 area units on our graph. The pass band allows 0.51 of this through, or 9.5 units. Therefore the error area is 0.044/9.5 or 0.5% of the Kα transmission.

Similar calculations for the tungsten-tantalum pair give the error area as 4% of the $K\beta_2$ radiation. It is to be expected that the error area of a tantalum-hafnium pair will constitute a smaller proportion of the $K\beta_1$ radiation.

These figures for the significance of the error area in relation to the characteristic radiation within the pass band are satisfactorily low. Of course, it may be that the errors are not real, but are introduced by the method of calculating the absorption coefficients, but at least the calculations suggest that there is no likelihood of the error interfering seriously with the measurements of characteristic radiation, provided that balance can be achieved either side of the pass band.

3.5 Choice and design of ionization chambers

For reasons mentioned in the introduction, it was desirable to measure the ratio of characteristic to total radiation in terms of exposure, and so the obvious choice of detector for the transmission measurements was an ionization chamber. This also had the advantage that by using two similar chambers/

chambers with different polarities of H.T., it was possible to measure directly the difference in ionization currents and therefore the difference in transmission between two filters. The accuracy of measurement was thereby improved considerably, and the results rendered relatively independent of variations in tube output.

Let us now consider the factors influencing the design of the ionization chambers. In order to accommodate the chambers side by side in a uniform part of the beam and allow the insertion of filters, it seemed best to use cylindrical chambers in an "end-window" geometry. In order that the difference ionization current should be as large as possible it was desirable to have a large chamber volume. On the other hand, the area of the filters would be limited, as would the size of X-ray beam of reasonable uniformity and exposure rate. These in turn set a limit to the diameter of the chambers. Considering these various factors, it was decided that a diameter of about 5 cm and a length of about 7 cm would be suitable.

The next point to consider was the requirement for saturation conditions in the ionization chamber, since quite high exposure rates might be used. Use was made of Boag's (1956) formula for a cylindrical chamber:

$$f = \frac{2}{1 + \sqrt{1 + \xi^2}} \quad \text{where} \quad \xi = \frac{md^2\sqrt{q}}{V}$$

f = fraction of saturation current

d = effective spacing of electrodes in cm

q = charge flowing in e.s.u./cc/sec

V = volts

m = 15.9 for these units

Let/

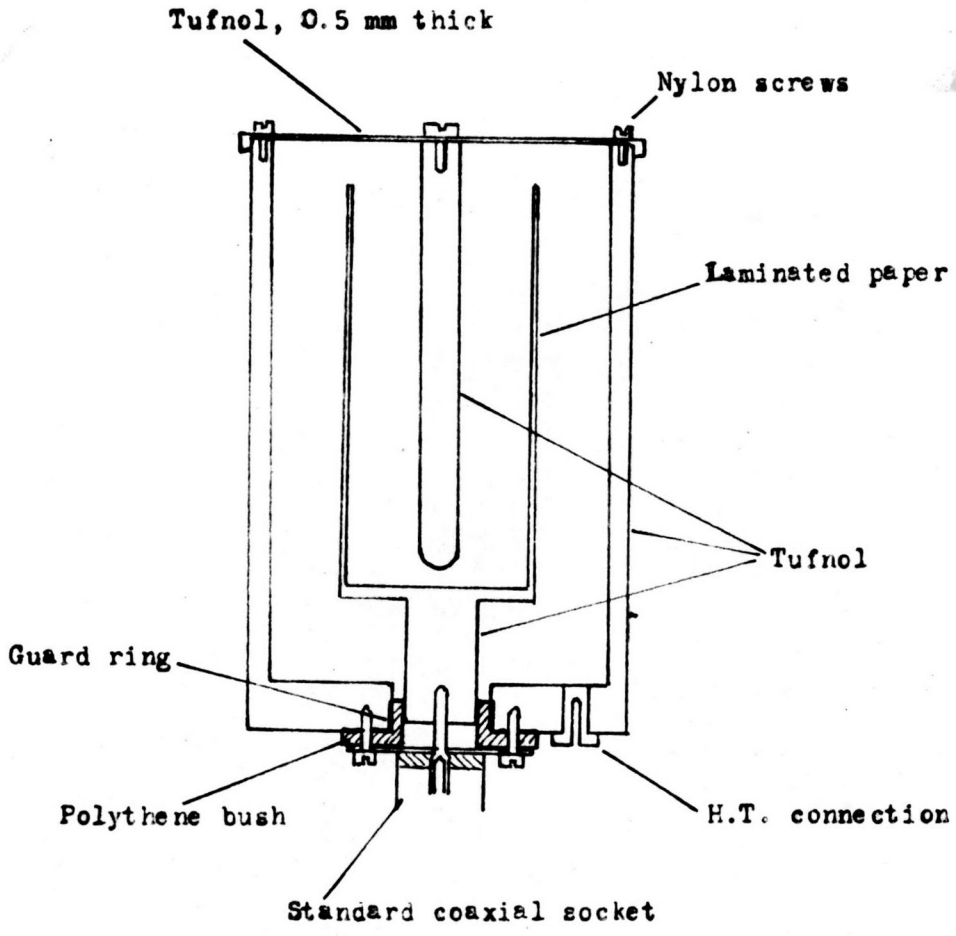

Figure 29.

Ionization chamber for balanced filter measurements

Let $f = 0.99$, then $\xi = 0.2$

For an exposure rate of 60 R/min (q = 1 e.s.u./cc/sec),

when V = 100, d = 1.12

when V = 200, d = 1.65

when V = 300, d = 2.02

If the radii of the inner and outer cylinders are b and a, d = (a - b) K and for a cylinder K = 1.18. If a = 2.5 cm and b = 0.25 cm, d = 2.65 cm

It is clear that saturation would not easily be achieved with a chamber of these dimensions, so it was decided to adopt a double cylinder arrangement, the central cylinder being connected to the outer case, with the collecting electrode as a concentric cylinder in between. In this way d would be not much over 1 cm and saturation should be easily achieved.

The design adopted for the chamber is shown in Figure 29. A standard coaxial socket serves to make connection to the cylindrical collecting electrode. The socket is inserted in a polythene bush, the outer surface of which is graphited to act as a guard ring, being connected to the braid on the coaxial cable. All inside surfaces, with the exception of the annulus adjoining the guard ring, are graphited.

The instrument used to measure the ionization currents was an E.I.L. dosemeter, type 37A. This is normally used with an ionization chamber of 35 cm^3 volume, and is calibrated directly in mR or mR/sec. Since our chamber volume is greater, a given reading will correspond to a smaller exposure or exposure rate. However, since we are concerned throughout with relative exposures, this is of no consequence, and for convenience the observed readings/

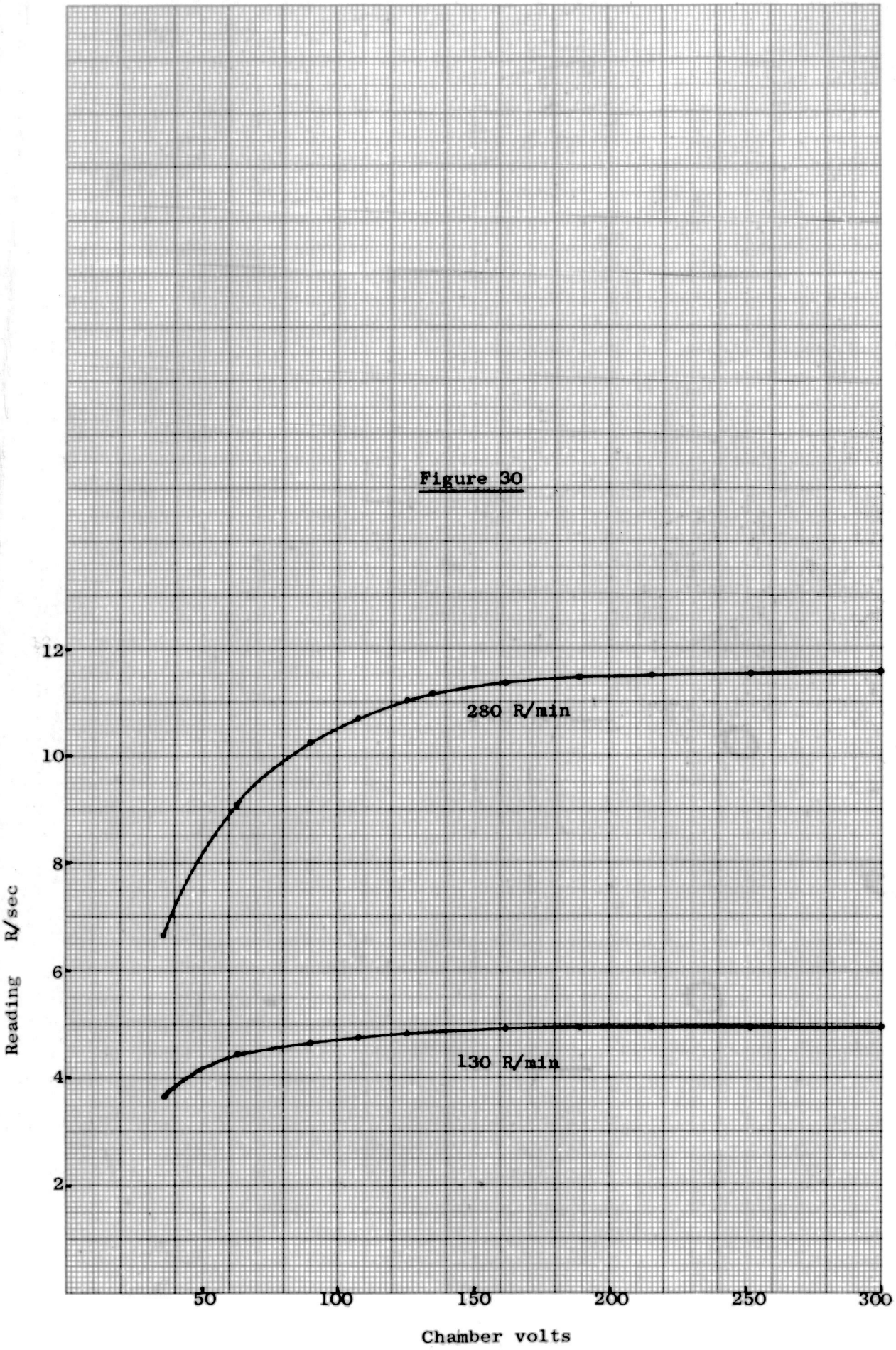
Figure 30
12
10
8
6
4
2
280 R/min
130 R/min
Reading R/sec
50
100
150
200
250
300
Chamber volts

readings will be quoted. With the E.I.L. dosemeter, exposure is measured by allowing the ionization current to charge one of a series of capacitors and measuring the potential developed. For exposure rate measurements the ionization current is passed through one of a number of resistors. One of its advantages is the wide range of currents that can be dealt with. With our chamber it was possible to measure exposures giving readings ranging from about 1 to 100,000 mR.

3.6 Experimental determination of saturation conditions

The first measurements made with the chamber were to check saturation. The chamber was set up in the beam from the Siemens Stabilipan set under conditions which gave an exposure rate of 280 R/min, as measured with a Baldwin-Farmer dosemeter. The H.T. volts on the chamber were varied and the exposure rate reading noted. The conditions were then changed to give an exposure rate of 130 R/min and the measurements repeated. The results are illustrated in Figure 30. It will be seen that for the lower exposure rate saturation was complete at 200 V. It was very nearly so for the higher exposure rate also, but since there was no difficulty in using a chamber voltage of 300, the latter was adopted.

3.7 Quality dependence of chambers

The next measurements were of the quality dependence of the chambers. It is obviously desirable that this dependence should be minimal, and the chamber materials and wall thickness had been chosen with this end in view. The experimental determination was carried out by placing the chamber alongside the chamber of a Baldwin-Farmer dosemeter. Both were then irradiated/

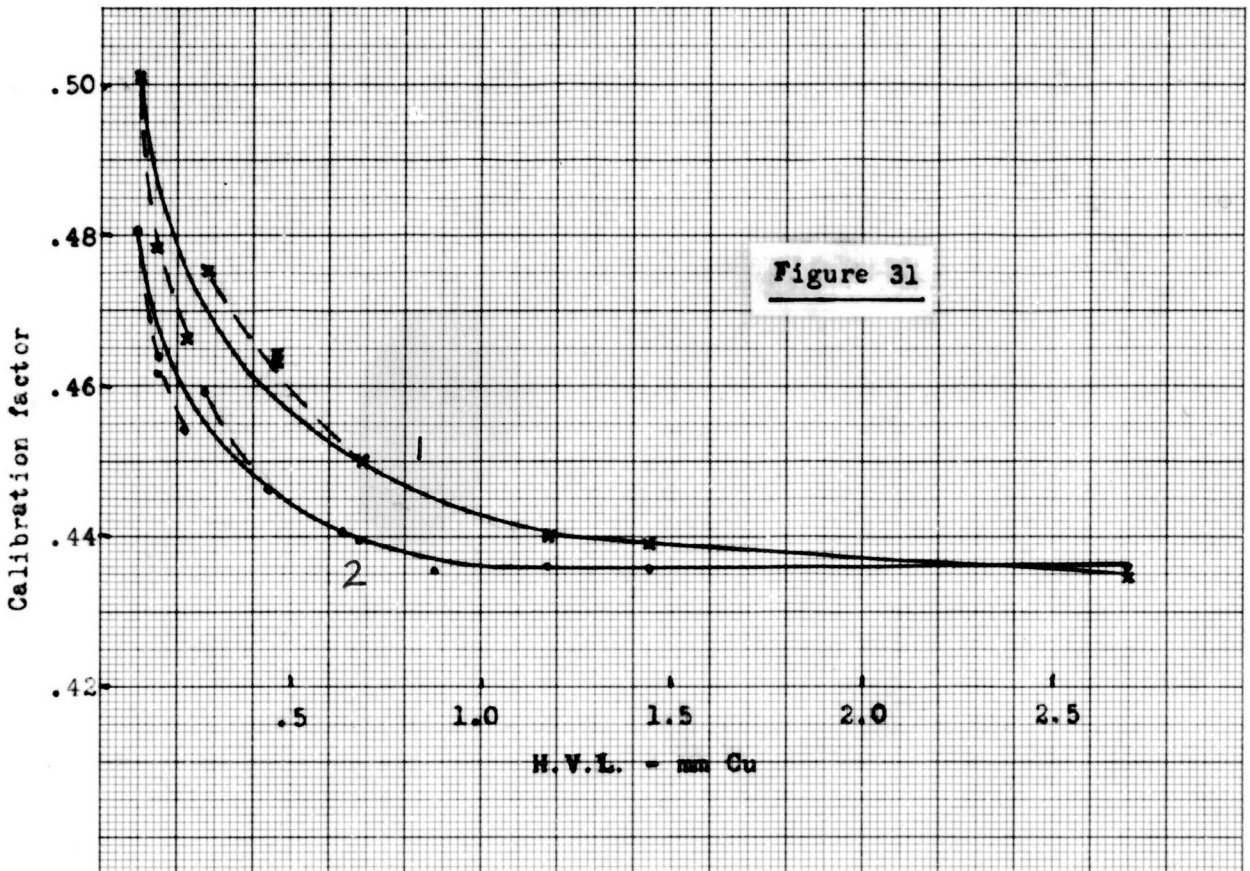

Figure 31

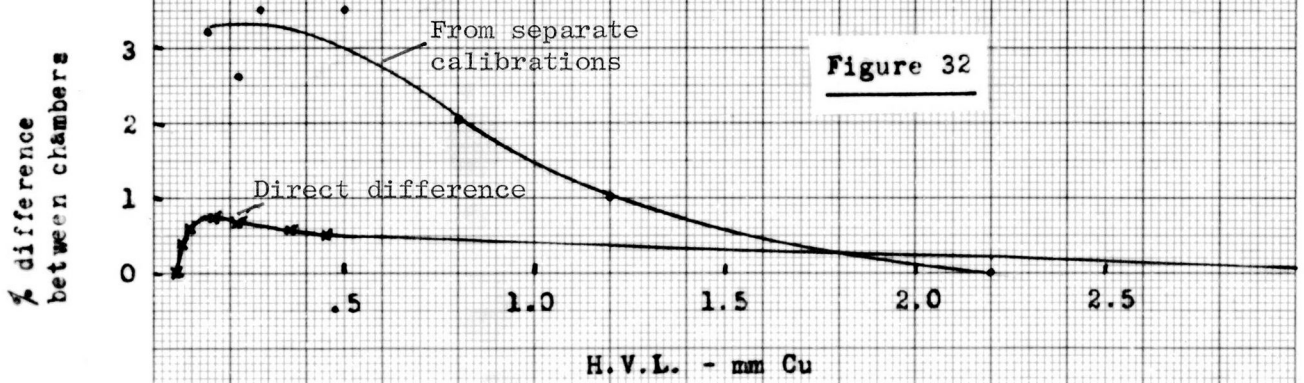

Figure 32

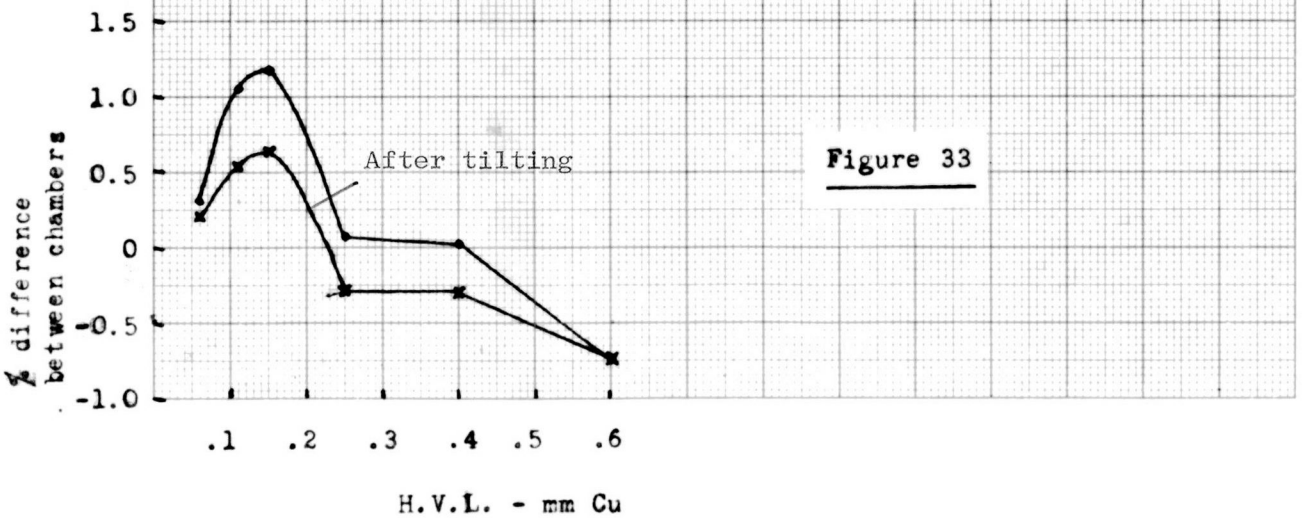

Figure 33

irradiated under a variety of conditions to give a range of half-value layers. The known correction factors were applied to the Baldwin-Farmer dosemeter readings, and the ratios of the readings of the two instruments gave correction factors for the experimental chamber. These are plotted in Figure 31; the ordinate is in arbitrary units. It will be seen that the quality dependence is reasonable, there being the usual reduction of sensitivity for softer qualities. The apparent discontinuity at approximately 0.25 mm copper H.V.L. is due to a change in filtration of the beam used to derive the calibration, and is indicative of the inadequacy of half-value layer alone as a criterion of quality in the calibration of such a chamber.

The variation of correction factor with beam quality is needed to correct the relationship between characteristic and total radiation, as will be described in section 3.12. Of more importance is the difference between the correction factors for the two chambers, since this will result in a change of balance conditions with beam quality. The percentage difference between the chambers as derived from the separate calibrations against the Baldwin-Farmer dosemeter is plotted against half-value layer in Figure 32. The maximum difference of about 3% is more than one would hope for in two chambers that are nominally identical. It is also more than that found on direct determination of the difference ionization current for balanced chambers without Ross filters as will be described later. One curve derived from such an experiment is also shown in Figure 32. It may be, of course, that the larger difference is due to inaccuracies in the separate calibrations. However, it was found during the balanced filter experiments/

experiments that the small departure from balance for operating voltages other than that chosen for balance was not the same on different occasions. It seemed that there might be some factor other than inherent differences in the chambers to account for quality dependent changes of balance. The most likely possibility seemed to be the effect of orientation of the chambers with respect to the beam, and this was investigated.

The chambers were set up in their holder in the beam from the KX-10 set and balanced at 60 kVp. The difference current was recorded as the operating conditions were changed to vary the beam quality. Then the holder was tilted through 2^{o} and the calibration repeated. The results are shown in Figure 33. Once again, discontinuities may be due to changes of filtration. It will be seen that tilting the chambers does change the difference current quality dependence. While this is probably not the only factor leading to changes of balance under different operating conditions, it does suggest that it is necessary to devise a method of correcting the results obtained in a balanced filter experiment. This will be dealt with in section 3.11.

3.8 Mounting of chambers and filters

The two chambers were mounted side by side with a filter holder over each. These were made to tilt, to provide a fine control on the effective thickness. In an early arrangement the filters were close to the ends of the ionization chambers. It was realised, however, that with this geometry much of the fluorescent radiation produced in the filter material would enter the chamber. While it was likely that a similar amount would enter each chamber, and therefore not seriously affect the balance, it was thought best to move the filters further away. It was found necessary to shield the

chambers/

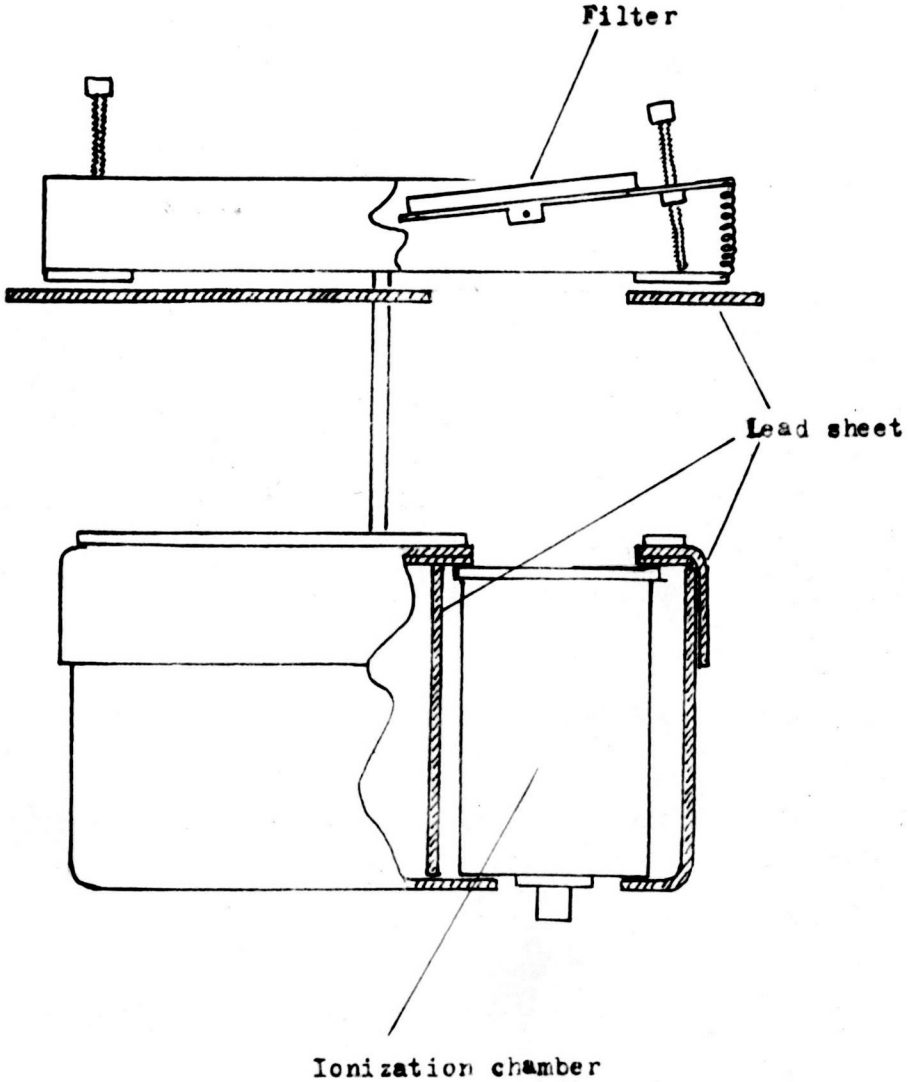

Figure 34

chambers with lead to cut out scattered radiation. The final set-up adopted is shown in Figure 34.

3.9 Form and construction of filters

The next matter to consider is the form of the filters. Tungsten and tantalum were available in the elemental form as metal sheet, and so posed no problems. Erbium, thulium and ytterbium are rare earths, and at the outset of this investigation were not available in sheet metallic form. In any case they are very expensive, and it was necessary to use the cheapest form available, which was the oxide. Kirkpatrick suggests several ways of making filters, including the incorporation of powdered materials into wax. This seemed suitable for our rare earth oxides, and preliminary experiments were carried out with other materials to determine suitable proportions and techniques. The method consists of mixing the powder and wax while applying heat - in our case from an infra-red lamp. The soft mixture is then sandwiched between two glass plates, heat still being applied. Spacers limit the thickness to the desired value. It was found that, although wax mixtures of lighter materials separated satisfactorily from the glass after cooling, provided that the surfaces of the latter were coated with silicone fluid, the erbium-wax mixture, for example, was much thinner, and separation was impossible without damaging the filter.

This snag was overcome by lining the glass plates with 0.001 in thick Melinex plastic sheet, stretched tight by heating. There was then no difficulty in separation. However, it proved impossible to obtain filters that were completely uniform. Even those which appeared satisfactory were shown to have areas of low or high density upon radiography. The use of wax-powder mixtures was therefore abandoned, and the oxides recovered by

dissolving the wax away.

Attention was next turned to the possibility of using the filters in liquid form. There was a dearth of information about the solubility of salts of the rare earth metals, so a pilot experiment was performed with 10 mg of erbium oxide. It was found that this was soluble in nitric acid, and that the resulting nitrate was very soluble in water. This was encouraging, and full-scale conversion was undertaken. Excess strong nitric acid was added to a weighed amount of oxide and the mixture heated in a boiling water bath. When solution was complete the nitric acid was driven off in an oven and the nitrate dried to constant weight. It was found that 4.8 g of Yb_2O_3, for example, yielded 10.0 g of nitrate, suggesting a formula of $Yb(NO_3)_3 . 3 H_2O$. This was then soluble in 4 ml of water. By noting the weights of oxides and nitrates it was possible to adjust solutions of the different salts to the same concentration.

Cells were made to contain the solutions. These were flat cylinders, made of Perspex. The internal diameter was 5.7 cm, to suit the ionization chambers, and the internal thickness 0.3 cm, to suit the volume of concentrated solution available. The faces of the cells were 0.16 cm thick, and it was calculated that the Perspex plus water attenuated the characteristic radiation by about 10%. The amount of filter material had been chosen to give optimum thickness when spread over the area described.

Another element of interest as a filter was hafnium. The most soluble salt of this was found to be the oxychloride. 9g were obtained, which bearing in mind eight molecules of water of crystallisation, is equivalent to 3.9g hafnium. The tantalum sheet with which a balance was required, had a thickness/

thickness of 0.088 g/cm^2. The hafnium, distributed over a circle diameter 5.7 cm, as with the other filter solutions, would give 0.150 g/cm^2, not quite thick enough to balance with two sheets of tantalum. Efforts to reduce the thickness of the tantalum sheet failed, so it was decided to increase the thickness of the hafnium solution by using the same volume in a cell of smaller diameter. The diameter chosen was 5.05 cm, and with the concentrated solution this called for a thickness of 3.7 cm. In order to achieve a balance with the tantalum sheets, a similar cell was constructed and filled with water. This was then used in conjunction with the tantalum.

3.10 Check of balance outside pass band

It is necessary to check experimentally the balance of the filters outside the pass band, and this is obviously best done with the detectors used in the main measurements, and with the chambers set up normally. It is easy to check the balance at wavelengths longer than that of the pass band by operating the X-ray tube at an energy below that required to give any radiation in the band. In our case this was achieved at 60 kVp. It is more difficult to check balance on the short wavelength side of the pass band. An attempt was made to use lead K characteristic radiation excited by higher energy X-rays, but it proved impossible to obtain a beam that did not include some radiation in the pass band.

A solution was found using heavily filtered 250 kVp X-radiation. Cormack et al (1955) described the use of such means to derive nearly monochromatic beams for calibrating a scintillation spectrometer, and Hettinger and Starfelt show spectra obtained with such a spectrometer of heavily filtered X-ray beams. The possibility was investigated by taking Hettinger and Starfelt's spectrum/

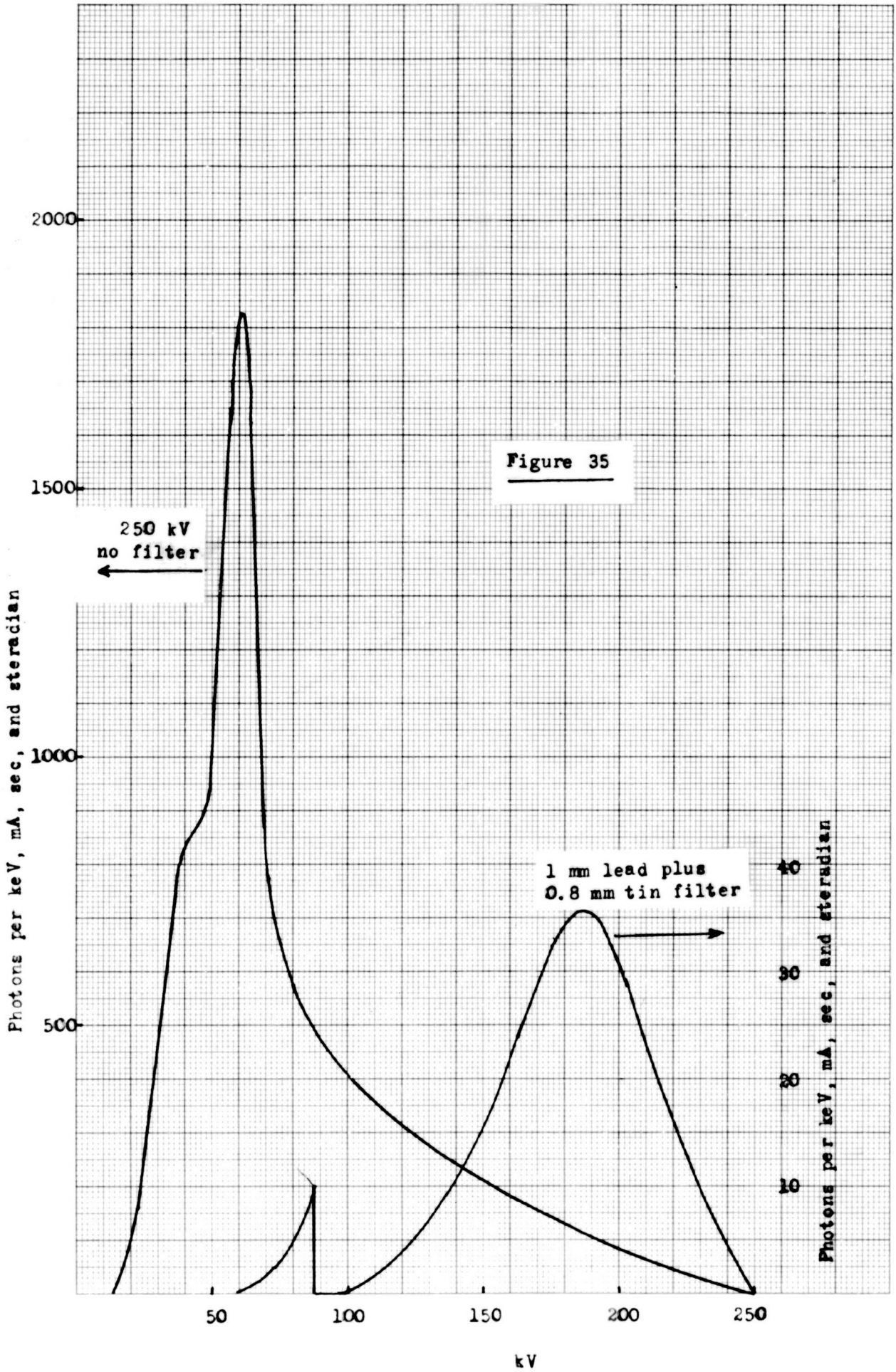
Figure 35
250 kV
no filter
1 mm lead plus
0.8 mm tin filter
2000
1500
1000
500
40
30
20
10
50
100
150
200
250
kV
Photons per keV, mA, sec, and steradian
Photons per keV, mA, sec, and steradian

spectrum for unfiltered 250 kVp radiation and calculating the attenuation due to 1 mm lead + 0.8 mm tin, the latter being added to reduce the 'leakage' of radiation of energy below that of the lead K absorption edge. The transmitted spectrum is shown in Figure 35. There is no radiation within the pass band, and the peak of the spectrum is at 190 keV. In practice the 1 mm lead was added to a "Thoraeus III" filter, the increased thickness of tin (1.2 mm) reducing further the transmission at energies just below the lead absorption edge. This composite filter reduced the exposure rate for 250 kVp radiation to about 3% of the unfiltered beam, but this was quite adequate for balancing purposes.

3.11 Technique of using filters

The technique of using the balanced filters was as follows: The holder containing the ionization chambers was arranged at approximately 60 cm from the tube focus with the line joining the centres of the chambers perpendicular to the tube axis. This was to minimise the effects of assymetry of the beam. The collecting electrodes of the chambers were connected to a junction box, from which a single lead went to the E.I.L. 37A dosemeter. + 300 V was supplied to the H.T. connection of one chamber, and -300 V to the other. In this way the dosemeter would record only the differences in ionization current. To reduce the effects of stray radiation on the chambers and on the cables, the X-ray beam was limited by a 15 x 7.5 cm clinical applicator. With no filters in position, the chambers were balanced as well as possible, particularly at 60 kVp and at 250 kVp with the lead filter. Initially this balance was carried out by varying the aperture over one chamber with a screw-operated lead diaphragm. It was found more convenient, however, to make use

of/

of the lack of uniformity of the beam and affect the balance by slight sideways movements of the chamber holder. With the chambers balanced as near as possible at the extremes of quality, measurements were made of the out of balance current at intermediate tube voltages. It was impossible to achieve perfect balance under no-filter conditions at all energies. This is perhaps not surprising, as the direct measurement of the difference between the two currents provided a very sensitive means of measuring lack of balance, amounts down to 10^{-5} of the current from one chamber being detectable. The out of balance current observed did not exceed 1% of the single chamber current. It will be shown how corrections were made for this lack of balance.

The next step was to measure the current from one chamber alone over a range of tube voltages. This was done after blocking the beam to the other chamber and removing its H.T. supply. Then the filters were introduced, one over each chamber, and balancing carried out at 60 kVp and 250 kVp with lead filtration. This step was performed as carefully as possible, as no correction could be applied for any lack of balance at this stage. The main adjustment to achieve balance was accomplished by tilting one of the filters to increase its effective thickness. In order to allow for slight differences of matching either side of the absorption edge it was necessary, as suggested by Kirkpatrick, to add a thin filter of low atomic number material to one filter. The material chosen was sheet polythene, 0.13 mm thick or 0.43 mm aluminium, and successive adjustments of number of sheets and angle of filters were usually necessary to obtain balance at the chosen points above and below the absorption edge. Then measurements were made of the difference current over a range of tube voltages with the filters in position, to give the pass band transmission. Finally the filtered current from one chamber alone was

measured/

measured, in the way already described.

Let us now turn to the method of correcting for the degree of unbalance found. If the chambers are balanced at 60 kVp, any differences of ionization current at higher voltages must be due to differences of quality dependence. The initial measurements made without the Ross filters present constitute a measure of this difference of quality dependence. Given a knowledge of the half-value layer of the beam at the different operating voltages, we can construct a calibration curve of percentage difference against H.V.L. One such curve has already been shown in Figure 33. The insertion of the Ross filters changes the quality of the beam and therefore the correction to be made at a given operating voltage. If the filtered H.V.L. is also known, the calibration curve derived from the unfiltered beam can be used to apply the necessary correction.

3.12 Results of measurements and corrections needed

A typical set of measurements is displayed in Table 5. Exposures are quoted in mR as read on the dosemeter for a 30 sec radiation time. The Ross filters used were ytterbium and erbium, and no additional filtration was applied to the X-ray beam. To obtain balance, the erbium filter was tilted and four sheets of polythene added to the ytterbium filter.

TABLE 5

kV	No Ross filters		With Ross filters	
	1 - 2	1	1(Yb) - 2(Er)	Yb
60	0	9850	1.5	700
90	125	19900	307	2500
130	319	35200	1070	6750
170	515	55000	2070	14350
210	720	75000	3210	24800
250	900	99000	4300	38100
250 + Pb	6.7	2890	5.5	2210

The corrections for lack of balance are shown in Table 6.

TABLE 6

kV	% difference unfiltered	H.V.L. unfiltered mm Copper	H.V.L. filtered mm Copper	% difference filtered	corrected Yb - Er	As % of 1
60	0	.05	.15	.90	- 4.8	- .05
90	.63	.08	.26	.94	284	1.43
130	.90	.13	.43	.91	1009	2.87
170	.92	.20	.66	.9	1940	3.53
210	.96	.30	1.1	.8	3010	4.01
250	.91	.45	1.5	.7	4030	4.06
250 + Pb	.23	5	5	.23	.4	.01

It will be seen that there is a small residual lack of balance at the two end points, which is an indication of the error there might be in the final result.

Further corrections have to be applied to these figures before they represent the ratio of characteristic to total radiation. There is a small correction for the energy dependence of the ionization chambers, due to the difference in response of the chamber to the total beam (variable half-value layer) and to the pass band (H.V.L. = 0.5 mm copper). This difference is negligible for beams with additional filtration, but amounts to a few percent for lower energies with an unfiltered beam. The other corrections are for the attenuation of the pass band radiation in the Ross filter and the amount of continuous radiation in the pass band.

3.13 Attenuation of filters

Since we wish to know the amount of characteristic radiation in the incident beam before it is affected by the filters, we must correct for attenuation in the filter of higher atomic number. This can be calculated, but in view of the uncertainty of the attenuation coefficients at wavelengths above the absorption edge and the effect of water and Perspex it was thought better to measure the attenuation. For this the americium-241 source and proportional counter described in Chapter 2 were used. The transmission of the pass band energy in the ytterbium filter could be measured directly, and the 59.6 keV γ-ray could also be used to measure transmission in the hafnium, tantalum and tungsten filters. The source was arranged 15 cm from an aperture in a lead diaphragm, with the counter a further 15 cm beyond. The pulse height analyser was set to include the whole of the 59.6 keV peak, and count rates recorded with and without a filter over the aperture. It was necessary to relate the measured transmission for the tantalum filter, for example, to that/

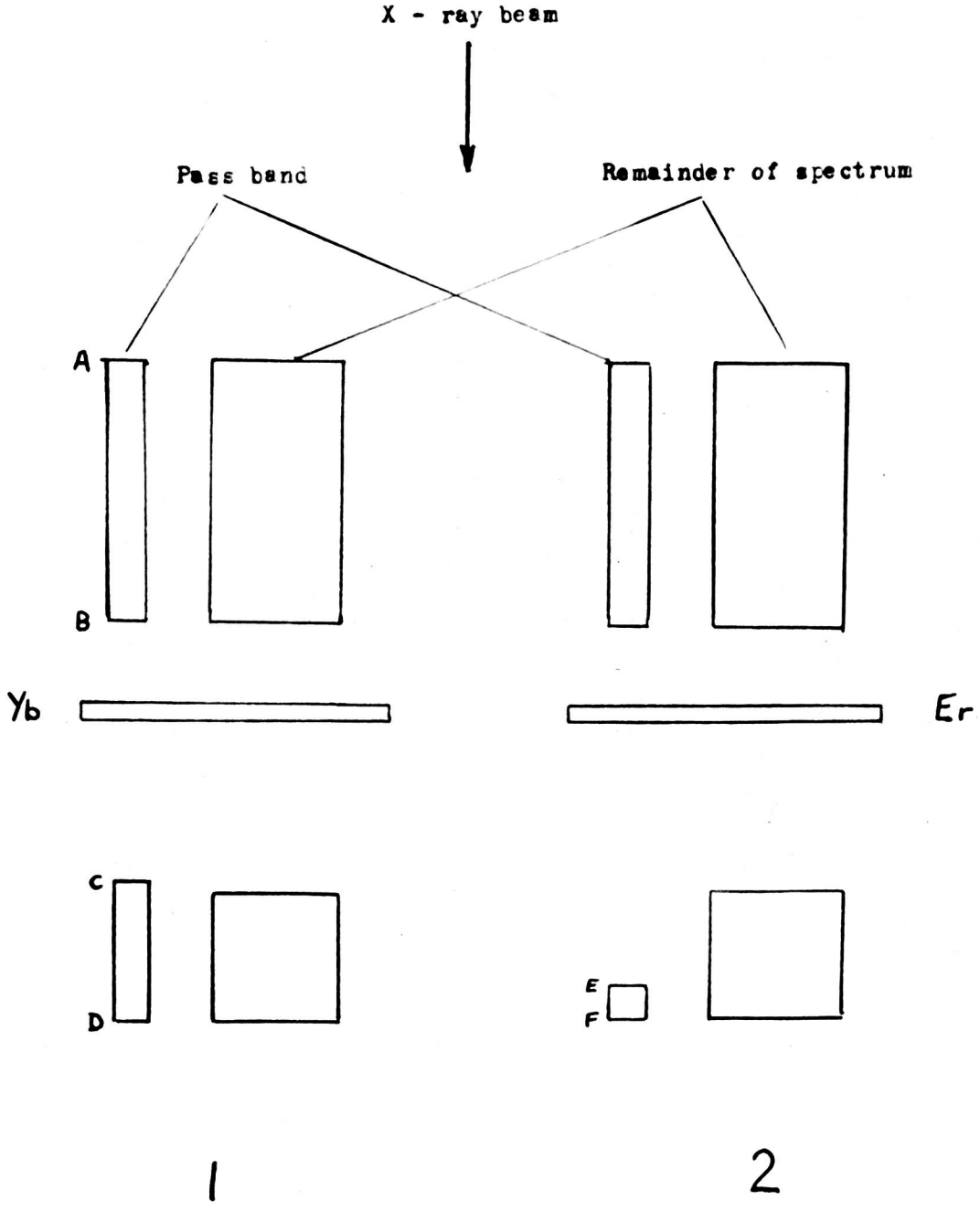

Figure 36. Transmission of different components through filters

that for the appropriate pass band by using the relationship between the attenuation coefficients at 59.6 and 67.5 keV.

The americium-241 γ-ray has an energy just above the absorption edge of thulium, and so it was necessary to use a lower energy beam. This was accomplished by using the americium source to excite fluorescent radiation from the erbium filter, giving a 49.2 keV beam. As the intensity was now lower it was necessary to have the lead diaphragm only 7 cm from the fluorescent source and from the counter, so the geometry was not so satisfactory. Once again the attenuation coefficients were used to correct the measured transmission to the pass band transmission required. The deduced transmissions of most interest were: tantalum 0.58, ytterbium 0.54, thulium 0.56.

It is not sufficient to correct the observed pass band ionization current by these transmission factors, as can be seen from Figure 36, which illustrates in diagrammatic form the effect of filtration on the different components of the spectrum. We measure the difference between CD and EF, and need to know AB. Therefore we must measure the transmission of the pass band energy in the lower atomic number filter, in this case the erbium. The americium source was again used for this, and a transmission of 0.12 found. Then AB = (CD - EF) / (0.54 - 0.12) = (CD - EF) / 0.42

3.14 Correction for continuous spectrum in pass band

The final correction to be made to the measurements is for the amount of the continuous spectrum that is included in the pass band. An attempt was made to use the proportional counter measurements described in Chapter 2 to give the required information. However, the presence of the scatter background and low energy coincidences made the level of the true continuous/

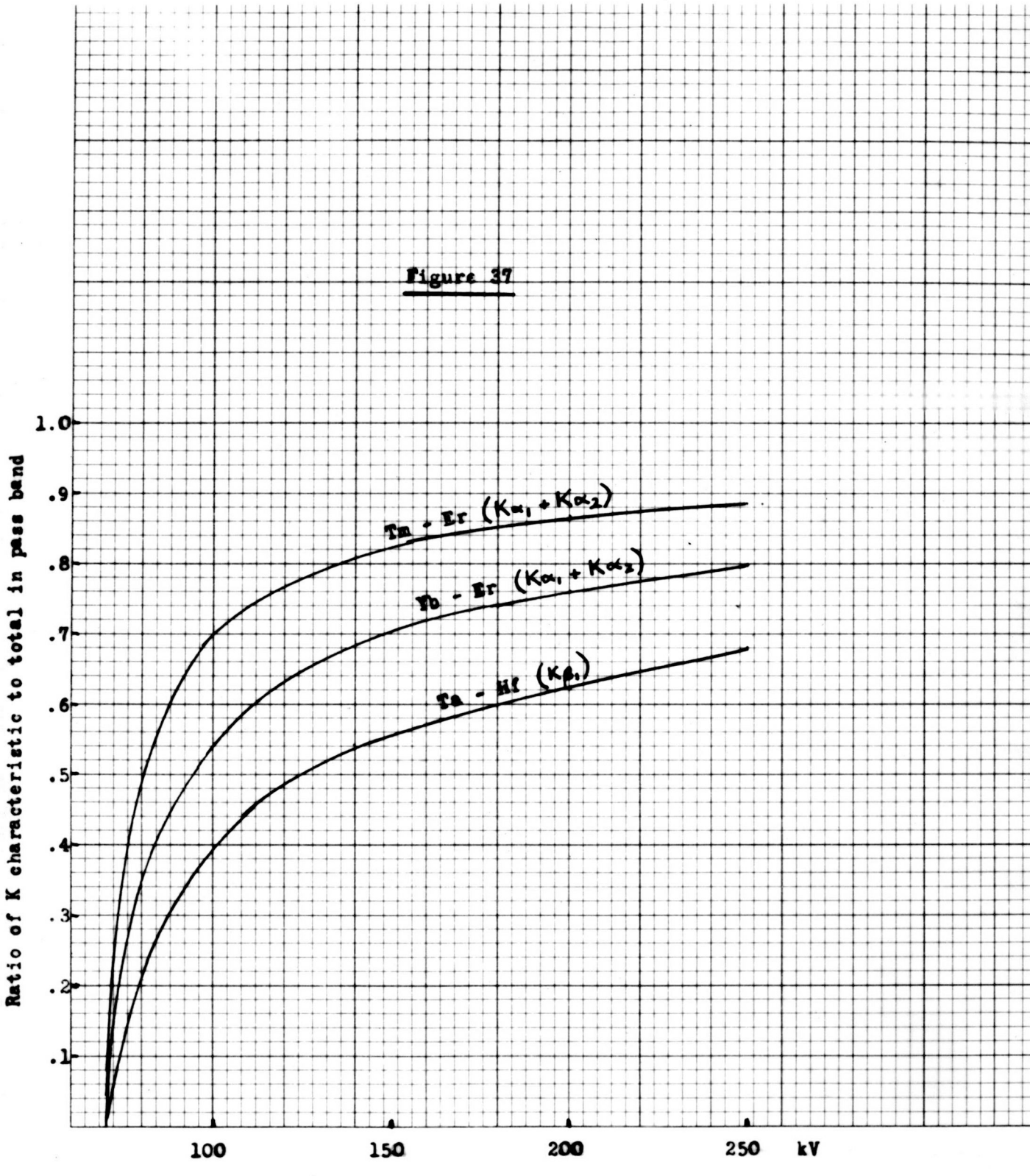
Figure 37
Ratio of K characteristic to total in pass band
1.0
.9
.8
.7
.6
.5
.4
.3
.2
.1
Tm - Er (Kα1 + Kα2)
Yb - Er (Kα1 + Kα2)
Ta - Hf (Kβ1)
100
150
200
250
kV

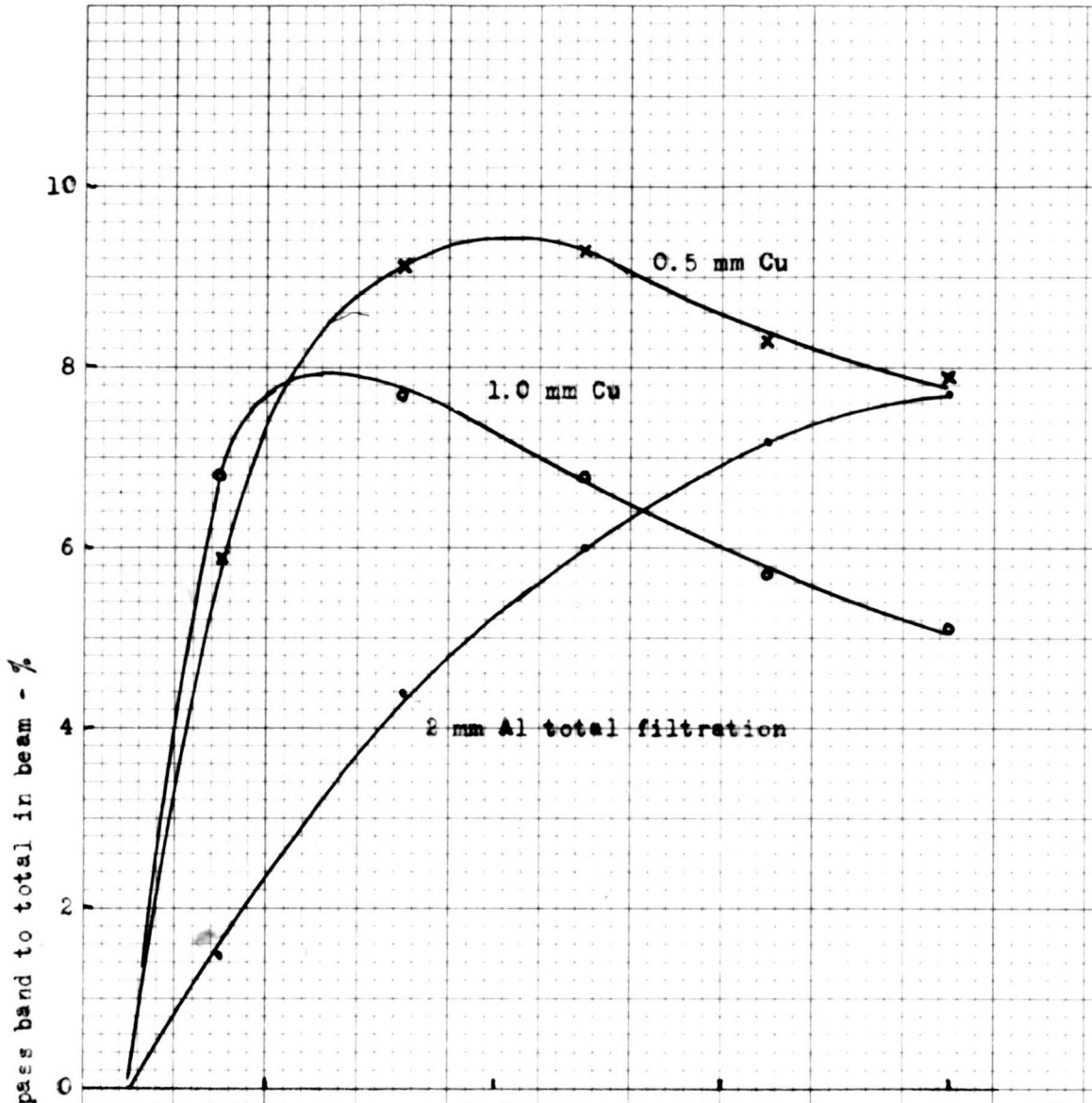

Figure 38. Yb - Er ($K\alpha_1 + K\alpha_2$)

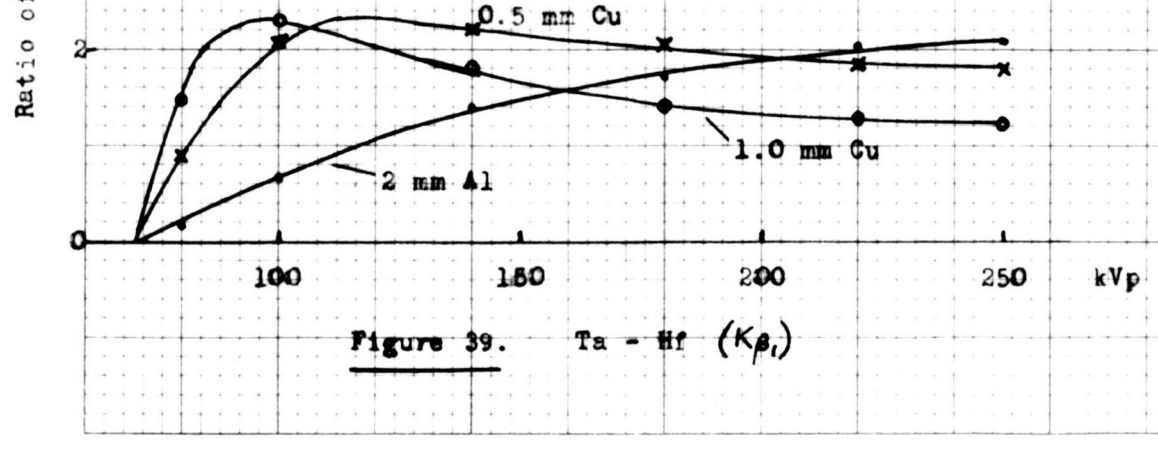

Figure 39. Ta - Hf ($K\beta_1$)

continuous spectrum uncertain. It seemed preferable, therefore, to derive the required ratio from Hettinger and Starfelt's spectra. These were replotted on a convenient scale and the continuous spectrum drawn in under the peak. The area of the peak was measured and compared with the area of the continuous radiation in the pass band as derived from the measured height and known energy width. The relative intensities of the different lines of the K radiation were used to give the appropriate ratio in a given pass band. The most useful results are presented in Figure 37, the ratio characteristic/(total in band) being plotted for convenience.

3.15 Corrected results of filter measurements

When all the corrections had been applied, values were obtained of the ratio of characteristic radiation in the appropriate pass band to total radiation in the beam, once again the relationship being expressed in terms of exposure rate. The results are plotted in Figure 38 - 40. Figure 38 shows the results for the ytterbium - erbium pair of filters, and represents the $K\alpha_1$ and $K\alpha_2$ peaks. It is therefore directly comparable with the proportional counter results shown in Figure 20. The ratios for the tantalum - hafnium pair are shown in Figure 39; these encompass the $K\beta_1$ line. It will be seen that the shapes of the curves are similar to the corresponding ones in Figure 38, the actual values being lower, of course, due to the lower intensity of the characteristic line. It is of interest to examine the relationship between these two sets of results; this can perhaps be best displayed in a table of ratios of % characteristic radiation (Table 7).

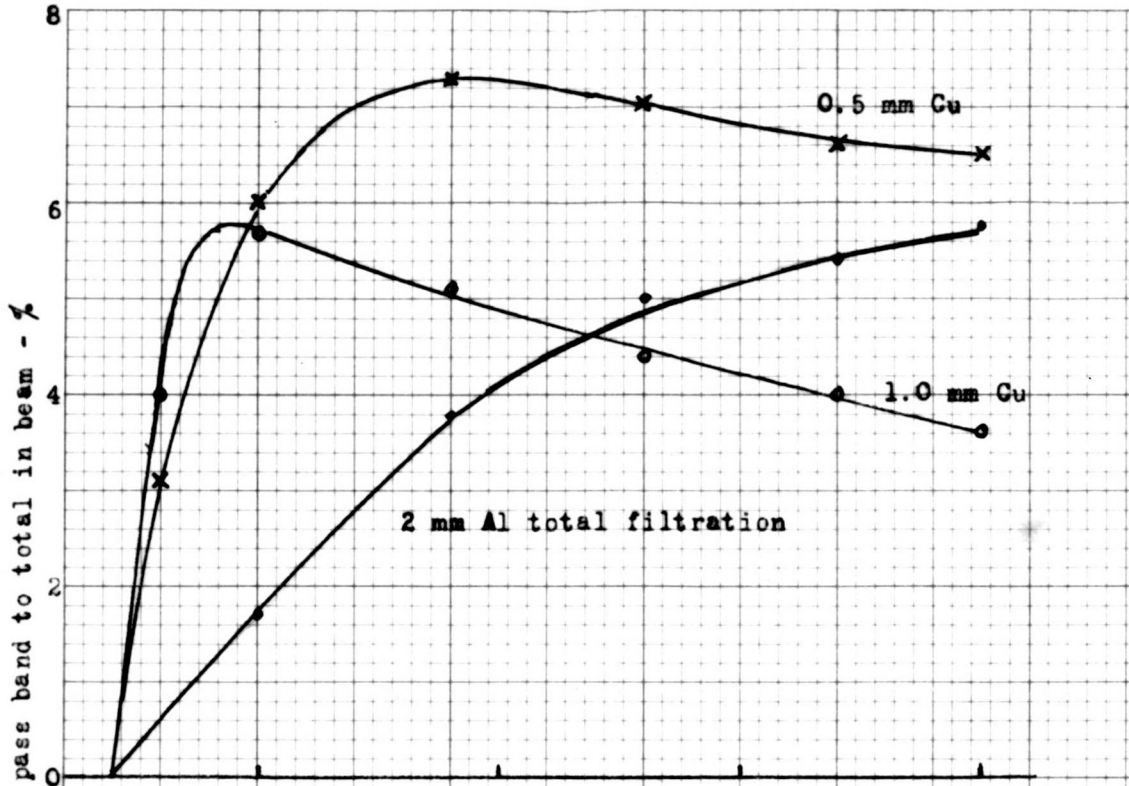

Figure 40. Tm - Er

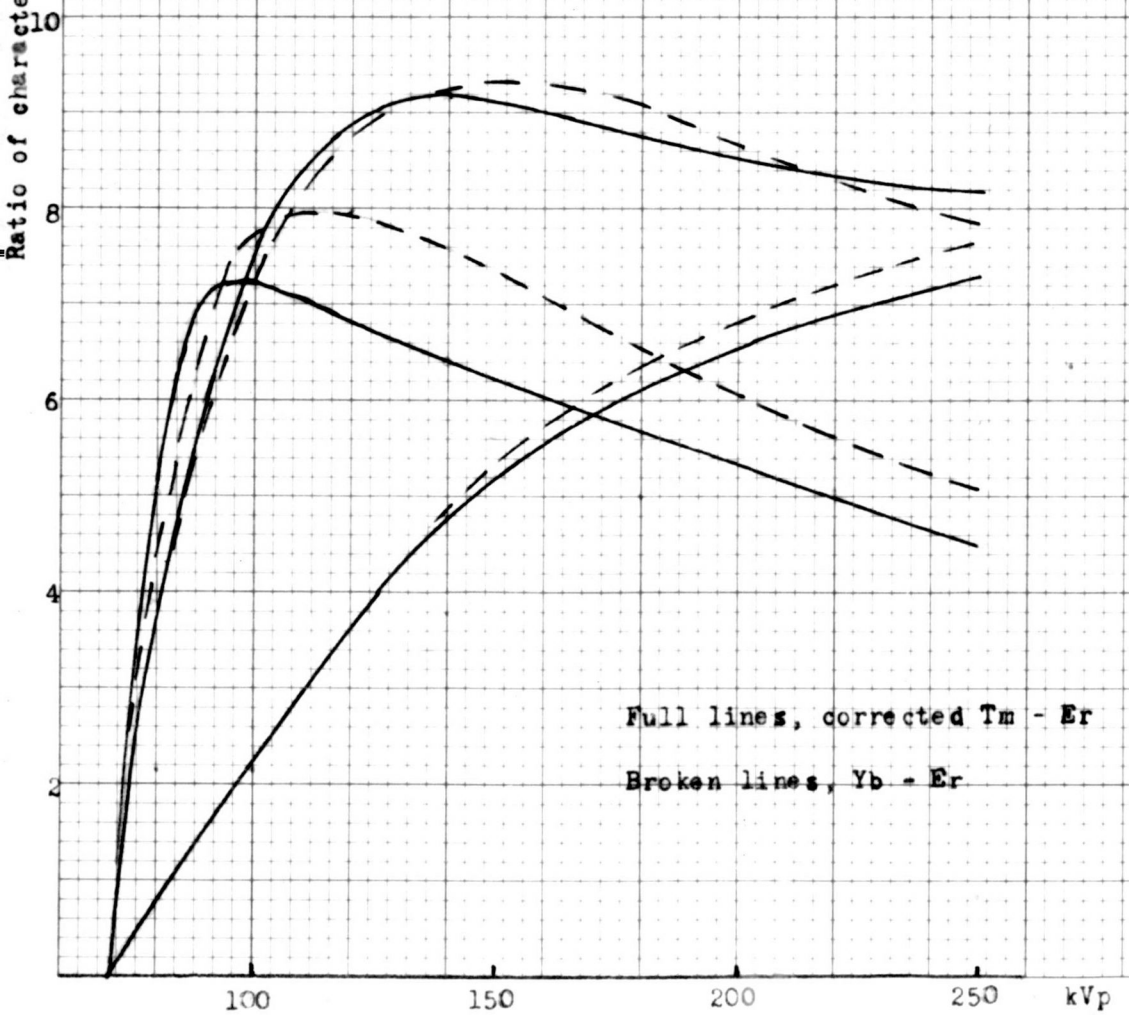

Figure 41.

TABLE 7

kV	Ratio $K\beta_1$ / ($K\alpha_1$ + $K\alpha_2$) for filtration of:		
	2 mm Al	0.5 mm Cu	1.0 mm Cu
100	.28	.29	.30
140	.29	.24	.24
180	.27	.23	.22
220	.27	.23	.23
250	.27	.23	.24

These values can be compared with the expected ratio of .23. The amount of K radiation generated at a tube voltage of 100 kVp is very small and these results will be the least accurate. Similarly, the proportion of characteristic radiation is least for the 2 mm aluminium total filtration and here the balance on the high energy side of the pass band was worse than with the filtered radiation. For the most accurate results, namely filtered radiation at tube voltages above 100 kVp, the agreement with theory is excellent. Because of the lower intensity of the $K\beta_1$ line, its determination is correspondingly less accurate than that of the $K\alpha$ lines, and the tantalum - hafnium results probably do not contribute appreciably to the knowledge of the proportions of characteristic radiation. However, they do serve as useful confirmation of the method of balanced filters.

The results for the thulium - erbium pair are shown in Figure 40. While the shapes are similar to those of Figure 38 the actual values are lower. This suggests that fears expressed in section 3.3 about the finite width of the $K\alpha_1$ line encroaching on the very close thulium absorption edge may be

well/

well founded.

3.16 Transmission of thulium filter

The difference between the expected and experienced transmission of the thulium filter should show up on attenuation measurements, if the $K\alpha_1$ line itself is used instead of the americium-241 source, with its slightly different energy. To test this, fluorescent K-radiation was excited by directing the beam from the KX-10 set, operated at 140 kVp, on to sheets of tungsten. The excited beam was defined by an aperture in a lead diaphragm and allowed to fall on the proportional counter. Filters were placed in turn over the aperture and spectral scans performed. In order to allow for variations in output of the X-ray set, several repeats were made of each scan. Some continuous radiation was present to form a baseline on the spectrum, and it was difficult to determine the position of this, particularly as the filter would introduce a discontinuity at the energy of the absorption edge. After the best estimate of the baseline had been made, areas under the peaks were measured, and means taken. The ratio of the transmission of the Kα peak in the thulium filter to that in the ytterbium filter was 0.87.

Since the transmission of the ytterbium filter as measured with the americium source was 0.54, this implies that the transmission of the Kα lines through the thulium filter was 0.47. The erbium transmission was 0.12, so the pass band transmission for the thulium - erbium pair would be 0.35, instead of 0.44 as assumed. The ratio of these figures, 1.26, may be applied as a correction to the values of Kα/total radiation in Figure 40, to give the curves in Figure 41 (full lines). For comparison, the curves from Figure 38, derived from the ytterbium - erbium pair, are superimposed. It is seen that the agreement is good, confirming the deductions concerning the amount of $K\alpha_1$ radiation/

radiation escaping the thulium edge.

A further check was made on the relative transmissions of the thulium and ytterbium filters at the Kα energies by using a thallium-204 β source to excite characteristic radiation from a sheet of tungsten. Once again the filters were placed in turn over an aperture between the source and the proportional counter. As the intensity was rather low it was necessary to have the detector quite close to the source, so the geometry was not good. However, it was possible to use the pulse height analyser associated with the ratemeter to exclude the fluorescent radiation excited in the filter. The analyser was set just to include the tungsten Kα peak, and count rates recorded with and without the different filters in position. Once again the attenuation was greater in the thulium, the ratio of transmissions being 0.89, in reasonable agreement with the figure of 0.87 obtained from the X-ray measurements. The experiment was repeated using tantalum as the target. This gave a Kα peak well clear of the thulium absorption edge and served to check on the similarity of the filters to radiation of energy just below that of the absorption edges. The measured transmissions were only 1% different.

3.17 Discussion of results of balanced filter measurements

Many factors enter into the assessment of the accuracy of the determination of the ratio of characteristic to total radiation, as expressed in Figures 38, 39 and 41, but the chief one is the degree of balance obtainable for parts of the spectrum outside the pass band. It has been seen that perfect balance was unobtainable over a range of operating voltages, even before the Ross filters were introduced. Causes of such variation of balance with quality have been suggested and a method devised for correcting them.

Nevertheless/

Nevertheless, the amount of characteristic radiation within the pass band is a small proportion of the total, and errors of balance are correspondingly more important. There are no means of correcting for the residual lack of balance observed in the measurements with radiation outside the pass band. In general this was no more than 3% of the maximum pass band transmission, but of course represented a bigger proportion of the lower values.

The procedures for obtaining balance either side of the pass band need critical examination. There is no doubt that operation of the X-ray set at 60 kVp gives radiation that is entirely of energy below that of the pass band. However, the spectral shape will not be the same as for the same energy band with higher operating voltages, and there is no guarantee that balance will be maintained. The calculated attenuation coefficients gave results that were encouraging in this respect, suggesting that a balance obtained at a given effective energy would be maintained over a wider range.

Turning to the check of balance at the high energy side of the pass band, we rely on calculations based on published scintillation spectra to ensure that no radiation lies within the pass band itself. While there seems no doubt that this is true in theory, in practice there will be some degraded radiation from scatter with air and other materials between the lead filter and the Ross filters. The amount of this contributing to radiation within the pass band cannot be assessed, though it is likely to be small in comparison with the high energy beam itself. Again, the spectral shape of the balance-checking radiation will be different from the high energy part of the beam under examination.

Errors of measurement can be more easily assessed. The accuracy of measurement of the ionization currents was limited more by the stability

of/

of the X-ray set output than by the electrometer. Repeated measurements agreed well, usually within 3%. The correction for the amount of continuous radiation within the pass band introduces another possible source of error. As described in section 3.14, this correction was based on scintillation spectra published by Hettinger and Starfelt. Particularly for the higher energies, one cannot be certain of the position of the continuous baseline of the spectrum, and this may introduce an error. However, at higher energies the characteristic radiation constitutes a large proportion of the total in the pass band, so errors in its assessment are minimised. It is unlikely that the error involved in the estimation of the contribution of continuous radiation exceeds 5%.

The other factor entering into the derivation of the ratio of characteristic to total radiation is the transmission of the pass band. The measured value for the most important filters, the ytterbium-erbium pair, was determined with the greatest accuracy, since it was possible to use the americium-241 source to give radiation of essentially the required energy. The accuracy was probably within 2%. For the derivation of the pass band transmissions for the other pairs of filters it was necessary to make corrections for the fact that the pass band energy was different from that used to measure the transmission. Even so, the accuracy should not be much worse than that for the ytterbium-erbium pair.

As previously mentioned, the most reliable results are likely to be those from the ytterbium-erbium pair, in spite of the fact that they are not of adjacent atomic number, and therefore more subject to errors of balance, and containing more continuous radiation within the pass band. This is because

a/

a fraction of the $K\alpha_1$ peak escapes the thulium edge, and the correction for this probably introduces more error than those found with the ytterbium-erbium pair. Nevertheless, the good agreement obtained between the corrected results for the three pairs of filters is heartening, and confirms the validity of the method and corrections used. For all the filter pairs and for all the degrees of primary beam filtration the measurements at lower tube voltages are less accurate than those at higher kVp because the actual amount of characteristic radiation is much less, even though under some conditions it constitutes a higher proportion of the total.

Because of the uncertainties regarding the degree of balance, a figure of overall accuracy cannot be suggested, but apart from this consideration, the error in determining the ratio of $(K\alpha_1 + K\alpha_2)$ to total radiation should be less than 10% for the highest tube voltages, becoming greater at lower energies.

A comparison between the results from the Ross filter experiments and those from the work with the proportional counter and from other sources will be made in Chapter 5.

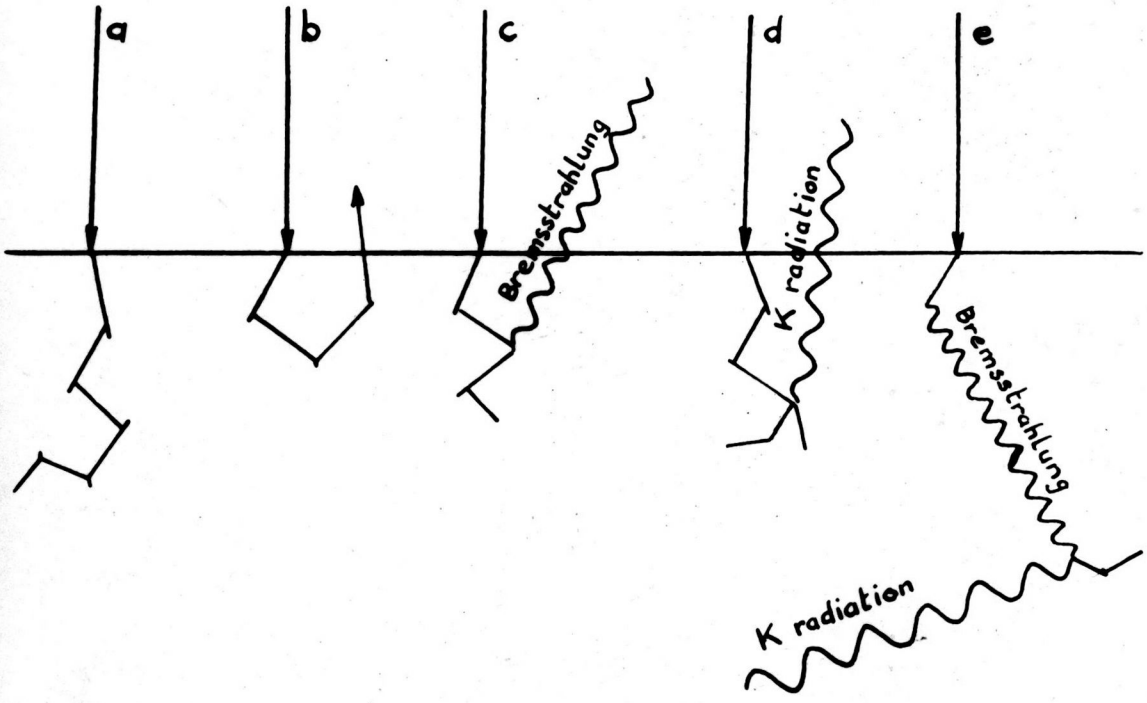
a
b
c
d
e
Bremsstrahlung
K radiation
Bremsstrahlung
K radiation

Figure 42

CHAPTER 4

Theoretical calculations of the ratio of characteristic to continuous radiation

4.1 Introduction

When high speed electrons strike a target, their energy may be dissipated in a number of ways. Some of the possibilities are illustrated in Figure 42. In general, the electrons will be scattered many times and follow a very tortuous path in the target material. The majority behave as at (a), the electron undergoing multiple non-radiative interactions with the electrons of the target material until all its energy has been dissipated as heat. During this multiple scattering, some electrons re-emerge from the target surface, as at (b). The third type of behaviour is illustrated at (c), where the electron, passing close to a nucleus, has given up part of its energy in the production of bremsstrahlung, to contribute to the continuous spectrum. Alternatively, a target atom may be ionized, leading to the emission of a photon of characteristic radiation, (d). Finally, a photon of bremsstrahlung may penetrate into the target; there is a chance that it will in turn give up its energy in the fluorescent production of a characteristic photon, (e).

Calculation of the amount of characteristic and continuous radiation emitted in a given direction is complicated by the diffusion of electrons in the target, and by self absorption of X-ray photons. No theoretical study has taken into account all the possible effects, and it is necessary to make simplifying assumptions. We shall be helped in our particular case by the fact that we need consider only one target material, one target angle and a limited range of electron energies. The main value of such calculations is likely to be an assessment of the relative importance of various parameters.

4.2/

4.2 Other studies

Most analyses of the production of characteristic radiation have considered relatively low energy electrons and low to medium atomic number target materials. The higher values we shall deal with lead to an increased proportion of indirect characteristic radiation production and increased problems of self absorption.

In one of the more important studies of the production of characteristic radiation, Worthington and Tomlin (1956) assume a straight line penetration of electrons into the target. They conclude, however, that electron scattering must be an important factor in determining the intensity of X-ray emission and that more quanta are emitted close to the surface than their calculations suggest. Use is made of Bethe's non-relativistic expressions for electron stopping power and ionization cross-section. These are considered adequate up to electron energies of 80 keV; they would not suffice in our case. Allowance is made for self absorption, based on the deduced relationship between electron energy and depth. Numerical evaluation of the resulting integrals is necessary. Indirect K X-ray production is allowed for in an all-embracing correction factor derived from experimental data.

In another recent study, Green and Cosslett (1961) avoid the need to assume an electron trojectory by ignoring target self-absorption. Experiments show that over the range of energies and materials considered, the error introduced is small, being less than 10% if $Z\ E_o/E_K$ is less than 100, where Z is the atomic number of the target material, E_o the electron energy, and E_K the K ionization energy. In our case $Z\ E_o/E_K$ may be up to 250, so the assumption is unjustified. Once again Bethe's formula for total ionization cross-section is used, but to simplify integration, his energy loss relationship

is/

is discarded in favour of the experimental Thomson-Whiddington formula. Indirect ionization is calculated by assuming that the origin of the continuous radiation is close to the surface compared with the range of continuous quanta in the target, so that half the bremsstrahlung is absorbed in the target. Kulenkampff's expression is used for the energy distribution of the bremsstrahlung.

Since indirect production of characteristic radiation is likely to play an important part in our case, and Green and Cosslett's method offers a better opportunity of assessing it, it seems worthwhile to consider how far their assumptions and approximations are justified, and whether their method needs any modification.

4.3 Self absorption of directly produced K radiation

We need to know the effective depth of K characteristic production. The Thomson-Whiddington energy loss relation (Whiddington 1912) gives the range of electrons capable of ionizing a target atom, x_k , from the equation $E_o^2 - E_k^2 = c\rho x_k$, where ρ is the density and c a parameter that changes rather slowly with E_o . Green and Cosslett compiled a table of values of c from the experimental data of various workers, but did not consider energies greater than 50 keV.

Klemperer et al (1960) derive an expression for c from Bethe's energy loss relation which gives values that agree well with experimental results at 25 and 50 keV. Their expression has therefore been used to obtain c for higher energies; ρx_k can then be calculated for a number of values of E_o .

TABLE 8

E_o (keV)	100	150	200	250
c $(keV^2 . cm^2 . g^{-1})(x\ 10^{-5})$	5.4	5.7	5.9	6.1
ρx_k $(g . cm^{-2})$	.010	.031	.059	.094

Green (1963) has shown in a Monte Carlo calculation of characteristic X-ray production in copper that takes into account the diffusion of electrons in the target, that virtually all the direct K-shell ionizations occur in less than half the effective electron range, and the bulk of them in less than a quarter. In our case, then, the deepest value for effective production is probably less than $\rho x = .02$.

With a 30^o target, the path length for characteristic radiation emission is $x \cot 30^o = 1.7x$ if x is measured in the direction of the incident electrons. μ/ρ for K_α radiation in tungsten = 3.0, therefore the maximum likely attenuation is given by $\mu t = 3.0 \times .02 \times 1.7 = .10$. This leads to a transmission of .90, so we are justified in following Green and Cosslett and ignoring self absorption of the directly produced K radiation, since other uncertainties are likely to introduce errors exceeding 10%.

4.4 Relativity effect on ionization cross section

This was ignored by Green and Cosslett and also Worthington and Tomlin, since they were primarily concerned with relatively low energy electrons. We must examine how much it alters the calculations at higher energies. Mott and Massey (1949) derive from Bethe's (1930) expression both a relativistic and non-relativistic formula for the ionization cross section, Q_k. Using

Green/

Green and Cosslett's notation, these are:

$$Q_k = \frac{2\pi e^4}{E E_k} \; b \left[\ln \frac{4E}{B} - \ln\left(1 - \frac{v^2}{c^2}\right) - \frac{v^2}{c^2} \right]$$

$$\text{and} \quad Q_k = \frac{2\pi e^4}{E E_k} \; b \; \ln \frac{4E}{B}$$

where e is the electronic charge, $B = 1.65\ E_k$ and $b = 0.35$. v is the electron velocity and c the velocity of light.

It is worth while evaluating the expression in squared brackets for a number of electron energies to examine the effect of the relativistic term.

TABLE 9

keV	$\frac{v}{c}$	(1) $\ln\left(\frac{4E}{B}\right)$	(2) $- \ln\left(1 - \frac{v^2}{c^2}\right) - \frac{v^2}{c^2}$	% effect of term (2)
100	.548	1.241	+ .057	4.5
150	.635	1.579	.113	7.3
200	.695	1.934	.177	9.0
250	.740	2.159	.247	11.6

We are concerned with electrons whose energy will range from that of the incident beam, E_o, to the ionization energy, E_k, so the average energies will be less than those used in the above calculation. If the initial energy is 250 keV, the relativity effect will be less than 11.6%, and so on for the other energies. It seems reasonable, therefore, to ignore it.

Green and Cosslett actually use a modified form of the ionization cross section equation that fits experimental data better, but the above arguments regarding relativity are not affected.

4.5 Direct ionization

It seems, therefore, reasonable to use Green and Cosslett's method for calculating direct ionization per electron, n_k (direct). Their final formula is

$$n_k \text{ (direct)} = 9.535 \times 10^4 \frac{R}{A_c} \left[U_o \ln U_o - (U_o - 1) \right]$$

where A is the atomic weight of the target material, c the constant in the Thomson-Whiddington equation already mentioned, U_o the ratio E_o/E_k, and R a figure introduced to allow for back scattering of electrons. It is not clear that the inclusion of R is valid for an X-ray tube, since presumably a backscattered electron will either return to the target under the influence of the electric field, and there make its contribution to interactions, or escape to the tube walls and not contribute to the measured tube current. In any case, we are concerned with a ratio of characteristic to continuous radiation, and both will be affected by loss of electrons by backscattering, so we shall ignore R .

Using the values of c already established, we can calculate n_k (direct)

TABLE 10

keV	100	150	200	250
U_o	1.43	2.15	2.85	3.60
n_k (direct)(x 10^{-5})	8	46	102	170

4.6 Penetration of continuous quanta into the target

Turning to the indirect production of characteristic radiation, we need to examine Green and Cosslett's assumption that the origin of the continuous radiation is close to the surface of the target compared with the range of the continuous quanta in the target material. This seems likely, as only the higher energy radiation is effective, and the electrons will not have penetrated far into the target before giving rise to such radiation. It may be useful to have quantitative confirmation of this argument.

Farr (1955) estimates that the effective depth of production of X-rays at 250 kV in tungsten is 5 μm. This corresponds to 0.01 $gm.cm^{-2}$. Stoddard (1935) gives figures for the mean depth of production of continuous radiation in gold which correspond to $\rho x = 0.011$ at 150 kV, and 0.016 at 180 kV. These figures can be compared with the value of 0.02 $gm.cm^{-2}$ derived earlier as the maximum likely effective depth of production of direct k radiation. Since we are concerned with higher energy radiation, a shallower depth is to be expected.

The maximum value of $\frac{\mu}{\rho}$ for tungsten at wavelengths below that of the K absorption edge is about 10 $cm^2.g^{-1}$. If we assume an attenuation to 0.1, $\rho x = 0.23$, much greater than the effective depth of continuous radiation production. It is reasonable, therefore, to assume that the continuous quanta are produced close to the surface in comparison with their penetration into the target. However, this depth of penetration of the continuous radiation does suggest that absorption of indirectly produced characteristic radiation may be too much to ignore.

4.7/

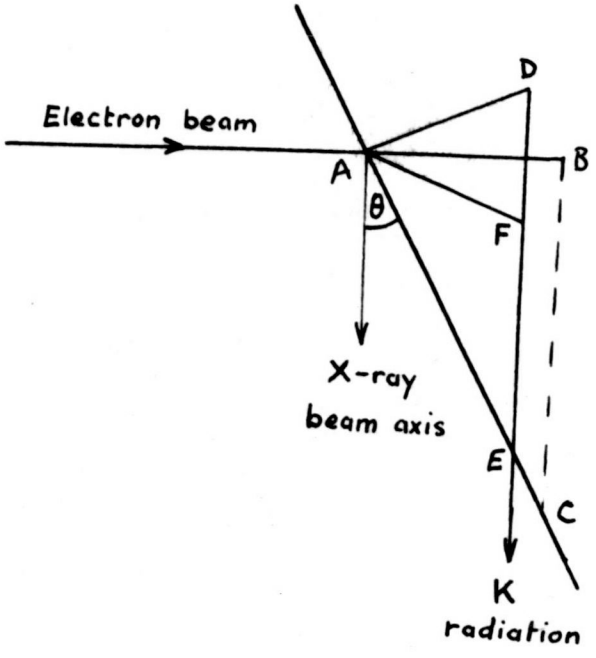

Figure 43

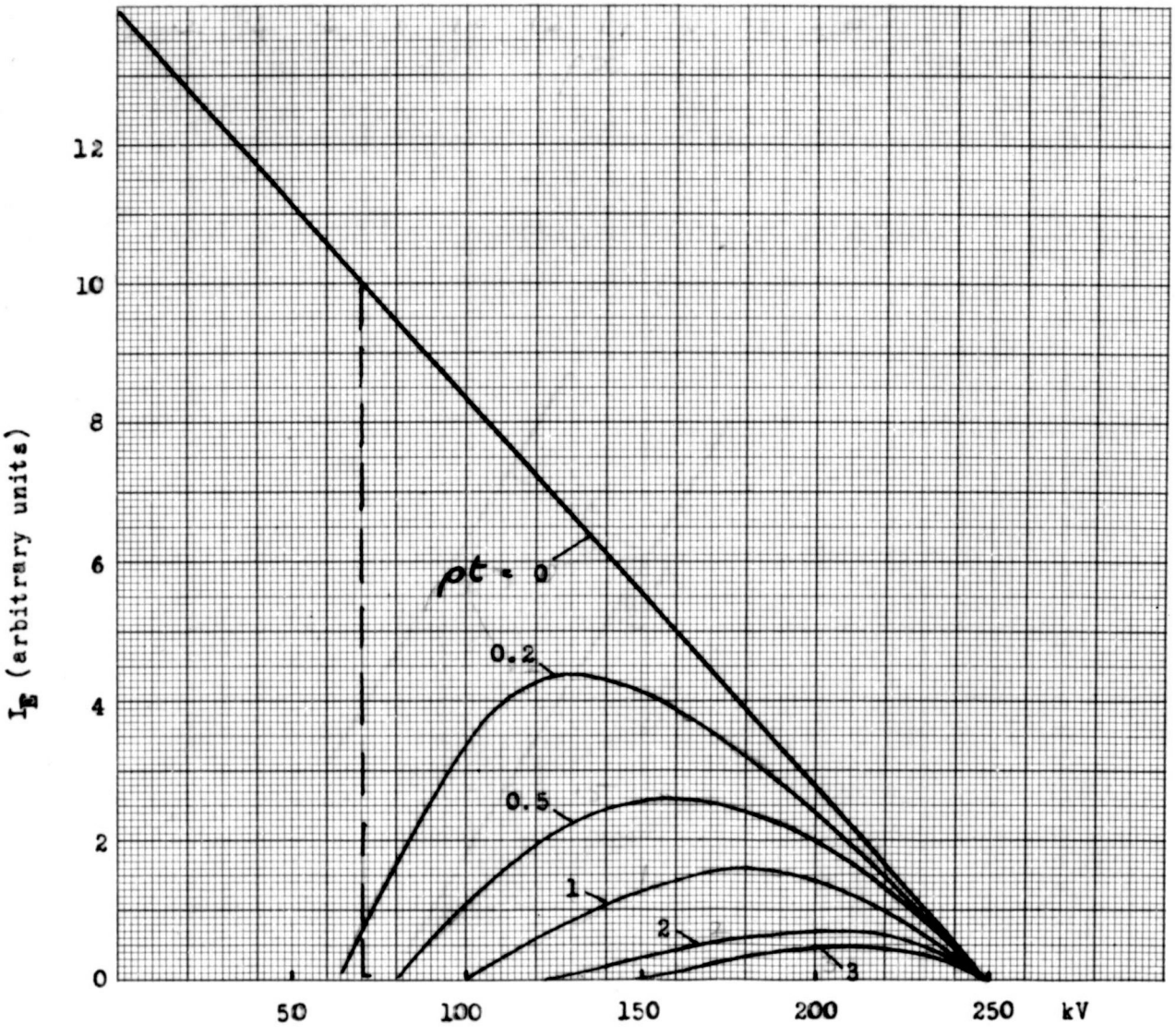

Figure 44

4.7 Self absorption of indirectly produced characteristic radiation

This subject is not very amenable to generalised analytical treatment, as consideration has to be given to attenuation of the continuous radiation as it penetrates the target, and changes in its spectral distribution, as well as attenuation of the characteristic radiation in emerging from the target. Numerical calculation is possible, however, if some simplifying assumptions are made. Consider Figure 43.

It is assumed that the continuous radiation is emitted close to the target surface, (e.g. at A), and that its distribution is isotropic. We have already shown that the first assumption is reasonable. The second also is likely. As soon as electrons have undergone a few deviations, their direction, and therefore that of the bremsstrahlung is likely to be random. Continuous quanta arising from relatively undeviated electrons will be mostly emitted at an angle to the direction of the electron beam, but this direction is just as likely to be A F as A D, and the relatively long path length, D E, for K radiation emitted at D will be offset by the shorter path F E for other K photons.

Assume that the energy distribution of the bremsstrahlung follows the Kulenkampff-Kramers relationship, $I_E = K (E_o - E)$ where I_E is the intensity per unit energy interval and K a constant (see section 4.10). Penetration of the X-rays to a distance t will cause attenuation, particularly of the lower energies. We can calculate the attenuation for different energies and various depths and produce a family of spectra (Figure 44). This calculation was performed for several values of incident electron energy. The ability of the continuous radiation to ionize the K shell of a target atom

after/

after penetrating a distance t is governed not only by the total intensity at that distance (the area under the curves in Figure 44), but also by the effective quality of the beam at that distance, as revealed by the spectral shape. The chance of an absorption of a quantum of a given energy is proportional to the photoelectric absorption coefficient (τ) at that energy, so we can assign to each of the spectra in Figure 44 a value proportional to its ability to cause K shell ionization, by calculating the sum of the products of ordinate height and τ. We consider only the parts of the spectra of energy greater than 70 keV, the K absorption edge of tungsten. Taking the value for the unattenuated spectrum as unity, values for the spectra for other distances of penetration can be plotted against distance to give a transmission curve of effective continuous radiation in the target material (Figure 45).

Now we consider a plane parallel to the target surface at a depth x (Figure 46). All characteristic radiation arising in this plane and emerging in the direction of the X-ray beam has to traverse the same thickness of target, $x \cot \theta$, which $= 2x$ for $\theta = 30^{\circ}$. Continuous radiation reaching this plane from A has traversed a thickness of $x \sec \phi$ where ϕ is the angle between the direction considered and the perpendicular from the target face. The total radiation reaching the plane will be the integral over 2π of the radiation per unit solid angle at angle ϕ, taking into account the attenuation. Since the distribution is symmetrical about the perpendicular line, we can, for each of a range of values of x, integrate numerically from $\phi = 0$ to $\phi = 90^{\circ}$, deriving the attenuation appropriate to each value of $x \sec \phi$ from the curve already deduced for the particular accelerating voltage, (Figure 45). In this

way/

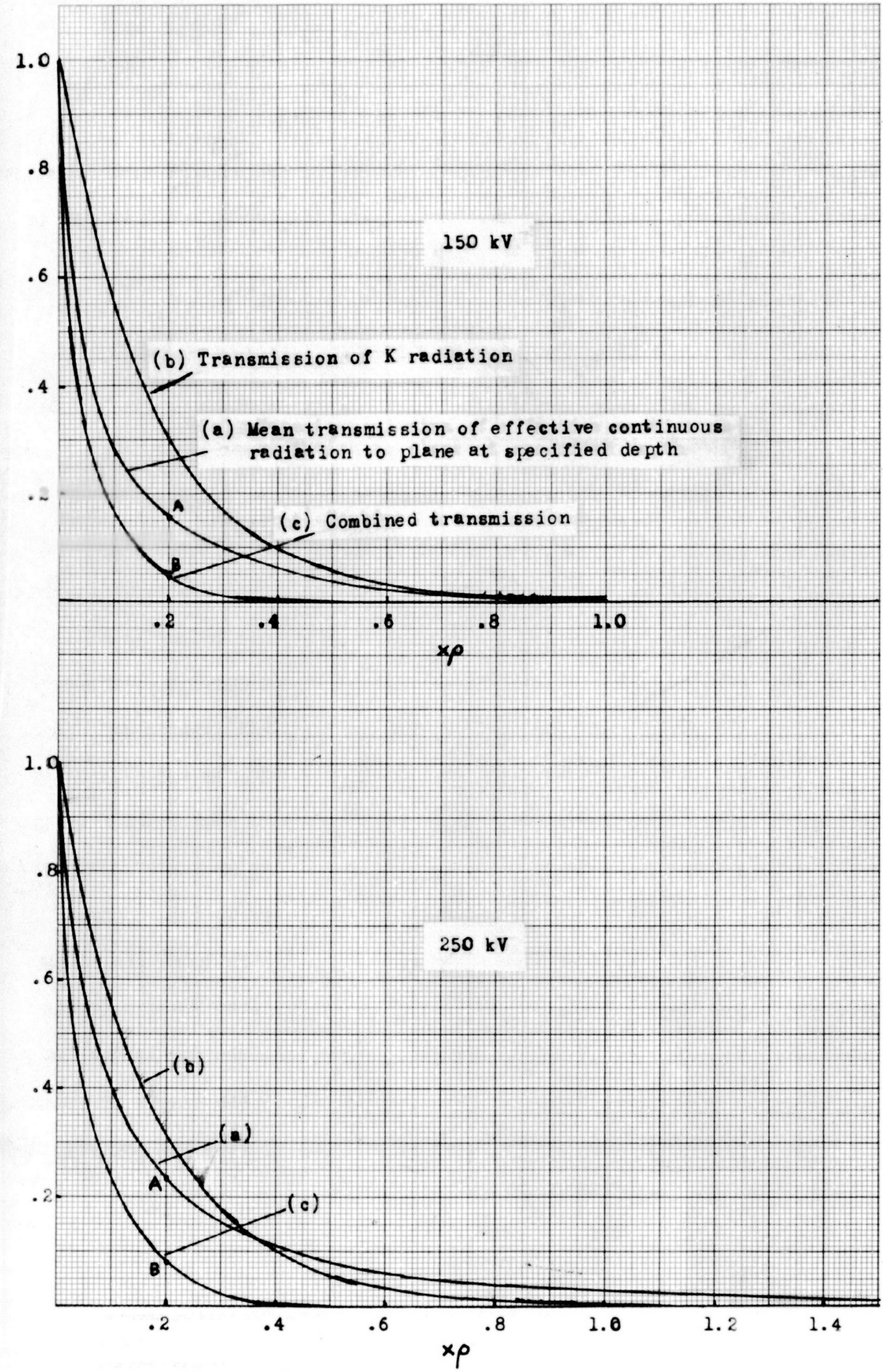
1.0
.8
.6
.4
.2
150 kV
(b) Transmission of K radiation
(a) Mean transmission of effective continuous radiation to plane at specified depth
(c) Combined transmission
A
B
.2
.4
.6
.8
1.0
xρ
1.0
.8
.6
.4
.2
250 kV
(b)
(a)
(c)
A
B
.2
.4
.6
.8
1.0
1.2
1.4
xρ

Figure 47

way, after rather extensive calculations, we can arrive at a mean attenuation for each depth of plane, and can plot this against x, as is shown at (a) in Figure 47.

As already mentioned, K radiation coming from a depth x passes through a thickness 2x beforeemerging. We can calculate the attenuation corresponding to each value of x ; this curve is also plotted, at (b), in Figure 47. The combination of the two degrees of attenuation is also plotted, (c). In the absence of any attenuation of the characteristic radiation the intensity of K lines arising from a particular depth would be proportional to the intensity of effective continuous radiation at that depth, as derived from 47(a). The total intensity of K radiation would be proportional to the sum of that from each depth, i.e. to the area under curve (a). Because, in fact, the characteristic radiation is attenuated, that arising at a given depth such as $x\rho = 0.2$ in Figure 47, and therefore having an intensity proportional to the height A, is reduced to an intensity proportional to the height B before emerging. The total intensity of emerging K characteristic radiation will then be proportional to the area under curve (c). Thus, attenuation reduces the intensity of K radiation by the ratio of the areas under curves (a) and (c). The deeper penetrating continuous radiation is largely wasted as far as K fluorescence is concerned, since the latter has a small chance of leaving the target. This reduction of the amount of escaping K radiation has been calculated for a number of initial electron energies and the results are presented in Table 11.

TABLE 11

kV	100	150	200	250
Transmission of indirect K radiation in target	.59	.44	.39	.37

It will be seen that the degree of attenuation is considerable, particularly at higher energies.

4.8 Indirect ionization

Making use of this assessment of absorption, we can now calculate the amount of indirect ionization by Green and Cosslett's method. We have shown that their assumption that the origin of the continuous radiation is close to the surface is reasonable in our case, and this leads to half the number of continuous quanta being available for fluorescent characteristic production. If r_k is the ratio of the photoelectric absorption coefficient on the high energy side of the k absorption edge to that on the low side, then the fraction of absorptions which cause K shell ionization is $(r_k - 1)/r_k$. For tungsten this fraction is 0.82. Then number of K shell ionizations per electron, $n_k = 0.5 \times 0.82\ N$ where N is the number of continuous quanta per electron with energies greater than the K ionization energy. Green and Cosslett derive N from integration of the Kulenkampff-Kramers energy distribution as adapted by Dyson (1959b). This leads to

$$N = 2.76 \times 10^{-6}\ Z\ E_k \left[U_o \ln U_o - (U_o - 1) \right]$$

from which we can calculate the values of n_k (indirect) shown in Table 12, and apply the corrections for K attenuation already deduced.

TABLE 12

kV	100	150	200	250
n_k (indirect) ($\times 10^{-5}$)	48	295	680	1180
K transmission	.59	.44	.39	.37
Ionizations leading to K emission ($\times 10^{-5}$), n_k (indirect, effective)	28	130	265	437

4.9 Total emission of K radiation

The results presented in Tables 10 and 12 can be combined to give the total number of K shell ionizations, and by bringing in the fluorescence yield, ω_k , the total K radiation emission per electron, N_k , can be deduced. ω_k for tungsten = 0.94

TABLE 13

kV	100	150	200	250
n_k (direct)(x 10^{-5})	7	46	102	170
n_k (indirect, effective)(x 10^{-5})	28	130	265	437
N_k (x 10^{-5})	33	165	345	570

It may be noted that in practice we are concerned with the number of quanta per unit solid angle in a particular direction rather than the total number emitted, but as we shall derive a ratio, the correction factor will cancel out.

4.10 Emission of continuous radiation

The starting point of this calculation is the Kulenkampff-Kramers energy distribution already referred to. This relation was found experimentally by Kulenkampff (1922) for the production of X-rays up to 40 kV in a thick target, and was derived theoretically by Kramers (1923). The formula has been found more recently (ICRU, 1964) to agree well with experimentally determined spectra over a wide energy range, when allowance is made for self-absorption in the target and attenuation in the tube window and housing. The formula can be expressed as $I_E = A\ (E_o - E)$, where I_E is the intensity distribution function, E the/

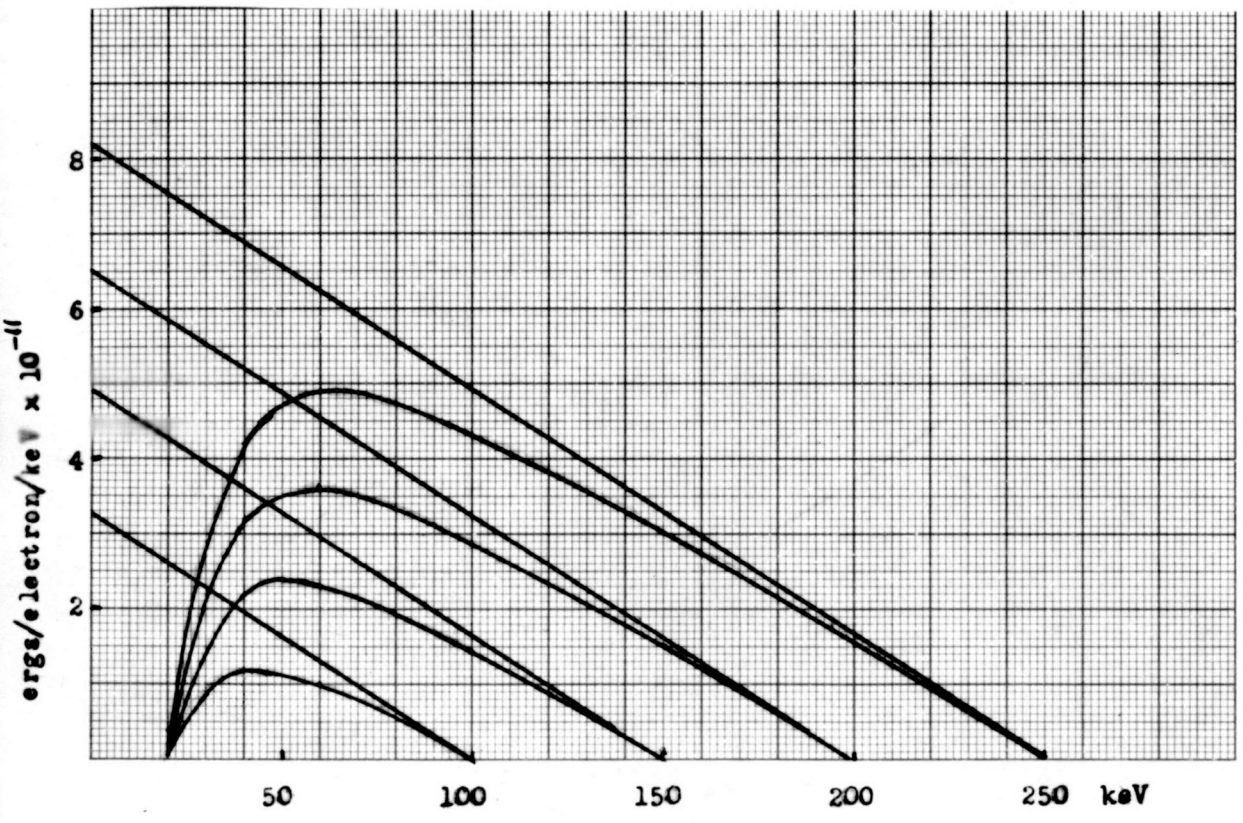

Figure 48

the photon energy at which I_E is evaluated and E_o the maximum value of E . A is a constant, and was quoted by Green and Cosslett as being $2.76 \times 10^{-6} Z$, when I_E is expressed as keV/electron/keV energy interval. Using Z = 74 and the more usual unit for energy, the erg, instead of keV, the constant = 3.25×10^{-13}.

Using this formula, we can plot the energy distributions at several values of accelerating voltage (straight lines in Figure 48). These spectra will be subject to attenuation, both within the target itself and in the tube window and housing. Target self absorption is difficult to assess, since it involves a knowledge of the variation with depth of the quantity and also the spectral distribution of the continuous radiation. Higher energy radiation is virtually unaffected, as it is produced close to the target surface and attenuation coefficients are low. The effective depth of production will vary both with the photon energy considered, and the incident electron energy, E_o . If we take as previously, a mean effective depth of 0.01 g/cm^2, and a target angle of 30^o

100	keV	radiation	is	attenuated	to	.92
80	"	"	"	"	"	.86
60	"	"	"	"	"	.93
40	"	"	"	"	"	.85
20	"	"	"	"	"	.34

The inherent filtration of the Siemens tube is stated to be equivalent to 2 mm aluminium. We can combine the attenuation due to this with that derived for target self-absorption and use the figures to obtain the corrected spectra shown in Figure 48. With these assumptions, the target attenuation/

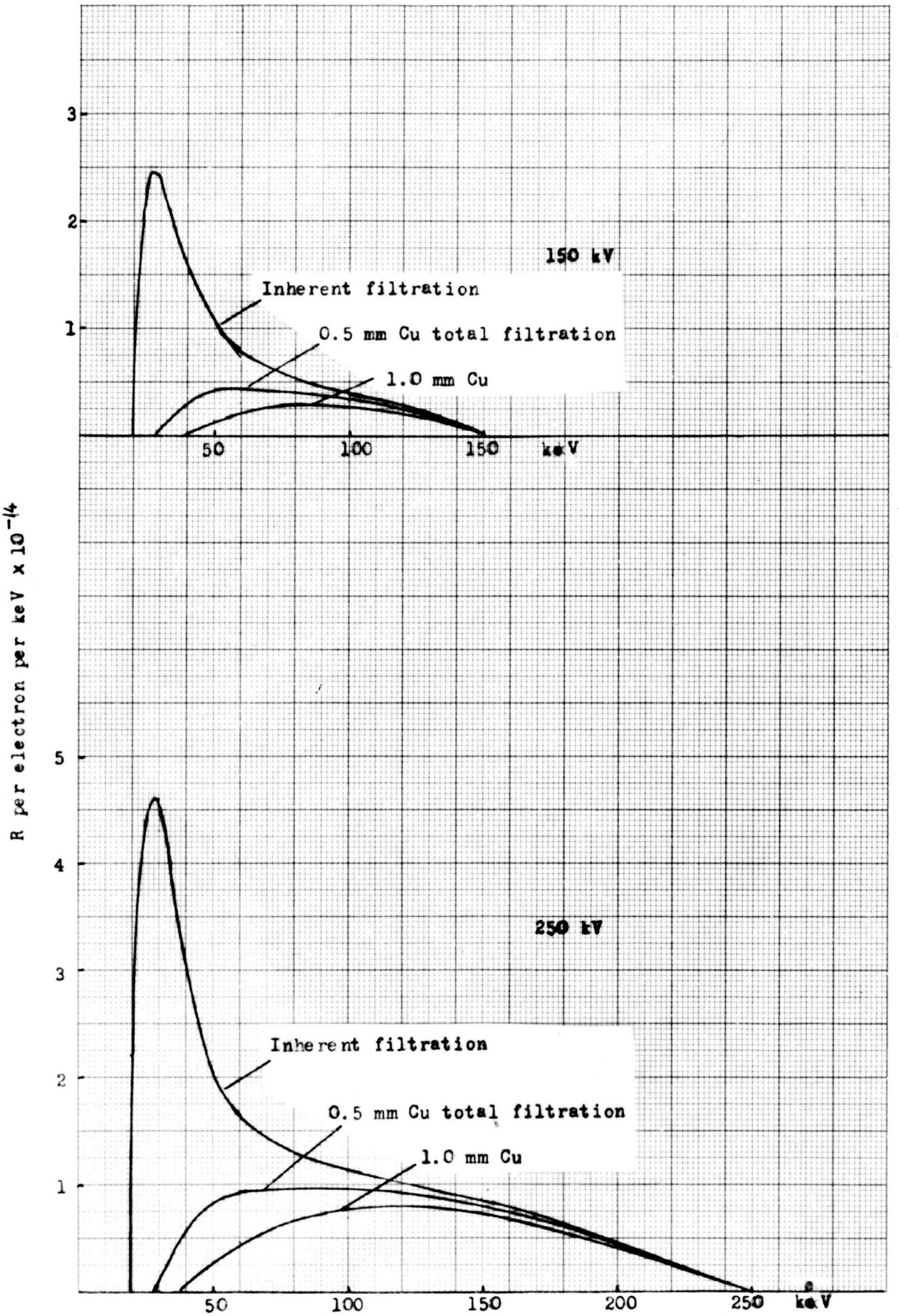
150 kV
Inherent filtration
0.5 mm Cu total filtration
1.0 mm Cu
50
100
150
keV
250 kV
Inherent filtration
0.5 mm Cu total filtration
1.0 mm Cu
50
100
150
200
250
keV
R per electron per keV x 10⁻⁴

Figure 49

attenuation is less important than that in the tube window and housing, so accuracy of its assessment does not matter so much. Inspection of unfiltered scintillation spectra confirms this idea.

If it were required to compare characteristic radiation with continuous radiation on a basis of intensity, the spectra shown in Figure 48 would suffice. However, it was pointed out in Chapter 1 that a more useful basis is in terms of exposure, and our experimental determinations have used this basis. It is necessary, therefore, to convert the spectra to those using R/electron/keV as the ordinate, making use of the real absorption coefficients of air. Spectra in these units were calculated for four incident electron energies, two of which are displayed in Figure 49. In addition to spectra for tube filtration only, the effects of additional filtration to bring the total to 0.5 mm and 1.0 mm copper were calculated. By measuring the areas under these curves the total exposures due to continuous radiation can be calculated. The results are shown in Table 14. To determine the ratio of characteristic to continuous radiation, the former has also to be expressed in terms of exposure, instead of numbers of photons. The relevant factor for 60 keV radiation is 313×10^8 photons/cm^2/R. It is also necessary to correct by the factor 0.87 for attenuation of the K radiation by the 2 mm aluminium equivalent inherent filtration. These results also are given in Table 14, together with ratios of total K and Kα radiation to continuous plus characteristic. The results for Kα/total are also presented graphically in Figure 50.

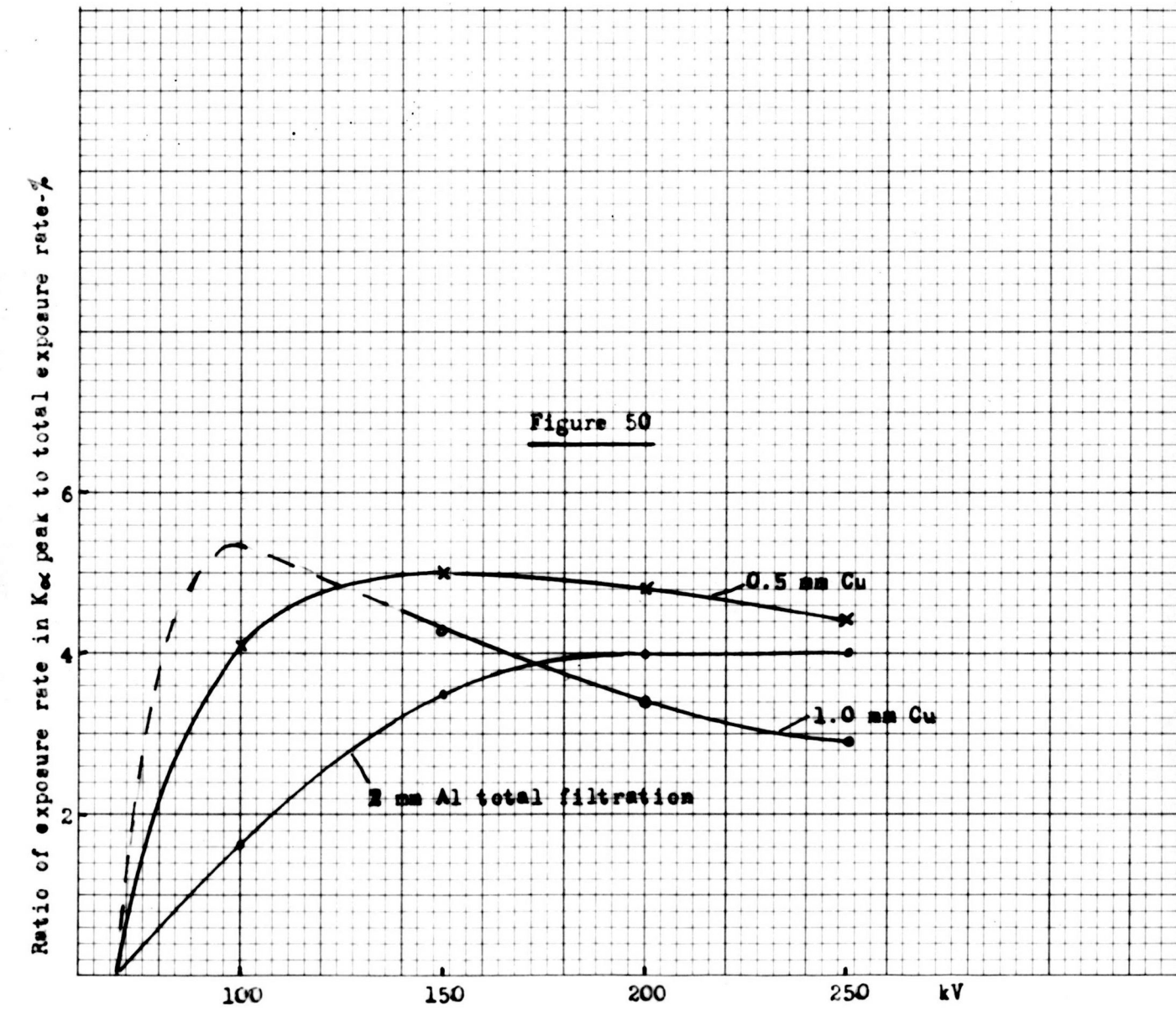
Ratio of exposure rate in Kα peak to total exposure rate-%
6
4
2
0.5 mm Cu
1.0 mm Cu
2 mm Al total filtration
100
150
200
250
kV

Figure 50

TABLE 14

kV	100	150	200	250
2 mm Al total filtration				
Continuous R/electron, x 10^{-14}	43	95	172	270
K radiation R/electron, x 10^{-14}	.92	4.6	9.6	15.9
Ratio K/total, %	2.1	4.6	5.3	5.3
Ratio Kα/total, %	1.6	3.5	4.0	4.0
0.5 mm Cu total filtration				
Continuous R/electron, x 10^{-14}	8.6	36	80	144
K radiation R/electron, x 10^{-14}	.51	2.6	5.5	9.0
Ratio K/total, %	5.5	6.7	6.4	5.9
Ratio Kα/total, %	4.1	5.0	4.8	4.4
1.0 mm Cu total filtration				
Continuous R/electron, x 10^{-14}		21	57	110
K radiation R/electron, x 10^{-14}		1.3	2.7	4.4
Ratio K/total, %		5.8	4.5	3.9
Ratio Kα/total, %		4.8	3.4	2.9

4.11 Discussion of results of calculations

Figure 50 can be compared with the experimental determinations of Kα/total radiation, as expressed in Figures 20 and 41 of Chapters 2 and 3. It will be seen that although the variation with operating voltage is similar, the actual values of the theoretical ratios are about 60% of the experimental ones. It is tempting to suggest that there is most scope for error in the assessment of the self-absorption of indirectly produced characteristic radiation.

This/

This is a large correction factor, and a reduction would lead to better agreement with experiment. However, it is thought that the treatment of this topic was fairly comprehensive and did not involve unjustified assumptions.

If the theoretical values of the continuous radiation without additional filtration are plotted against operating voltage on log-log graph paper, a straight line is obtained with a slope showing that the exposure is function of the square of the voltage. The Kulenkampff-Kramers expression implies that the intensity should vary in this way for the completely unfiltered beam, but it was found also to apply to the variation of exposure after allowing for inherent filtration. By contrast, the experimental variation was to the power of 1.6 of the voltage. The slope of this line is very sensitive to filtration, the greater the filtration, the more rapid the increase of exposure with voltage. It may be, then, that we have not used quite the right degree of inherent filtration in the calculations to match the experimental reality. When the theoretical and experimental derivations of filtered continuous radiation are compared, the variation with voltage is much more similar, though the theoretical curves are still slightly steeper.

The variation of characteristic radiation with voltage can be compared in a similar manner, this time plotting the exposure against $E - E_o$ on log-log paper. Again the theoretical graphs are steeper than the experimental ones, though this time, as one would expect, filtration does not change the slope. These comparisons do not suggest that any one factor is primarily responsible for the different between the theoretical and experimental determinations of the ratio of characteristic to total radiation, but/

but rather that there may be differences in several factors.

In view of the number of assumptions and approximations made, it is not surprising that agreement between the theoretical and experimental results is not better. However, the main purpose of the calculations is not necessarily to obtain such agreement, but rather to gain some insight into the factors which determine the relationship between characteristic and continuous radiation. Perhaps the most interesting finding is the importance of indirect production of characteristic radiation. Even when fairly severe self-absorption is taken into account, this is something like two and a half times the emission due to direct characteristic production. The actual indirect ionization is about six times that from direct electron interactions. This is in marked contrast to the findings with lower atomic number target materials and lower accelerating potentials. Here the reverse is true, and direct production predominates.

4.12 Expression of ratios in other units

As we have derived complete spectra for the bremsstrahlung, we can express the ratios of characteristic to continuous radiation in terms other than those of exposure used hitherto. It may be of interest to see what difference this makes. We start with the spectra expressed in terms of energy flux (Figure 48) and can measure the area under the curves to obtain the total continuous radiation in this form. Using the relationship between photon flux and energy flux at 60 keV, we can convert the value for the K characteristic radiation to the same units, and so obtain the ratio required. This has been done for 250 kV tube voltage and the ratio 5.5% obtained for the ratio Kα/total radiation, compared with 4.0% when exposure units are used. Similarly, both

types/

types of radiation can be expressed as photon flux, giving a ratio of 7.2%

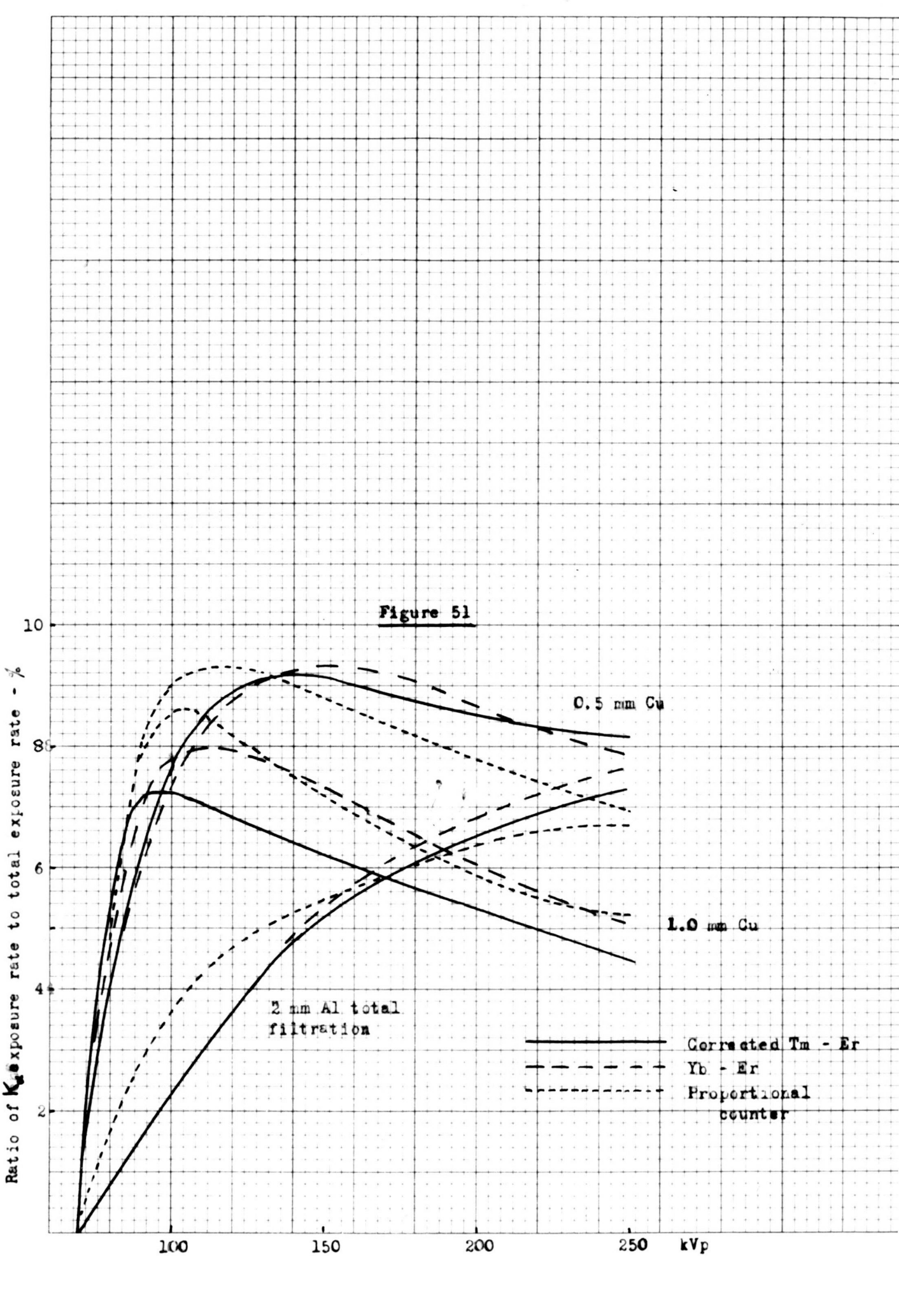
Figure 51
10
8
6
4
2
Ratio of K_a exposure rate to total exposure rate - %
0.5 mm Cu
1.0 mm Cu
2 mm Al total filtration
Corrected Tm - Er
Yb - Er
Proportional counter
100
150
200
250
kVp

CHAPTER 5

Comparisons between results and derivations from them

5.1 Comparison between experimental results

In this final chapter the results from the proportional counter experiments and from the balanced filter studies will be compared with each other and with other published values of the ratio of characteristic to total radiation from a tungsten target. In addition, some other relationships derived from the experiments will be discussed.

The balanced filter results obtained with the ytterbium-erbium pair have already been compared with the corrected thulium-erbium results in Figure 41. These graphs are reproduced in Figure 51, together with the proportional counter results from Figure 20. The agreement is very satisfactory, and as the two methods are very different, it suggests that the values of the ratio are substantially correct in absolute, as well as relative terms.

5.2 Comparison with results of other workers

Before scintillation spectrometry became available, the only estimate of the relationship between characteristic and continuous radiation for tungsten seems to have been by Greening (1947). In developing the method of spectral determination from attenuation data, he proposed a means of correcting for the presence of characteristic radiation. This made it possible to estimate the contribution of the K-radiation. Greening expresses his results as a ratio of the intensities of the K lines to the continuous radiation. Converting to the ratio Kα/total radiation to permit comparison with our results, we obtain:

kV	100	150	200	250
Ratio intensity kα/total	.15	.28	.33	.35

While the shape of the curve is similar to ours for an unfiltered beam, the values of the ratios are much higher, some five times in fact. Considering the ratios in terms of exposure instead of intensity would probably lead to lower values, but a substantial disparity would remain. Greening claims no great accuracy for his estimates, and indeed would not support entirely the validity of the method (private communication). It is of interest to note that Cormack et al (1955) in using Greening's method to obtain a spectrum of 280 kVp, 1.7 mm copper H.V.L. radiation to compare with one determined by scintillation spectrometry, found it necessary to assume that the K characteristic radiation amounted to 15% of the total.

Data derived from scintillation spectrometry provide the other results with which ours can be compared. For example, Cormack et al (1955) estimated that with 280 kVp, 1.73 mm copper H.V.L. radiation 10% of the photons were contributed by K characteristic radiation. However, in a later determination of the spectrum from the same radiation, these workers proposed a figure of 25% (Cormack et al 1958).

The most careful analysis of characteristic radiation from scintillation spectrometry seems to have been made by Hettinger and Starfelt (1958). Expressed as number of K-photons per total number of photons, they give ratios of 0.10 at 100 kV, 0.145 at 150 kV, 0.165 at 200 kV and 0.18 at 250 kV for radiation from an X-ray tube with inherent filtration equivalent to 4 mm aluminium, but no additional filtration. In order to compare these results with ours it is necessary to convert their published spectra to ordinates/

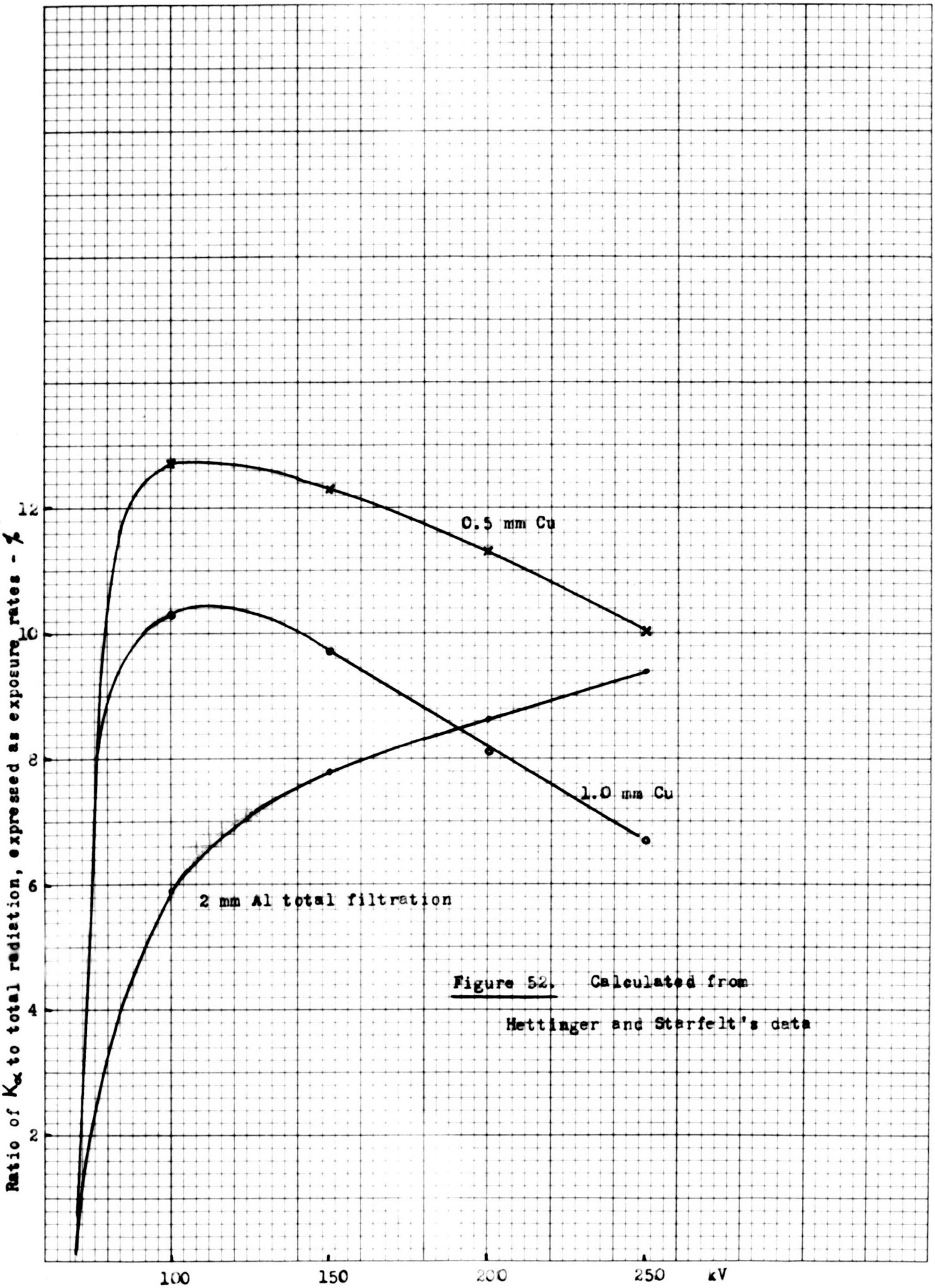

Figure 52. Calculated from Hettinger and Sterfelt's data

ordinates of exposure instead of photon flux, and also to allow for the differences in inherent filtration. The latter was achieved by dividing each ordinate by the transmission in 2 mm aluminium for the appropriate energy. In addition to the spectra for an unfiltered beam, the effect of the addition of 0.4 mm and 0.9 mm copper was calculated. Areas under the curves corresponding to the characteristic peak and also the continuous radiation were measured, and ratios of Kα/total radiation were calculated, assuming that the Kα lines constitute 75% of the total K radiation. The results are presented in Figure 52.

It will be seen that although the curves are similar in shape to ours, the values of the ratios are generally some 40% higher (compare with Figure 51). Because of the relatively poor resolution of a scintillation spectrometer, it is not always easy to draw in the line corresponding to the continuous radiation under the characteristic peak. This would reduce the accuracy of determination of the ratio. However, errors introduced by such considerations are not likely to be large or consistent enough to account for the discrepancy. Errors in the assessment of inherent filtration, for which one must rely upon the manufacturer, might lead to sizeable differences in the ratio of characteristic to total radiation for beams with no added filtration. The low energy end of the spectrum is particularly enhanced when expressed in terms of exposure, and is, of course, most affected by filtration. However, these differences would become less for filtered beams. In the present case, there is nearly as much difference between our experimental results and those derived from Hettinger and Starfelt's data for filtered as for unfiltered beams, so inherent filtration is unlikely to account for the disparity.

One respect in which our X-ray apparatus differed from that used by Hettinger and Starfelt was in the target angle, this being 30° for our Siemens tube and quoted by the manufacturers as 21½° for the Philips tube used in the Swedish experiments. Hettinger and Starfelt do not state the direction of their beam relative to the tube axis, but it is assumed that, as in our experiments, it was perpendicular to the direction of the electron beam, so that the target angle assumed its normal importance. It can be expected that this angle will influence the ratio of characteristic to total production, although in a direction opposite to that necessary to explain the present differences, since indirectly produced K-radiation is likely to be most affected by the increased attenuation consequent upon a steeper target angle.

Hettinger and Starfelt used the whole focus for their collimated beams, while the centre portion only was used with the proportional counter in our experiments. However, there was no systematic difference between the counter results and those using balanced filters, and Cormack and Burke (1960) showed that different parts of the focus gave the same spectral shape, even when the intensity was very different. This factor is therefore unlikely to contribute to a difference.

One factor that might contribute to a difference, but which cannot be assessed, is the condition of the target. Kuntke (1957) has shown that the radiation yield of an X-ray set decreases with operating time, owing to increasing roughness of the target, which increases the electron backscatter and absorption of X-rays within the target. However, as with the effects of filtration and target angle, the low energy part of the spectrum is most affected, and again differences due to this factor would be expected to be much less important for beams with additional filtration. While one or more of the

factors/

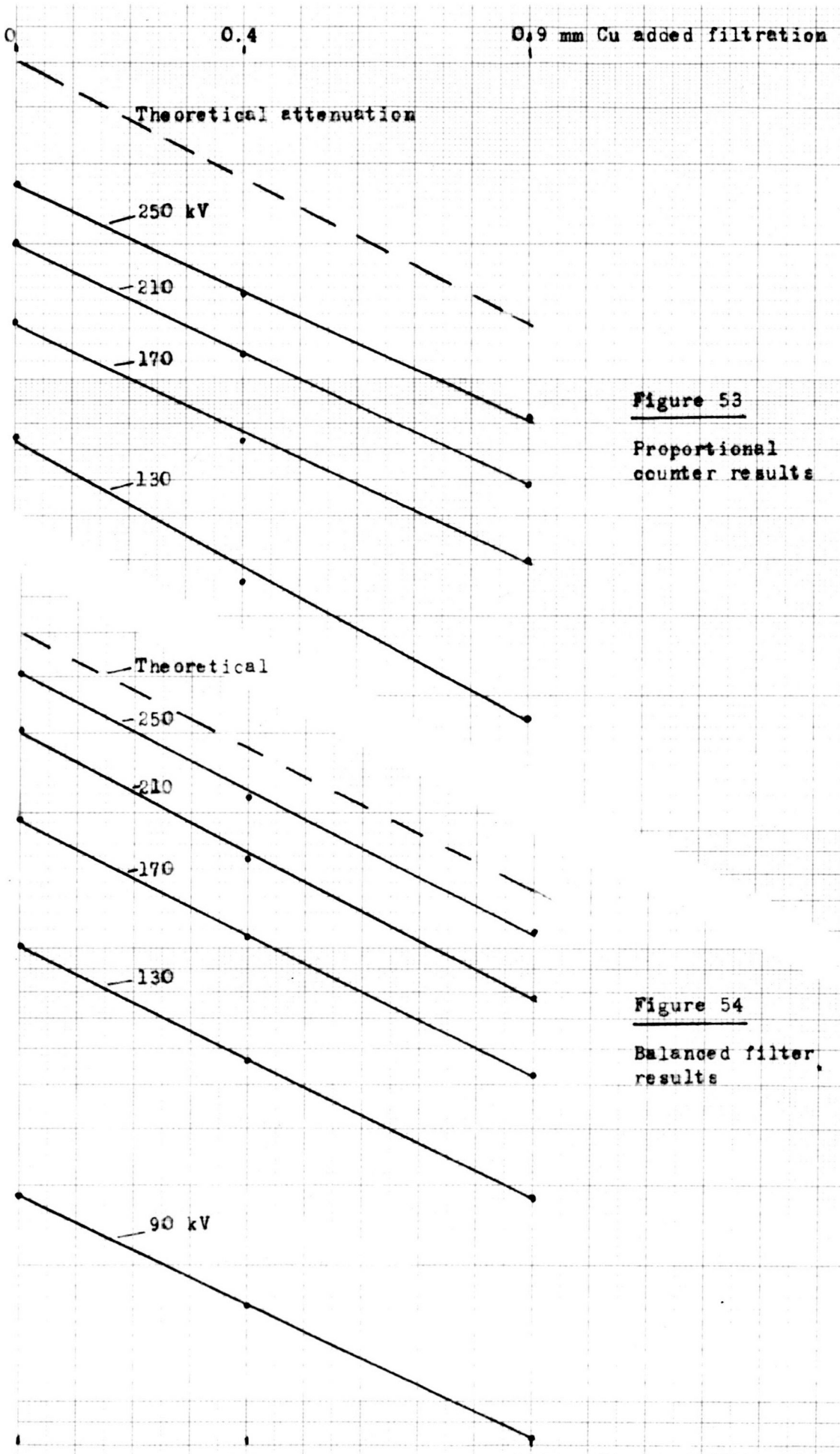

Figure 53

Proportional counter results

Kα exposure rate

Figure 54

Balanced filter results

factors considered may contribute towards the differences noted, it is not clear what the reason is.

5.3 Effect of filtration on ratio of characteristic to total radiation

We may now turn to some general discussion about the experimental results. The first consideration is the effect of filtration upon the relative importance of characteristic X-ray production. In the experiments reported here the characteristic and total radiation have been measured for three different degrees of filtration. It would be expected that the effect of filters on the Kα exposure rates should agree with predictions based on attenuation data, since the radiation is practically monochromatic, and the geometry good. Indeed, this was a necessary assumption in the calculations arising from the proportional counter experiments. Figure 53 shows how far the criteria were achieved, Kα exposure rates being plotted against filter thickness for a range of tube voltages.

When similar data from the balanced filter experiments are plotted in the same way, as in Figure 54, the agreement with the theoretical attenuation is even better. This agreement inspires confidence in the method.

It is reasonable to assume that the exponential attenuation of the characteristic radiation would be maintained over a wider range of filtration, and this would enable the ratio of characteristic to total radiation to be derived for any other filtration for which the attenuation of the total radiation could be measured. Indeed, the Kα/total ratios for our three degrees of filtration could be derived from one set of Kα measurements, together with the relatively easy determination of variation of total radiation with filter thickness. However, in the case of the balanced filter measurements, the use

of/

of different primary beam filtration provided useful confirmation of the results, while with the proportional counter it was an integral part of the method of deriving the baseline of the spectrum.

The attenuation of the total radiation is far from exponential, of course, owing to the heterogeneity of the beam, and the attenuation curves derived in these experiments cannot be extrapolated with any accuracy. However, enough information can be obtained to give some idea of the effect of greater amounts of filtration on the ratio of characteristic to total radiation. At 250 kV, for example, the measured value of Kα/total is 5.2% for 1 mm copper filtration and falls to 1.5% at 2 mm and 0.4% at 3 mm. The change in the ratio is less at lower energies, owing to the more rapid attenuation of the continuous radiation. For example, at 130 kV, the ratio Kα/total falls from 7.8% for 1 mm copper filtration to 3.2% at 2 mm and 1.0% at 3 mm. Characteristic radiation evidently becomes negligible when filtration is heavy. This is only to be expected, since it is attenuated more than the higher energy parts of the spectrum that are inevitably present.

It is the heterogeneity of the continuous radiation and the departure from an exponential form of its attenuation in copper that leads to the differences in shape between the curves of Kα/total radiation against voltage for different degrees of filtration. For low operating voltages, an increase of filtration initially increases the ratio, as the continuous radiation contains a substantial proportion of low energy X-rays which are attenuated more than the K characteristic radiation itself. On the other hand, at 250 kV there is a reduction of the ratio almost as soon as filtration is increased.

5.4/

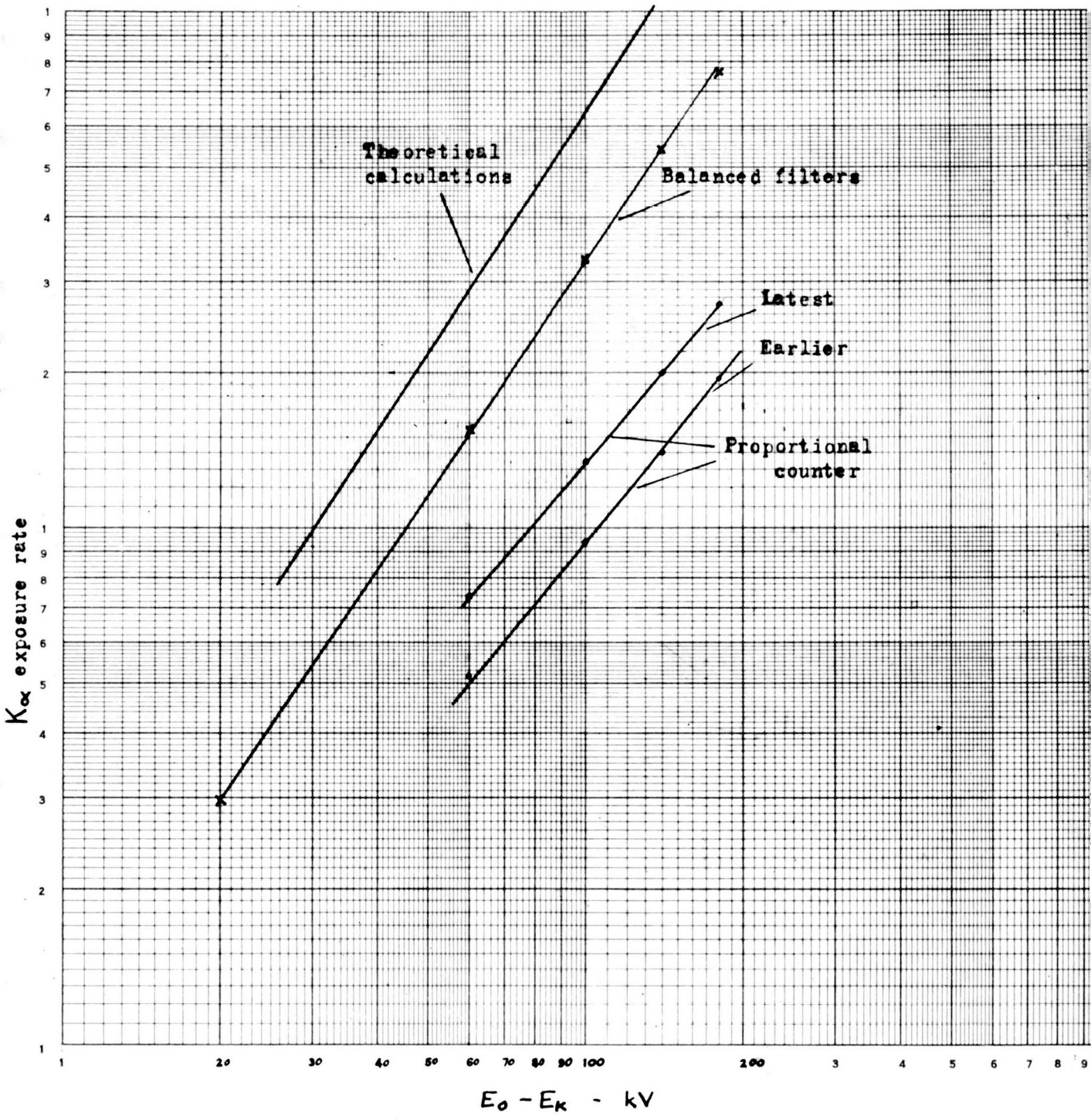
Theoretical calculations
Balanced filters
Latest
Earlier
Proportional counter
K_α exposure rate
$E_o - E_K$ - kV

Figure 55

5.4 Variation of characteristic and continuous radiation with tube voltage

Many workers have found that the variation of intensity of characteristic X-ray production with electron energy can be expressed in the form $I = A (E_o - E_k)^n$, where A and n are constants. Surveying a number of results, Compton and Allison (1935, p 81) concluded that the most reliable value of n was 1.65, and that the relationship was valid up to values of E_o equal to 4 E_k. It is of interest to plot our results on log-log graph paper to investigate the relationship. This is done in Figure 55. The form of the relationship certainly applies, but for the balanced filter measurements, n = 1.4, for the proportional counter measurements illustrated by Figure 18, n = 1.2, and for earlier proportional counter measurements, n = 1.33. It must be borne in mind that the variation of Kα exposure rate with voltage might not be as accurately determined as the ratio to total exposure rate, since no special effort was made to maintain stability of X-ray output over long periods or to measure accurately the low values of tube current necessary in some proportional counter measurements. These figures may be compared with the value of n = 1.23 reported by Hettinger (1960). All these values are lower than that chosen by Compton and Allison, and it may be that the difference is due to the choice of tungsten as target material. The high electron energies giving rise to K characteristic production lead to greater attenuation of the indirectly produced component. The earlier measurements were mostly made with targets of atomic number no higher than that of silver (47), and voltages below 100 kV. The theoretical calculations of Chapter 5 lead to a figure of n = 1.55.

The continuous or total radiation exposure rate without additional filtration can also be plotted against voltage on log-log paper (Figure 56).

Here/

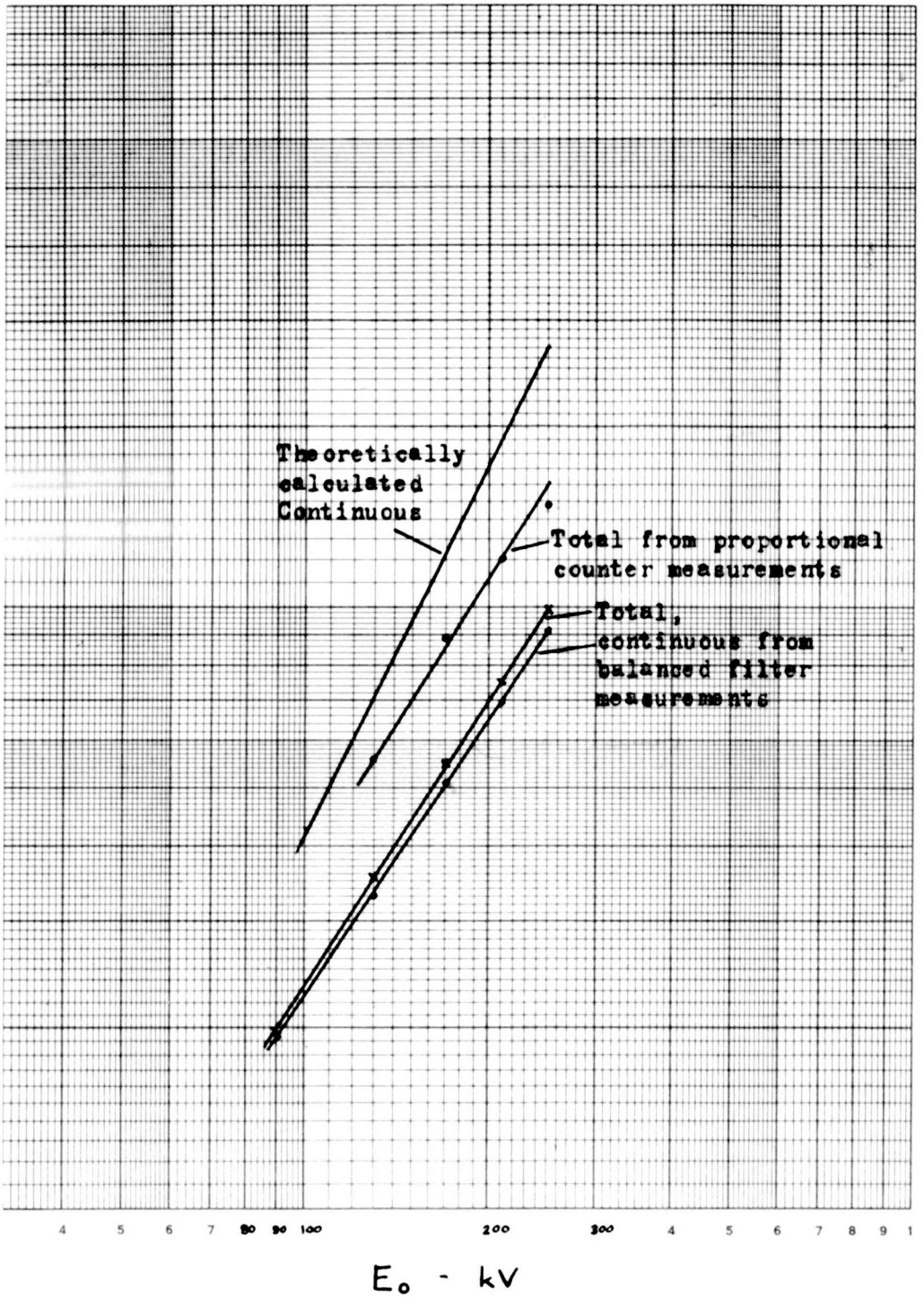
Theoretically calculated Continuous
Total from proportional counter measurements
Total, continuous from balanced filter measurements
Exposure rates
4 5 6 7 80 90 100 200 300 4 5 6 7 8 9 1
E_o - kV

Figure 56

Here the exposure rate varies as the voltage raised to the power 1.54 for the continuous radiation alone, and 1.57 for the total radiation. The theoretical calculations of continuous radiation lead to a variation of exposure rate as the square of the voltage, with the assumed degree of target and tube absorption. The addition of filtration not only leads to an increase in the slope of the continuous radiation/voltage curve, but also to a departure from a power law relationship.

The relationships considered above can be used to express some of our results for unfiltered radiation in the form of an equation. Since the characteristic exposure rate is proportional to $(E_o - E_k)^n$, and the total exposure rate to E_o^m, the ratio, R, of one to the other $= \frac{B\,(E_o - E_k)^n}{E_o^m}$

With the energies expressed in keV and the ratio as a percentage, for the balanced filter measurements, $R = \frac{0.29\,(E_o - 70)^{1.4}}{E_o^{1.57}}$

for the latest proportional counter measurements, $R = \frac{0.76\,(E_o - 70)^{1.2}}{E_o^{1.57}}$

and as a mean between the two, $R = \frac{0.42\,(E_o - 70)^{1.33}}{E_o^{1.57}}$

5.5 Points for further study

The chief parameter that was not studied was the effect of the direction of the X-rays on the ratio of characteristic to total radiation. All the measurements were made on the axis of the beam, and the calculations referred to this direction also. The ratio might be expected to change as a direction more towards or away from the cathode was considered, since the attenuation/

attenuation of X-rays, particularly of indirectly produced characteristic radiation, within the target would alter. While it may be that with a given X-ray tube the beam axis is the direction of most interest, such studies would provide information about the effect of target angle. In view of the difficulty of setting up the proportional counter, the balanced filter method would probably be the simpler to use.

The relative importance of characteristic radiation might be expected to change also, though to a lesser extent, with the waveform applied to the X-ray tube. For a known waveform, it is possible that the results reported here for constant potential operation could be applied by deriving the characteristic and total exposure rates over a range of voltages, and integrating over the waveform considered. The measurement techniques could, of course, be applied to a beam of pulsating potential. The theoretical calculations could probably be refined, though at the cost of considerable effort. It might be possible to allow for effects that were considered small enough to neglect, such as the absorption of directly produced K radiation in the target, and the effect of relativity on ionization cross section. The former would require a knowledge or assumption of electron trajectory. It would be interesting to examine the effect on the calculations of different models of electron trajectory. For example, Archard (1960) has proposed an empirical model which fits the experimental evidence much better than the straight trajectory assumed by Worthington and Tomlin. A later proposal (Archard, 1961) provides a further improvement.

While such developments of the calculations might provide a more accurate picture of the processes involved in X-ray production, and possibly closer agreement with experimental results, it is not certain that they would be entirely worth while, since it is unlikely that the calculations can ever

be/

be sufficiently comprehensive or the data sufficiently accurate to permit the complete prediction of characteristic and continuous emission.

A C K N O W L E D G E M E N T S

It is a pleasure to record my gratitude to Dr. J. R. Greening, Director of the Department of Medical Physics, University of Edinburgh, for his continued guidance and encouragement.

I must also pay tribute to my wife, without whose support and forbearance the work would have been impossible.

I am grateful to the Radiochemical Centre, U.K.A.E.A., for the loan of the 100 mc source of americium-241.

REFERENCES

Archard, G. D. (1960). X-ray Microscopy and X-ray Microanalysis, Elsevier, Amsterdam, p.331.

Archard, G. D. (1961). Back scattering of electrons, J. Appl. Phys, 32, 1505.

Barnes, S. W. and Palmer, L. D. (1933). The rocking curve correction in the determination of the width of X-ray lines, Phys. Rev. 43, 1050.

Barrett, C. S. (1952). The Structure of Metals, McGraw-Hill, New York.

Beckman, O. (1955). Relative intensities of the X-ray K lines of heavier elements, Ark. f. Fysik. 9, 495.

Bendit, E. G. (1958). The ratio of characteristic to white X-radiation from a copper target, Brit. J. Appl. Phys. 9, 312.

Bethe, H. A. (1930). Zur Theorie des Durchgangs schneller Korpuskularstrahlen durch Materie, Ann. Phys. Lpz. 5, 325.

Bisi, A. and Zappa, L. (1955). Statistical spread in pulse size of the proportional counter spectrometer, Nuovo cimento, 2, 988.

Blokhin, M. A. (1957). The Physics of X-rays. The State Publishing House of Technical-Theoretical Literature, Moscow. Translated by the United States Atomic Energy Commission, AEC-tr-4502.

Boag, J. W. (1956). Chapter 4 of Radiation Dosimetry edited by Hine and Brownell. Academic Press, New York.

Cabrera, J. (1923). Sur les limites d'absorption K de quelques elements, Compt. rend. 176, 740.

Compton, A. H. and Allison, S. K. (1935). X-rays in Theory and Experiment. D. van Nostrand, New York.

Cormack, D. V., Till, J. E., Whitmore, G. F. and Johns, H. E. (1955). Measurement of continuous X-ray spectra with a scintillation spectrometer, Brit. J. Radiol. 28, 605.

Cormack, D. V., Davitt, W. E., Burke, D. G. and Rawson, E. G. (1958). Spectral distributions of 280 kVp X-rays, Brit. J. Radiol. 31, 565.

Cormack, D. V. and Burke, D. G. (1960). Spectral distributions of primary and scattered 140 kVp X-rays, Radiology, 74, 743.

Cosslett, V. E. and Dyson, N. A. (1957). Measurements of spectral and angular distribution of X-rays from thin targets. X-ray Microscopy and Microradiography. Academic Press, New York, p.405.

Dolby, R. M. (1960). Absolute intensity measurements of the carbon and aluminium X-ray K-lines with a proportional counter, Brit. J. Appl. Phys. 11, 64.

Dyson, N. A. (1959). Efficiency of characteristic Kα X-ray production in copper between 9 and 15 kV, Brit. J. Appl. Phys. 10, 505.

Dyson, N. A. (1959b). The continuous X-ray spectrum from electron-opaque targets, Proc. Phys. Soc. 73, 924.

Farr, R. F. (1955). The distribution of dose-rate across the field of an X-ray therapy tube. Brit. J. Radiol. 28, 364.

Gatrousis, C., Heinrich, R. and Crouthamel, C. E. (1961). Recent advances in counting techniques, Progress in Nuclear Energy, Series 9, Analytical Chemistry, Vol. 2, Pergamon Press.

Green, M. and Cosslett, V. E. (1961). The efficiency of production of characteristic X-radiation in thick targets of a pure element, Proc. Phys. Soc. 78, 1206.

Green, M. (1963). A Monte Carlo calculation of the spatial distribution of characteristic X-ray production in a solid target, Proc. Phys. Soc. 82, 526.

Greening, J. R. (1947). The determining of X-ray energy distributions by the absorption method, Brit. J. Radiol. 20, 71.

Grodstein, Gladys W. (1957). X-ray attenuation coefficients from 10 keV to 100 MeV, N.B.S. Circular 583.

Handbook of Chemistry and Physics (38th edition) 1956. Chemical Rubber Publishing Co., Cleveland.

Hettinger, G. and Starfelt, N. (1958). Bremsstrahlung spectra from roentgen tubes, Acta Radiologica. 50, 381.

Hettinger, G. (1960). Spectra of primary and secondary roentgen radiation, Radiation Physics Department University of Lund.

I.C.R.U. (1964). Physical aspects of irradiation, recommendations of the International Commission on Radiological Units and Measurements, Report 10b, 1962. N.B.S. Handbook 85.

Johansson, S. A. E. (1951). The use of scintillation counters in the measurement of the energy of X-rays and low energy gamma rays, Ark. Fysik. 3, 533.

Johns, H. E. (1961). The Physics of Radiology, 2nd edition. Charles C. Thomas, Springfield.

Kaye, G. W. C. and Laby, T. H. (1957). Tables of Physical and Chemical Constants. Longmans Green and Co., London.

Kirkpatrick, P. (1939). On the theory and use of Ross filters, Rev. Sci. Inst. 10, 186.

Kirkpatrick, P. (1944). Theory and use of Ross filters, II, Rev. Sci. Inst. 15, 223.

Kirkpatrick, P. and Baez, A. V. (1947). Absolute energies of Kα radiation from thick targets of silver, Phys. Rev. 71, 521.

Klemperer, O., Thetford, A. and Lenz, F. (1960). Transmission of slow electrons through thin films, Proc. Phys. Soc. 76, 705.

Kramers, H. A. (1923). On the theory of X-ray absorption and of the continuous X-ray spectrum, Phil. Mag. 46, 836.

Kulenkampff, H. (1922). Über das kontinuierliche Röntgenspektrum, Annal. Phys. 69, 548.

Kuntke, A. H. G. (1957). Untersuchungen über die Anderung der Röntgenstrahlen - Ausbeute an Drehanoden - Röntgenröhren, Fortschritte Rontgenstr. 87, 397.

Mott, N. F. and Massey, H. S. W. (1949). The Theory of Atomic Collisions. Clarendon Press, Oxford.

Ross, P. A. (1928). A new method of spectroscopy for faint X-radiations, J. Opt. Soc. Am. and Rev. Sci. Inst. 16, 433.

Smick, A. E. and Kirkpatrick, P. (1945). Absolute K ionization cross-section of the nickel atom under electron bombardment at 70 kV, Phys. Rev. 67, 153.

Spiers, F. W. (1946). Effective atomic number and energy absorption in tissues, Brit. J. Radiol. 19, 52.

Stoddard, K. B. (1935). Direct and fluorescence excitation of the K level in thick targets of gold, Phys. Rev. 48, 43.

Strominger, D., Hollander, J. M. and Seaborg, G. T. (1958). Table of isotopes, Rev. Mod. Phys. 30, 585.

Victoreen, J. A. (1948). The absorption of incident quanta by atoms as defined by the mass photoelectric absorption coefficient and the mass scattering coefficient, J. Appl. Phys. 19, 855.

Victoreen, J. A. (1949). The calculation of X-ray mass absorption coefficients. J. Appl. Phys. 20, 1141.

West, D. (1953). Energy measurements with proportional counters. Progress in Nuclear Physics, Vol 3, p.18 edited by O. R. Frisch, Pergamon Press, London.

West, D. and Bradley, E. F. (1957). Proportional counter measurements of π^--mesonic X-rays, Phil. Mag. 2, Series 8, 957.

Whiddington, R. (1912). The transmission of cathode rays through matter, Proc. Roy. Soc. A. 86, 360.

Williams, J. H. (1932). Wavelengths of the tungsten K series spectrum with the double spectrometer, Phys. Rev. 40, 791.

Worthington, C. R. and Tomlin, S. G. (1956). The intensity of emission of characteristic X-radiation, Proc. Phys. Soc. A. 69, 401.